Master's thesis

NTNU
Norwegian University of Science and Technology
Faculty of Natural Sciences
Department of Biotechnology and Food Science

Rosa Jodalen Rudberg

Production of Roseoflavin Using the Engineered Bacteria *Corynebacterium glutamicum*

Master's thesis in Industriell kjemi og bioteknologi
Supervisor: Dr. Fernando Pérez-García
Co-supervisor: Dr. Luciana Fernandes de Brito and Prof. Trygve Brautaset

June 2023

NTNU
Norwegian University of Science and Technology

Rosa Jodalen Rudberg

Production of Roseoflavin Using the Engineered Bacteria *Corynebacterium glutamicum*

Master's thesis in Industriell kjemi og bioteknologi
Supervisor: Dr. Fernando Pérez-García
Co-supervisor: Dr. Luciana Fernandes de Brito and Prof. Trygve Brautaset
June 2023

Norwegian University of Science and Technology
Faculty of Natural Sciences
Department of Biotechnology and Food Science

NTNU
Norwegian University of
Science and Technology

Preface

This thesis signifies the completion of my master's in Chemical Engineering and Biotechnology at the Faculty of Natural Science at Norwegian Univeristy of Science and Technology (NTNU). The thesis was completed in the spring of 2023 as part of the Cell Factory group under the guidance of Postdoctoral Fellow Fernando Pérez-García and Professor Trygve Brautset, who serves as the principal investigator of the group. The practical aspects of the research were carried out at the Microbial Biotechnology Division within the Department of Biotechnology and Food Science (IBT).

I am deeply grateful to Fernando Pérez-García for providing me with the opportunity to work on such a exciting projects and for his guidance, teaching and patience in addressing all my questions. Additionally, I express gratitude to Postdoctoral Fellow Luciana Fernandes de Brito for providing extensive guidance and supervision. Furthermore, I would like to thank Ingunn Husøy and Monica G. Frøystad, my closely associated colleagues in the laboratory, for making each day joyful. Working alongside all of you has been a true pleasure.

I would also like to acknowledge the other members of the Cell Factories group for including me. Lastly, I am thankful for the support of my friends and family, during the five years of my master's program.

Abstract

This Master's thesis aimed to produce the antimicrobial compound roseoflavin using strains of *Corynebacterium glutamicum* that overproduces its precursor riboflavin as a microbial platform. Roseoflavin is currently produced by chemical synthesis, which is costly, employs hazardous compounds, and has a low molar yield of 5%. *C. glutamicum* is commonly used in industry and has been engineered to produce several value-added chemicals, including riboflavin. This study explored the roseoflavin biosynthetic pathway from *Streptomyces davawensis* in a *C. glutamicum* riboflavin-producing strain. In this regard, the genes *rosA*, *rosB*, *rosC*, and *ribM* were plasmid-based expressed. Additionally, the bifunctional riboflavin kinase / FMN adenylyltransferase gene *ribF* from *C. glutamicum* was overexpressed connecting the roseoflavin and riboflavin pathways. The genes *ribF-rosABC* belonged to the roseoflavin biosynthesis pathway, while the gene *ribM* coded for a flavin transporter protein. The newly constructed plasmids were transformed into a riboflavin-producing *C. glutamicum* strain, overexpressing the riboflavin operon *ribGCAH* (named *riboCg*), resulting in the following three strains: *C. glutamicum*(pSym-*riboCg*)(pVWEx1-*rosABC*) (named Roseo1), *C. glutamicum*(pSym-*riboCg*)(pVWEx1-*rosABC-ribM*) (named Roseo2), and *C. glutamicum*(pSym-*riboCg*)(pVWEx1-*ribF-rosAB-ribM*) (named Roseo3). Growth experiments in shaking flasks were performed to evaluate the cell growth, and HPLC was utilized to quantify the riboflavin and roseoflavin production. Antimicrobial tests were performed to evaluate the toxicity of roseoflavin in *C. glutamicum*, and to investigate the impact of the transporter proteins encoded by *ribM* from *S. davawensis*, and *ribX* from *C. glutamicum*. In the growth experiments, it was found that all the constructed strains, except for the control strain, produced roseoflavin. In comparison to the strains constructed in the Specialisation project of Rudberg (2022) [1], containing the genes *rosAB*, and *ribM*, it was found a decrease of roseoflavin production in the strains overexpressing *rosC*. Contrarily, overproducing *ribF* in the strain Roseo3 increased the roseoflavin production. Roseo3 achieved the highest roseoflavin titer of 4.065 ± 0.901 g/L. It is noteworthy that the roseoflavin final titers might have been influenced by an unknown analyte detected at a similar retention time as roseoflavin. Notably, the expression of the *ribM* gene proved to be beneficial since it decreased roseoflavin toxicity while increasing roseoflavin productivity. The antimicrobial tests indicated that *ribM* is an antiporter, co-transporting roseoflavin out of the cells while importing riboflavin. *ribX* was revealed to encode a riboflavin and a roseoflavin importer, due to the similar structures of the two compounds. Furthermore, the antimicrobial tests revealed a roseoflavin inhibitory constant of 0.05 g/L, which represents the threshold concentration of roseoflavin that limits the growth of *C. glutamicum* cells. This work lays a solid foundation for the sustainable and efficient microbial production of roseoflavin, offering a promising alternative to costly and hazardous chemical synthesis methods. However, further research is necessary to optimize the production method, separate the unknown compound influencing the roseoflavin titers, and explore potential applications for scaling-up production in bioreactors.

Sammendrag

Denne masteroppgaven hadde som mål å produsere det antimikrobielle stoffer roseoflavin ved bruk av riboflavin-overproduserende stammer av *Coreynebacterium glutamicum* som en mikrobiell platform. I dag produseres roseoflavin ved kjemisk syntese, som er kostbart, bruker farlige fobindelser og har et lavt molart utbytte på 5%. *C. glutamicum* brukes vanligvis i industrien og har blitt genmodifisert til å produsere flere verdifulle kjemikalier, inkludert riboflavin. I denne studien ble roseoflavin-biosyntesesporet fra *Streptomyces davawensis* testet i en riboflavin-produserende *C. glutamicum*-stamme. I den forbindelse ble genene *rosA*, *rosB*, *rosC* og *ribM* uttrykt ved hjelp av plasmider. I tillegg ble genet *ribF*, som koder for bifunksjonell riboflavin kinase / FMN adenylyltransferase i genomet til *C. glutamicum*, overuttrykt for å koble sammen roseoflavin og riboflavin sporene. Genene *ribF-rosABC* tilhørte roseoflavin biosyntese sporet, mens genet *ribM* kodet for en flavintransportprotein. De nykonstruerte plasmidene ble transformert inn i *C. glutamicum*-stammen som overproduserte riboflavin ved å overuttrykke riboflavin operonet *ribGCAH* (kalt *riboCg*). Dette resulterte i de tre følgende stammene: *C. glutamicum*(pSym-*riboCg*)(pVWEx1-*rosABC*) (kalt Roseo1), *C. glutamicum*(pSym-*riboCg*)(pVWEx1-*rosABC-ribM*) (kalt Roseo2), og *C. glutamicum*(pSym-*riboCg*)(pVWEx1-*ribF-rosAB-ribM*) (kalt Roseo3). Vekstforsøk ved bruk av flaskedyrking ble utført for å evaluere celleveksten, og HPLC ble brukt til å kvantifisere produksjon av roseoflavin og riboflavin. Antimikrobielle tester ble utført for å evaluere giftigheten til roseoflavin for *C. glutamicum*, og for å undersøke egenskapene til transportproteinene kodet av *ribM* fra *S. davawensis* og *ribX* fra *C. glutamicum*. Fra vekstforsøkene ble det funnet at alle de konstruerte stammene, bortsett fra kontrollstammen, produserte roseoflavin. Sammenlignet med stammene konstruert i Fordypningsprosjektet til Rudberg (2022) [1], som inneholdt genene *rosAB* og *ribM*, ble det funnet en reduksjon i roseoflavin-produksjon i stammene som overuttrykkte *rosC*. Derimot økte roseoflavin-produksjonen når *ribF* ble overuttrykt i Roseo3-stammen. Roseo3 oppnådde den høyeste roseoflavin konsentrasjonen på 4,065 ± 0,901 g/L. Verdien påvirkes imidlertid av konsentrasjonen til en ukjent forbindelse med liknende retensjonstid som roseoflavin. Det er verdt å merke seg at overuttrkkelse av *ribM* viser seg å være gunstig siden det reduserte roseoflavin-giftigheten samtidig som roseoflavin produksjonen økte. Fra de antimikrobielle testene ble det oppdaget at *ribM* fungerte som en antiporter som transporterte roseoflavin ut av cellene samtidig som den importerte riboflavin. *ribX* ble funnet til å kode for en riboflavin- og roseoflavin-importør på grunn av de liknenede strukturene til de to forbindelsene. Videre avslørte de antimikrobielle testene en roseoflavin-inhiberingskonstant på 0,05 g/L, som representerer terskelkonsentrasjonen av roseoflavin som begrenser veksten av *C. glutamicum* celler. Totalt sett legger dette arbeidet et solid grunnlag for bærekraftig og effektiv mikrobiell produksjon av roseoflavin, og tilbyr et lovende alternativ til kostbare og farlige kjemiske syntesemetoder. Imidlertid kreves det videre forskning for å optimalisere produksjonsmetoden, oppdage den ukjente forbindelsen som påvirker roseoflavin-titerne, og utforske potensielle anvendelser for produksjon i større skala i bioreaktorer.

Contents

List of Figures

List of Tables

Abbreviations list

Table 0.1: Abbreviations used in this work.

Abbreviation	Full name
AF	8-demethyl-8-amino-riboflavin
AFP	8-dimethyl-8-amino-riboflavin-5´-phosphate
AHC	S-adenosylhomocysteine
BHI	Brain hart infusion
bp	Base pair
Cg	*C. glutamicum*
Cg(pSym-*riboCg*)	*Cg*(pECXT-Psyn-*ribGCAH*)
CGXII	Minimal media
Erythose 4P	n erythose 4-phosphate
FAD	Flavin adenine dinucleotide
FMN (or RP)	Flavin mononucleotide (or riboflavin-5´-phosphate)
Fructose 6P	Fructose 6-phosphate
G6PDH	Glucose-6-phosphate dehydrogenas
GA3P	glyceraldehyde 3-phosphate
GCDBP	GTP cyclohydrolas II/3,4-dihydroxy-2-butanone-4-phosphate synthase
Glucose 6P	Glucose 6-phosphate
Glyceraldehyde 3P	Glyceraldehyde 3-phosphate
GMP	guanosine monophosphate
6PLG	6-phosphoglucono-lactonas
6PGDH	6-phos-phogluconate dehydrogenase
GTP	guanosine triphosphate
HOOC-RF	8-demethyl-8-carboxyl FMN
HPLC	High pressure liquid chromatography
IMP	inosine monophosphate
IPTG	Isopropyl-β-D-1-thiogalactopyranoside
LB	Lysogeny broth
MAF	8-demethyl-8-methylamino-riboflavin
NMR	Nulcear magnetic resonance
OD	Optical density
OHC-RF	8-demethyl-8-formyl FMN
PCR	Polymerase chain reaction
PGI	phosphoglucose isomerase
PP	Purine pathway
PPP	Pentose phosphate pathway
PRPP	phosphoribosyl diphosphate
RDR	Bifunctional riboflavin-specific deaminase/reductase
RF	Riboflavin
Ribulose 5P	ribulose 5-phosphate
RoFAD	Adenine dinucleotide
RoFMN	Moseoflavin mononucleotide
RoF	Roseoflavin
Roseo0/ Transport3	*Cg*(pSym-*riboCg*)-(pVWEx1)
Roseo1	*Cg*(pSym-*riboCg*)-(pVWEx1-*rosABC*)
Roseo2	*Cg*(pSym-*riboCg*)(pVWEx1-*rosABC-ribM*)
Roseo3	*Cg*(pSym-*riboCg*)(pVWEx1-*ribF-rosABC-ribM*)
Roseo4	*Cg*(pSym-*riboCg*)-(pVWEx1-*rosAB*)
Roseo5	*Cg*(pSym-*riboCg*)(pVWEx1-*rosAB-ribM*)
RPI	Ribose-5-phosphate isom-erase
RS	Riboflavin synthase
RSC	Riboflavin synthase beta chain
SAM	S-adenosylmethionine
Sedoheptulose 7P	sedoheptulose 7-phosphate
tac	Tac-promotor
TES	Trace element solution
Thi	Thiamine
Transport0	*Cg*(pVWEx1)
Transport1	*Cg*(pVWEx1-*ribM*)
Transport2	*Cg*(pVWEx1-*ribX*)
Transport3/Roseo0	*Cg*(pSym-*riboCg*)-(pVWEx1)
Transport4	*Cg*(pSym-*riboCg*)(pVWEx1-*ribM*)
Transport5	*Cg*(pSym-*riboCg*)(pVWEx1-*ribX*)
XMP	xanthine monophosphate
Xylulose 5P	xylulose 5-phosphate

1 Introduction

The antimicrobial agent roseoflavin is widely used in food industry to select roseoflavin-resistant strains for pasta and bread fermentation [2]. Current methods for producing roseoflavin rely on chemical synthesis, which is not only expensive but also poses significant risks due to use of hazardous compounds [3] [4]. Therefore, there is a pressing need for more sustainable approaches to producing roseoflavin.

Corynebacterium glutamicum (*C. glutamicum*) has emerged as a promising microbial host for the production of novel compounds in the industrial biotechnology sector [5]. Among these compounds, riboflavin has been successfully produced by overexpressing the native riboflavin operon *ribGCAH* or the sigma factor gene *sigH* which increases the expression of riboflavin biosynthesis genes [5] [6]. Notably, riboflavin serves as the precursor for roseoflavin, making the latter a novel target for production in *C. glutamicum*. According to literature, roseoflavin can be produced by overexpressing the genes *rosABC* and *ribF* in a riboflavin-overproducing strain, while overexpression of the genes *rosAB* should be sufficient for roseoflavin production [2]. Additionally, the overproduction of *ribM*, which encodes a flavin transporter protein, has been shown to increase the production of roseoflavin [1].

This study was envisioned to further optimize the production of roseoflavin from the work conducted in the Specialisation project, "Production of Roseoflavin Using the Engineered Bacteria, *Corynebacterium glutamicum*", during the fall of 2022 [1] (further named Rudberg's study [1]). Additionally, the study explores the hypothesis that the effect of the roseoflavin exporter gene *ribM* reduces roseoflavin´s antimicrobial effect, and the study tested if the riboflavin transporter-protein *ribX* is a roseoflavin transporter.

1.1 *Corynebacterium glutamicum* a workhorse in biotechnology

C. glutamicum is a Gram-positive bacterium belonging to the phylum *Actinobacteria*, and is commonly found in soil [7]. It is a facultative anaerobe, meaning that it can survive in both the presence and absence of oxygen. *C. glutamicum* possesses several characteristics which makes it well-suited for biotechnological applications. It is non-sporulating, non-pathogenic, has a stable genome, and does not secrete any extracellular protease [8]. Moreover, it is a fast-growing bacterium that grows at temperatures ranging from 25-37°C, with an optimal temperature of 30°C [9].

C. glutamicum is generally recognized as safe (GRAS) compared to *E. coli* [10] and has several advantages as a microbial cell factory. In industry, *C. glutamicum* has been used for many years as a microbial host for the production of novel compounds within cosmetics, health, food, and animal food [11]. It is capable of naturally producing the amino acid glutamate and has been genetically engineered to overproduce other amino acids such as isoleucine, threonine, and lysine [12] [8]. These amino acids have been produced by genetically engineered *C. glutamicum* in a million-ton scale for over 60 years [13], resulting in much available knowledge and tools to work with *C. glutamicum* [5]. The tools are used for gene cloning, expression, DNA transfer, gene deletion, protein secretion, gene replacement, and genome rearrangement. These methods enable researchers to manipulate genes, study gene function, and modify genomes [14]. Researchers have extensively studied the complete genome and genetic makeup of *C. glutamicum* [15]. By analyzing its genes and their functions, they have gained valuable insights, predicting the functions of over 60% of the identified genes [16]. To

investigate gene expression in *C. glutamicum*, specific DNA microarrays have been developed for transcriptome analysis [16]. In recent years, *C. glutamicum* has undergone extensive modifications to enable it to utilize various carbon sources, like glycerol, a byproduct of biodiesel production. Additionally, amino acids derived from fish industry waste and lignocellulosic sugars have been employed as alternative carbon sources for *C. glutamicum* [5] [13]. Furthermore, the fermentable sugar alcohol mannitol and the glucose-based polymer laminarin from brown seaweed, have been used as carbon sources for genetic metabolic engineered *C. glutamicum* [5]. Since *C. glutamicum* lacks a complex carbon catabolite repression system, it is a preferred bacteria to engineer, making *C. glutamicum* able to consume more than one substrate at the same time and also consume different substrates [5]. On the other hand, the bacteria *Bacillus subtilis* and *Escherichia coli* (*E. coli*) have more complex catabolite repression systems. As the number of novel compounds produced by *C. glutamicum* is increasing, there is potential to investigate other reaction pathways that could lead to the expansion of the compound portfolio produced by *C. glutamicum* [17].

1.1.1 *C. glutamicum* as a sustainable host for production of antimicrobial compounds

C. glutamicum has been proven by Hongnian et al. (2016) [10] to produce the antimicrobial component violacein. The study yielded high violacein titers, indicating that *C. glutamicum* is a robust bacteria with high capability for the production of antimicrobial compounds. Consequently, using *C. glutamicum* in the biosynthesis of various antimicrobial compounds, such as roseoflavin, hold promising prospects. Violacein is naturally produced by *Cromobacterium violaceum* (*C. violaceum*), and formed by condensation of two tryptophan molecules [10]. It is a pigment with antibacterial [18], antifungal, antitumor [19], and antiprotozoal properties, meaning it resists cell growth or causes cell death of certain bacteria, fungi, cancer, and protozoans [20]. In addition, violacein induces apoptosis and has a role as a bacterial metabolite [20]. From the study of Hongnian et al., violacein was produced by overexpression of the heterologous *vioABCDE* operon from *C. violaceum* in a *C. glutamicum* strain ATCC 21850 [21]. In industry the *C. glutamicum* strain ATCC 21850 is an established L-tryptophan hyper-producer, making it attractive for violacein production, due to tryptophan being a precursor of violacein. A titer of 5.4 g/L of crude violacein, a mixture of deoxy-violacein and violacein, was achieved in a batch reactor after optimization of the production method [10]. Such a high titer made microbial fermentation of violacein in *C. glutamicum* compatible with other methods for violacein production.

1.1.2 Glucose as feedstock in biotechnology

Microbial fermentation utilizing glucose, menthol, xylose, and complex carbon sources derived from lignocellulosic biomass offers a sustainable alternative to chemical synthesis reliant on non-renewable fossil fuels [22]. However, given the widespread use of glucose in the human food industry, its utilization as a carbon source for biobased metabolite production in *C. glutamicum* and other bacteria poses a competition for resources intended for food production [22]. Consequently, there has been a shift towards non-food sustainable carbon sources such as xylose, methanol, arabinose, and glycerol. Furthermore, there is a growing emphasis on exploring alternative renewable carbon sources including agricultural and industrial wastes, as well as seaweed [22].

The utilization of glucose as a carbon source offers several advantages for the growth of *C. glutamicum* compared to other sugars. One significant advantage is the faster growth rate supported by glucose when compared to alternative sugars [23]. Moreover, glucose possesses the capability to suppress the utilization of other carbon sources by most bacteria, except by *C. glutamicum*, known as carbon catabolic repression [23]. In natural environments, carbon catabolic repression promotes rapid bacterial growth by directing their focus towards glucose, the preferred sugar [23]. Consequently, in the presence of a mixture of sugars, glucose is the first sugar to be consumed. Glucose inhibits the utilization of other carbon sources through two main mechanisms: Inducer exclusion and the inhibition of the signaling molecule cAMP synthesis [23]. Inducer exclusion occurs through the uptake of glucose via the phosphotransferase system, leading to the formation of dephosphorylated enzyme EIIAGlc [24]. EIIAGlc, inhibits lactose permease (LacY) by binding to it, thereby inhibiting lactose transport and the utilization of the carbon source lactose [24]. cAMP activates the transcription factor CRP, which performs various functions, including the regulation of alternative sugar utilization systems [23]. As glucose serves as the carbon source yielding the fastest growth of *C. glutamicum*, glucose is the most commonly used carbon source when reaction pathways for the production of novel compounds are explored [25].

1.2 Riboflavin

Riboflavin is a water-soluble vitamin, known as B2-vitamin [26]. It is found in fish, meat, milk, and vegetables, and it has essential roles in the metabolism of carbohydrates, amino acids, fats, ketone bodies, and steroids. Additionally, riboflavin plays a role in cellular function and the cell's energy production [26]. Riboflavin is the precursor of the two cofactors flavin adenine dinucleotide (FAD) and flavin mononucletide (FMN) [27], which are active groups in flavo-coenzymes and flavoproteins [28]. Flavoproteins play important roles inside all prokaryotic and eukaryotic cells in physiological functions such as DNA repair, chromatin remodeling, protein folding, fatty acid β-oxidation, redox homeostasis, apoptosis prevention [29] and choline metabolism [28]. In visible light riboflavin is yellow, and it is fluorescent when it is exposed to UV light [30]. Riboflavin is also inactivated rapidly when exposed to visible- and UV light. The chemical structure of riboflavin is shown in Figure 1.1.

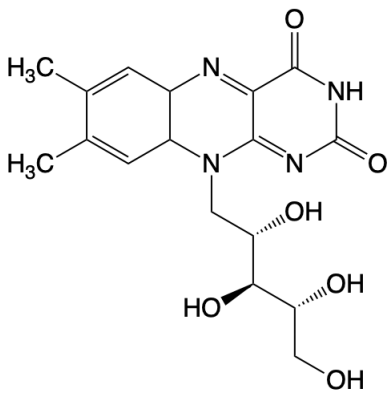

Figure 1.1: The chemical structure of riboflavin.

1.2.1 Production of riboflavin in industry

Industrial production of riboflavin can either be carried out as fermentation or through chemical synthesis [31]. Production through fermentation is cost-effective and occurs in one step. In addition, using fermentation reduces the energy required and the waste from the process [32]. Furthermore, renewable resources can be used for microbial fermentation. On the other hand, the production of riboflavin through chemical synthesis is achieved through multiple stages and is expensive [31]. Hence, today's production of riboflavin is by fermentation and genetically engineered microorganisms. The biosynthesis pathway of riboflavin, which is overexpressed in genetically engineered strains for riboflavin production is shown in Figure 1.2.

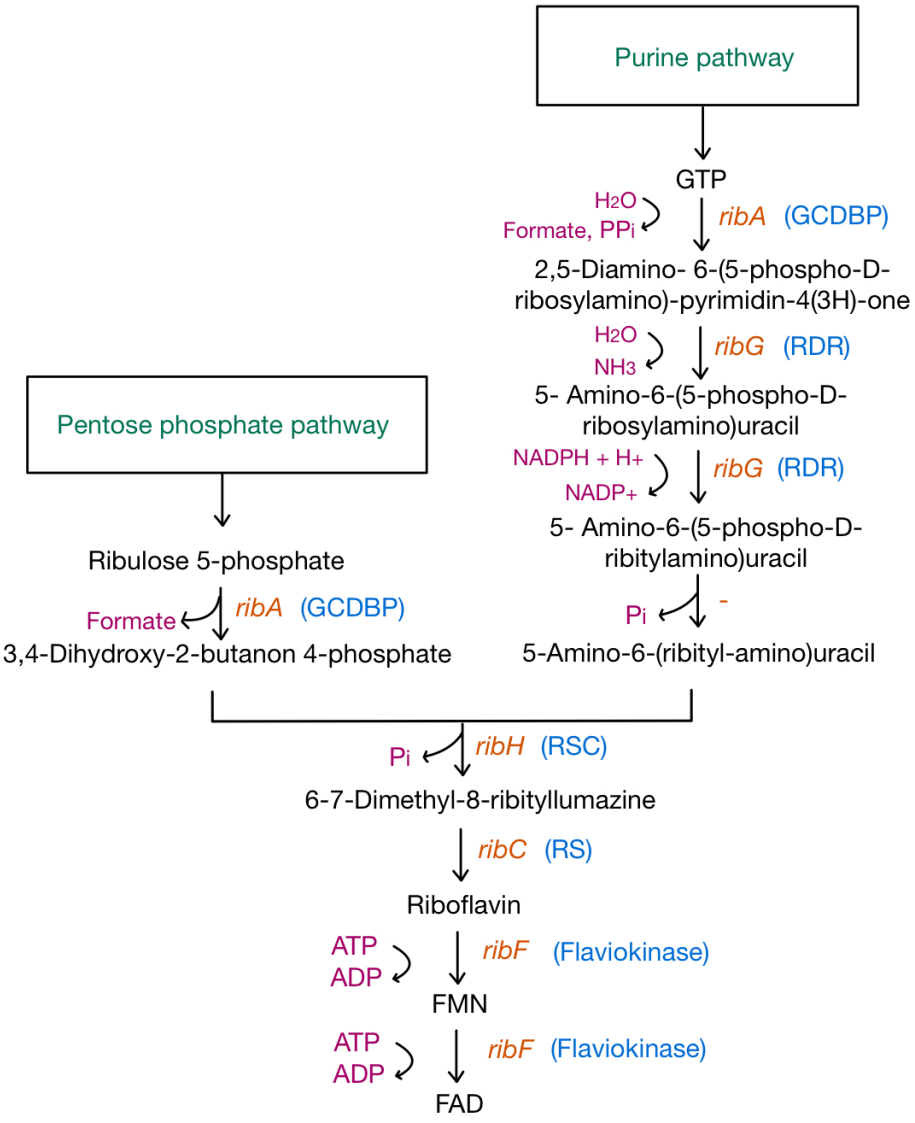

Figure 1.2: The riboflavin biosynthesis pathway starts with the precursors GTP and ribulose 5-phosphate from the purine pathway (PP) and pentose phosphate pathway (PPP), respectively. PP and PPP in marked green. The genes (marked orange), encoded for the enzymes (marked blue) producing the compounds (marked black). In pink are the electron carrier and cofactors participating in the reactions. The enzyme GTP cyclohydrolase II/3,4-dihydroxy-2-butanone-4-phosphate synthase (GCDBP) is encoded by the gene *ribA*, the bifunctional riboflavin-specific deaminase/reductase (RDR) is encoded by the *ribG* gene, the riboflavin synthase beta chain (RSC) is encoded by *ribH*, the enzyme riboflavin synthase (RS) is encoded by *ribC*, and the flavokinase is encoded by *ribF* [5] [33]. Flavokinase is also known as FAD- and FMN- synthetase [31].

The enzymes encoded by the genes *ribA*, *ribG*, *ribH*, *ribC* and *ribF* in Figure 1.2 catalyses different reactions in the riboflavin pathway [34]. A hydrolysis reaction is catalyzed by the enzyme GCDBP (GTP cyclohydrolase II/3,4-dihydroxy-2-butanone-4-phosphate synthase) producing 2,5-diamino-6-(5-phospo-D-ribosylamino)-pyrimidin-4(3H)-one, formate and PPi (inorganic pyrophosphate) from GTP (guanosine triphosphate) and water [34]. Further, GCDBP hydrolyses ribulose 5- phosphate (ribulose 5P) forming 3,4-dihydroxy-2-butanon 4-phosphate and formate [34]. The enzyme RDR (bifunctional riboflavin-specific deaminase/reductase) encoded by *ribG* deaminates 2,5-diamino-6-(5-phospo-D-ribosylamino)-pyrimidin-4(3H)-one to 5-amino-6-(5-phospo-D-ribosylamino)- uracil and ammonia [34]. After, it catalyzes a reduction reaction reducing 5-amino-6-(5-phospo-D-ribosylamino)- uracil to 5-amino-6-(5-phospo-D-ribitylamino)- uracil using NADP as the electron carrier. The phosphatase reaction producing 5-amino-6-(ribityl amino)- uracil from 5-amino-6-(5-phospo-D-ribitylamino)- uracil is catalyzed by an unknown enzyme [34]. From 5-amino-6-(ribityl amino)uracil and 3,4-dihydroxy-2-butanon 4-phosphate the enzyme RSC (riboflavin synthase beta chain) catalyzes the reaction producing 6-7-dimethyl-8-ribityllumazine [34]. Finally, a dimutation reaction [34] catalyzes the production of riboflavin from 6-7-dimethyl-8- ribityllumazine. The enzyme FMN syntethase catalyzes FMN from riboflavin, and FAD is adenylated from FMN by FAD synthetase [35]. The gene sequences of *ribG*, *ribC*, *ribA*, and *ribH* constitute the operon *ribGCAH* also known as *riboCg*. [5].

Strains developed to improve riboflavin production are the filamentous fungi, *Ashbya gossypii*, and the bacterium *Bacillus subtilis* [28]. The strains were genetically modified by overexpression of the riboflavin operon, and modification of the carbon metabolism to increase the precursors, such as ribulose 5P and GTP, of riboflavin [36].

1.2.2 Riboflavin production pathway in *C. glutamicum*

Today, *C. glutamicum* is investigated as a compatible strain for riboflavin production [5], and the study by Pérez-García et al. (2022) [5], present a achieved riboflavin titer of 1.291 g/L by overexpressing the riboflavin operon *riboCg*. Inside of *C. glutamicum*, the riboflavin pathway is connected to the purine pathway (PP) and the oxidative pentose phosphate pathway (oxidative PPP). PP is further connected to the reductive pentose phosphate pathway (reductive PPP). The precursors for the reductive PPP and oxidative PPP are the intermediate, glucose 6-phosphate (glucose 6P), in the glycolysis [37] [38]. Glucose, which is the substrate of glycolysis, is a possible feedstock for *C. glutamicum*. All the pathways connecting the feedstock glucose with the riboflavin product in *C. glutamicum*, is shown in Figure 1.3

The reaction pathway from glucose to riboflavin depicted in Figure 1.3 starts with phosphorylation of glucose to glucose 6P by hexokinase, and the energy carrier ATP is phosphorylated to ADP [41]. From glucose 6P, 6-phosphogluconolacetone is oxidized by G6PDH (glucose-6-phosphate dehydrogenase) when glucose 6P enters the oxidative PPP. At the same time, the coenzyme $NADP^+$ is reduced to NADPH. 6-phosphogluconolacetone is further hydrolyzed to 6-phosphogluconate by 6PGL (6-phosphogluconolactonase) before 6-phosphogluconate is decarboxylated oxidatively to ribulose 5P by 6PGDH (6- phosphogluconate dehydrogenase) in the presence of $NADP^+$ [40]. Further, ribulose 5P is transported into both the riboflavin biosynthesis pathway and the reductive PPP [37]. RPI (ribose-5-phosphate isomerase) isomerizes ribulose 5P to ribose 5P in the reductive PPP. Ribose 5P is the precursor of the PP, and PRPP synthetase (phosphoribosyl diphosphate

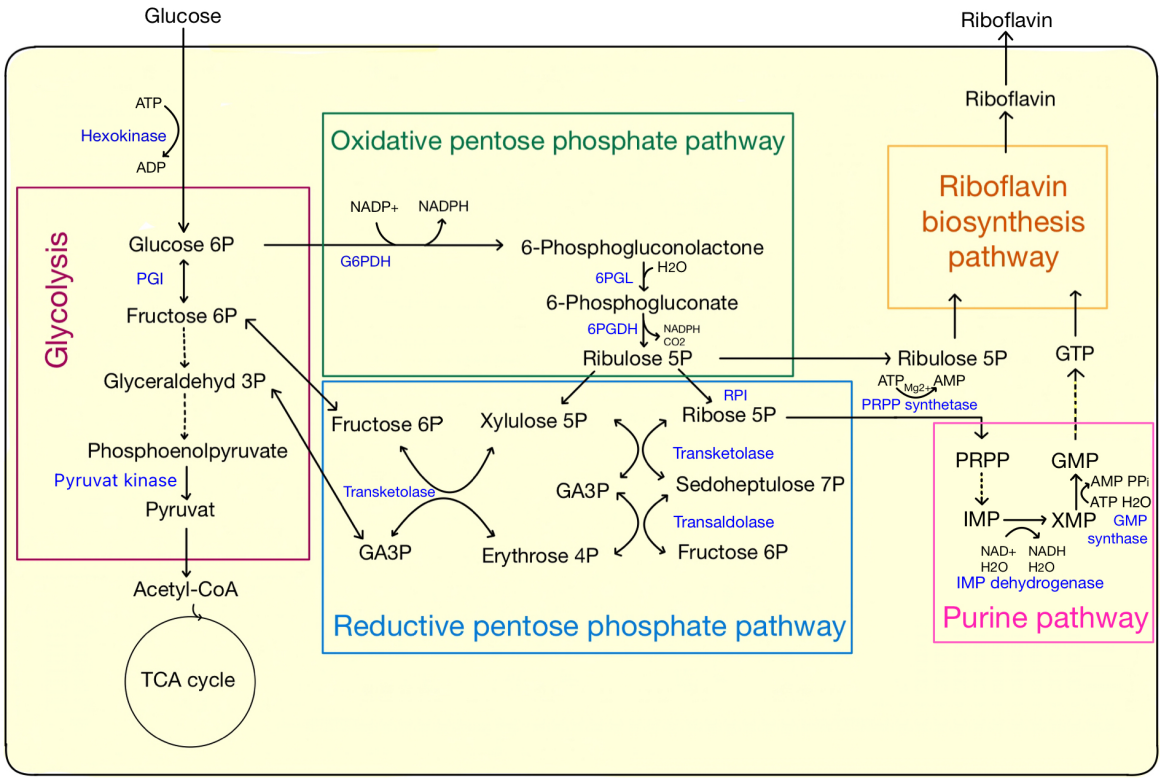

Figure 1.3: In the production of riboflavin from the feedstock glucosis in *C. glutamicum*, several metabolic pathways are connected [37] [38] [39] [40] [41] [42]. The glycolysis is shown in red color, oxidative PPP in green, reductive PPP in blue, PP in pink and riboflavin biosynthesis pathway in yellow color. Substrates, intermediates, and products of the different pathways are in black color, and the enzymes are in dark blue color. Cofactors utilized in the reactions are marked in black beside the reaction arrows. The enzymes are hexokinase, phosphoglucose isomerase (PGI), pyruvate kinase (PK), glucose-6-phosphate dehydrogenase (G6PDH), 6-phosphogluconolactonase (6PGL), 6-phosphogluconate dehydrogenase (6PGDH), ribose-5-phosphate isomerase (RPI) and PRPP synthetase, inosine monophosphate dehydrogenase (IMP dehydrogenase), GMP synthase, transketolase and transaldolase [43]. The substrates, intermediates, and products are glucose, glucose 6-phosphate (glucose 6P), fructose 6-phosphate (fructose 6P), glyceraldehyde 3-phosphate (glyceraldehyde 3P), phosphoenolpyruvate, pyruvate, 6-phosphogluconolacetone, 6-phosphogluconate, ribulose 5-phosphate (ribulose 5P), phosphoribosyl diphosphate (PRPP), inosine monophosphate (IMP), xanthine monophosphate (XMP), guanosine monophosphate (GMP), guanosine triphosphate (GTP), glyceraldehyde 3-phosphate (GA3P), xylulose 5-phosphate (xylulose 5P), erythose 4-phosphate (erythose 4P) and sedoheptulose 7-phosphate (sedoheptulose 7P) [43].

synthetase) phosphorylate ribose 5P to PRPP (phosphoribosyl diphosphate) [39] using the energy carrier ATP [43]. Through multiple steps, IMP (inosine monophosphate) is catalyzed and from IMP, XMP (xanthine monophosphate) is oxidized as NAD^+ is reduced to NADH by IMP dehydrogenase. XMP is phosphorylated by GMP (guanosine monophosphate) synthetase yielding GMP, which is further phosphorylated to GTP (guanosine triphosphate) through two steps. GTP is the precursor together with ribulose 5P for the riboflavin biosynthesis pathway.

In genetically engineered strains of *C. glutamicum* where the flux of glucose 6P into the oxidative PPP is increased, the strains tends to grow slower [37]. The increased flux of glucose 6P out of the glycolysis results in less production of acetyl-CoA, and less acetyl-CoA entering the TCA cycle for energy production. Cell growth requires energy produced in the electron transport chain, and the main compounds for the electron transport chain are produced in the TCA cycle [44]. Therefore, *C. glutamicum* strains that overexpress the riboflavin operon may show slower growth than the *C. glutamicum* wild-type strain.

1.3 Roseoflavin

Roseoflavin is an analog of riboflavin with antimicrobial activity [45]. The roseoflavin structure is similar to the riboflavin structure, Figure 1.4. The difference between the structures is an additional dimethyl amine group in roseoflavin, marked red in Figure 1.4. The similar structures make riboflavin transporters in bacteria able to import roseoflavin into the cytosol of the bacteria [46]. Due to roseoflavins antimicrobial activity, Gram-positive bacteria and Gram-negative bacteria, where roseoflavin is imported into the cells, are affected by roseoflavins toxic properties [47] [2]. As Gram-positive bacteria appear to contain many riboflavin transporters, Gram-positive bacteria are the main targets of roseoflavin [48] [49]. ImpX, RibM, RibN, RibZ, RfuABCD, RibXYZ, RfnT, and RibU are known riboflavin importers found in the bacteria of *Fusobacterium nucleatum*, *Streptomyces dawavensis*, *Rhizobium leguminosarum*, *Clostridium*, *Treponema pallidum*, *Chloroflexus aurantiacus*, *Ochrobactrum anthropi*, and *Lactococcus lactis*, respectively [48]. Hence, as these bacteria import riboflavin, they have also been found to import roseoflavin due to the similar structures of the two compounds [48]. Inside Gram-positive bacteria, promiscuous flavokinase enzymes catalysis roseoflavin mononucleotide (RoFMN) and FAD synthetase catalysis adenine dinucleotide (RoFAD) from roseoflavin. The production of RoFMN and RoFAD inside the bacteria abolishes flavoprotein's function since RoFMN and RoFAD replace FMN and FAD in the binding sites of flavoproteins. The flavoproteins function is crucial for cell function and cell growth, resulting in roseoflavin's toxic properties (see subsection 1.2 for flavoproteins functions). Another target of RoFMN is the FMN riboswitch. RoFMN feedback inhibits riboflavin production during binding to the FMN riboswitch [2]. The binding occurs at the aptamer portion which is the receptor domain in the FMN riboswitch during transcription by cellular RNA polymerases [47]. FMN riboswitches regulate the expression of the genes in the biosynthesis and in the transport of riboflavin after sensing the FMN level [47] [45]. When RoFMN binds to the riboswitches binding site, replacing FMN, the riboflavin production stops [50]. Since all bacteria depend on the flavoprotein function and many bacteria have FMN riboswiches, roseoflavin is considered an antimicrobial compound of a broad spectrum [45].

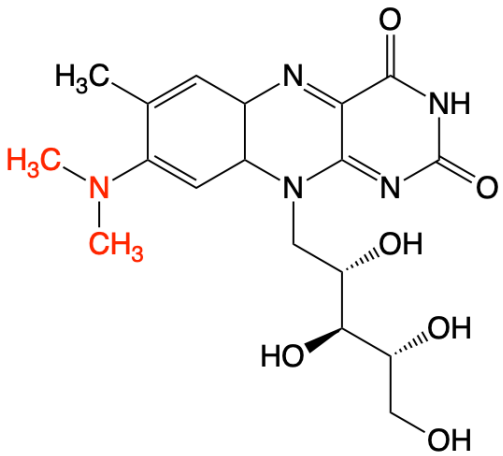

Figure 1.4: The chemical structure of roseoflavin. The dimethyl amine group, marked in red, distinguishes the roseoflavin structure from the riboflavin structure.

Today, roseoflavin is used to select roseoflavin-resistant strains in the food industry by inhibiting the growth of different bacteria and protozoa parasites [45]. Bacteria, whose growth is inhibited by

roseoflavin are *Staphylococcus aureus*, *Streptococcus pyogenes*, *Enterococcus faecalis*, and *Listeria monocytogenes*. Additionally, the protozoal parasites where the growth is affected by roseofalvin are *Leishmania mexicana*, *Trypanosoma brucei* and *Trypanosoma cruzi* [45]. Riboflavin is overproduced in the roseoflavin-resistant strains to increase the riboflavin content in the food. The roseoflavin-resistant strains contain mutations which lead to an enhanced expression of riboflavin biosynthetic genes and thus to riboflavin overproduction. *Lactobacillus plantarum* is an example of a roseoflavin-resistant strain used for pasta production and sourdough fermentation [45].

1.3.1 Production of roseoflavin in industry

The current production method of roseoflavin is chemical synthesis. Through several steps starting from N,N-dimethyl-o-toluidine, a small yield of approximately 5% roseoflavin is achieved [45]. Nitrating N,N-dimethyl-o-toluidine results in the formation of 2-dimethylamino-4-nitrotoluene. In the presence of Raney nickel, 2-dimethylamino-4-nitrotoluene is further reduced by hydrazine to 2-dimethyl-amino-4-aminotoluene, before it is condensed with D-ribulose and pressure hydrogenated in the presence of Raney nickel to 2-dimethylamino-4-o-ribitylaminotoluene [45]. Further, it is condensed with violuric acid, acetylated, recrystallized and hydrolyzed with NaOH, producing roseoflavin as the final product [45]. In addition to a small yield of roseoflavin, the compounds hydrazine and Raney nickel are hazardous [3] [51], meaning that the production method of roseoflavin is not sustainable. Moreover, the chemical compounds utilized in the synthesis are expensive [52], resulting in a costly roseoflavin product [45]. The price of roseoflavin in the market can reach up to 137 Euros per mg of roseoflavin [4], making alternative production methods of roseoflavin desirable.

1.3.2 Bioproduction of roseoflavin from riboflavin

The two bacteria known to naturally produce roseoflavin are *Streptomyces davawensis* (*S. davawensis*) and *Streptomyces cinnabarinus* (*S. cinnabarinus*). They both are Gram-positive, filamentous, and resistant to roseoflavin [45]. In Figure 1.5 the production pathway of roseoflavin, starting from riboflavin, in *S. davawensis* and *S. cinnabarinus*, is illustrated [45].

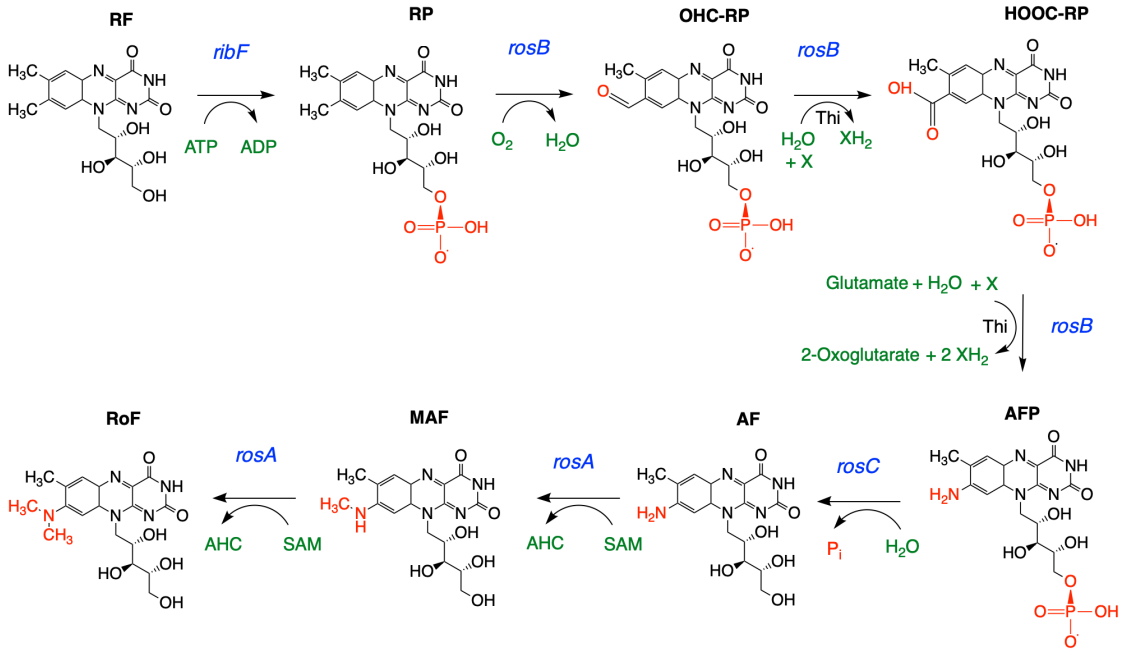

Figure 1.5: The roseoflavin biosynthesis pathway, starting from riboflavin. The chemical structures in the reaction pathway are shown with corresponding abbreviated names in black bold writing. The genes encoding for the enzymes catalyzing the reactions are colored blue, and the cofactors and energy carriers are colored green. The changes in the chemical structures are marked red. The abbreviated name, RF: riboflavin, RP: FMN which is also called riboflavin-5´phosphate, OHC-RP: 8-demethyl-8-formyl FMN, HOOC-RP: 8-demethyl-8-carboxyl FMN, AFP: 8-demethyl-8-amino-riboflavin-5´-phosphate, AF: 8-demethyl-8-amino-riboflavin, MAF: 8-demethyl-8-methylamino-riboflavin, RoF: roseoflavin, SAM: S-adenosylmethionine, and AHC: S-adenosylhomocysteine.

The genes in Figure 1.5 code for different enzymes. The enzyme bifunctional riboflavin kinase also known as FMN adenylyltransferase is encoded by *ribF*. *RibF* phosphorylates riboflavin which produces riboflavin- 5' phosphate, using ATP as the phosphate donor [53]. *RosB* codes for the enzyme complex 8-demethyl-8-amino-riboflavin-5´-phosphate synthase. In three steps it catalyzis the production of the toxic compound AFP (8-demethyl-8-amino-riboflavin-5´-phosphate). The first reaction produces the intermediate OHC-RP (8-demethyl-8-formyl FMN) in the presence of oxygen [2]. The second reaction producing HOOC-RP (8-demethyl-8-carboxyl FMN) requires thiamine (Thi), water, and an unknown hydrogen acceptor. Glutamate, water, and the unknown hydrogen acceptor are needed in the third reaction producing AFP [2] [45]. The enzyme AFP phosphatase is encoded by *rosC*. *RosC* dephosphorylates AFP to AF (8-demethyl-8-amino-riboflavin) in the presence of water [53]. Through two steps, the enzyme SAM-dependent dimethyltransferase, encoded by *rosA* produces roseoflavin. First, AF is methylated to MAF (8-demethyl-8-methylamino-riboflavin), before the second methylation results in the production of RoF (roseoflavin). As a side reaction in both steps, S-adenosylmethionine (SAM) is demethylated to S-adenosylhomocysteine (AHC) [2].

The natural producers *S. davawensis* and *S. cinnabarinus* are not used in industrial production. They adhere to surfaces and grow as aggregates, resulting in difficulties when the bacteria are grown in bioreactors [45]. Hence, it is hard to produce roseoflavin in bioprocesses, and therefore a more suitable microbial host as *C. glutamicum* is of great interest.

1.3.3 Genetic adaptions in *S. davawensis* to study the riboflavin and roseoflavin import and export

S. davawensis has several defense mechanisms, making the bacteria resistant to roseoflavin. A membrane protein, encoded by the gene *ribM*, transports riboflavin into the cells, and roseoflavin out of the cells [54]. Another mechanism is the tight bindings between AFP and roseoflavin, and roseoflavin and the enzymes encoded by *rosA* and *rosB* [55] [45]. The tight bindings prevent roseoflavin and AFP from binding to the flavoproteins. The last mechanism is the FMN riboswitch in *S. davawensis* which is non-sensible to RoFMN, making the riboflavin production unaffected by high roseoflavin concentrations [46] [45].

Several genetic adaptions regarding the import and export systems of riboflavin and roseoflavin were carried out in the roseoflavin producer *S. davawensis* in the study of Schneider et al. (2021) [49]. A riboflavin biosynthetic operon *ribE1MAB5H* was deleted resulting in riboflavin auxotrophic strains of *S. davawensis*. The operon *ribE1MAB5H* harbored the riboflavin transporter gene, *ribM*, which was assumed to be the only riboflavin importer. The deletion strain was not able to grow on media without riboflavin. Hence, a second riboflavin import system was hypothesized to be present. The former genes *rosXY* were found to encode a riboflavin importer and not a roseoflavin exporter and renamed as *ribXY* [48] [49]. The discovery was made through overexpression of *ribXY* in the roseoflavin sensitive bacteria, *S. coelicolor*, where the bacteria was roseoflavin resistant in the presence of riboflavin. This suggested that *ribXY* was importing riboflavin, not transporting roseoflavin. In addition, deletion of *ribXY* in *S. davawensis* did not affect the intracellular roseoflavin levels making it less likely for *ribXY* to be a roseoflavin exporter [49]. The riboflavin uptake system encoded by *ribXYZ* belongs to the taurine uptake family of ABC transporters [56]. The system consists of the genes *ribY* encoding for an extracellular substrate-binding component, *ribX* the trans-membrane protein, and *ribZ* the intracellular ATP-binding component [56]. The overexpression of *ribM* in the roseoflavin sensitive *S. coelicolor* only led to roseoflavin resistance when riboflavin was present [49], meaning that *ribM* was not a roseoflavin exporter without the presence of riboflavin. As a roseoflavin exporter, it should have protected *S. coelicolor* against the roseoflavin in the absence of riboflavin. Hence, riboflavin was suggested of being an agonist, accumulating and protecting cells from roseoflavins toxic effects in the study [49].

1.3.4 A *rosC* gene in *C. glutamicum*

The roseoflavin pathway is complete when the genes *ribF*, *rosA*, *rosB*, and *rosC* are present [45]. The enzyme AFP phosphatase encoded by *rosC* dephosphorylate AFP to AF in the roseoflavin pathway [53]. In the genome of *S. davawensis*, *rosC* is observed downstream of *rosA*. Previous, *rosC* has been misnamed in the Japanese KEGG database as phosphoglycerate mutase listed as BN159_8033 [57], while *rosC* (GeneBank CCK32411.1) is listed as BN159_8033 for the AFP phosphatase in the Genbank [57]. In Rudberg's study [1], the FASTA sequence of BN159_8033 was compared against the protein database of wild-type *C. glutamicum* ATCC 13032 in a BLASTp search, achieving the results in Figure 1.6.

The results from Rudberg's study in Figure 1.6 reviled that in the protein database of *C. glutamicum* WT, the protein in the histidine phosphatase family had 34% and 30% identical protein sequences compared to the protein sequence of the *rosC* gene. The protein phosphoglycerate

Description	Scientific Name	Max Score	Total Score	Query Cover	E value	Per. Ident	Acc. Len
Phosphoglycerate mutase/fructose-2,6-bisphosphatase [Corynebacterium glutamicum ATCC ...	Corynebacterium glutamicum ATCC ...	53.5	53.5	51%	1e-09	33.59%	214
histidine phosphatase family protein [Corynebacterium glutamicum]	Corynebacterium glutamicum	53.5	53.5	51%	1e-09	33.59%	233
histidine phosphatase family protein [Corynebacterium glutamicum]	Corynebacterium glutamicum	46.6	46.6	72%	3e-07	29.61%	236

Figure 1.6: The proteins, organsims, and the blast parameter of the BLASTp search from Rudberg's study [1]

mutase/fructose-2,6-bisphosphatase was 34% identical. AFP phosphatase encoded by *rosC* can not be identified as identical to the proteins phosphoglycerate mutase/fructose-2,6-bisphosphatase or the protein in the histidine phosphatase family since the values of the BLAST parameters, max score, query cover and e-value are not sufficiently high/low [58] [59] [60] [61]. Nevertheless, the values indicates the existence of an enzyme in *C. glutamicum* with similar catalytic function as AFP phosphatase has in *S. davawensis*.

1.4 Objectives

This study seeks to establish and optimize roseoflavin bioproduction, using microbial strain engineering techniques for competent roseoflavin production in the research platform of *C. glutamicum*. The main goal of this work was divided into the following specific objectives:

- Construction of optimized roseoflavin producing strains of *C. glutamicum* using the biosyntetic genes from *S. davawensis*.
- Evaluation of cell growth and productivity of newly roseoflavin producers through growth experiments and HPLC analysis.
- Assessment of flavin transport proteins encoded by *S. davawensis* and *C. glutamicum* for the optimization of roseoflavin production.
- Determination of a roseoflavin inhibitory constant through antimicrobial tests.

2 Materials and methods

2.1 Overview of methods

Figure 2.1 illustrates the main workflow used during this thesis. The methods will be further explained in the next sections. Extraction separated the plasmid (pVWEx1) from the rest of the cellular material of *Escherichia coli* (*E. coli*). To cut and linearize the plasmids, digestion was utilized. The wanted genes, *rosA*, *rosB*, *rosC*, *ribM* and *ribF* were amplified from *S. davawemsi*'s genomic DNA by polymerase chain reaction (PCR). Purification was used to purify the genes and the linearized plasmids. To clone the genes into the linearized plasmids, Gibson Assembly (Gibson) was used, resulting in the production of the recombinant plasmids, pVWEx1-*rosABC*, pVWEx1-*rosABC-ribM*, and pVWEx1-*ribF-rosABC-ribM*, containing the genes *rosABC*, *rosABC-ribM* and *ribF-rosABC-ribM*, respectively. Transformation was used to insert the recombinant plasmids into *E. coli* competent cells and colony PCR was used to verify positive clones. Plasmid extraction was utilized on the positive clones to separate the recombinant plasmids before the recombinant plasmids were transformed into *C. glutamicum* competent cells containing the pSym-*riboCg* plasmid. The result was the three new strains, *C. glutamicum*(pSym-*riboCg*)(pVWEx1-*rosABC*), *C. glutamicum*(pSym-*riboCg*)(pVWEx1-*rosABC-ribM*), and *C. glutamicum*(pSym-*riboCg*)(pVWEx1-*ribF-rosABC-ribM*). To see if the genes *rosC*, *ribM* and *ribF* increased the roseoflavin production in the newly constructed strains, two growth experiments were carried out. To analyze the components excreted from the strains of *C. glutamicum* in the growth experiments, high-pressure liquid chromatography (HPLC) was utilized. Gel electrophoresis was used to control that PCR, colony PCR, and digestion, went as anticipated. To measure the concentration of the solutions after extraction and purification a microvolume spectrophotometer was used.

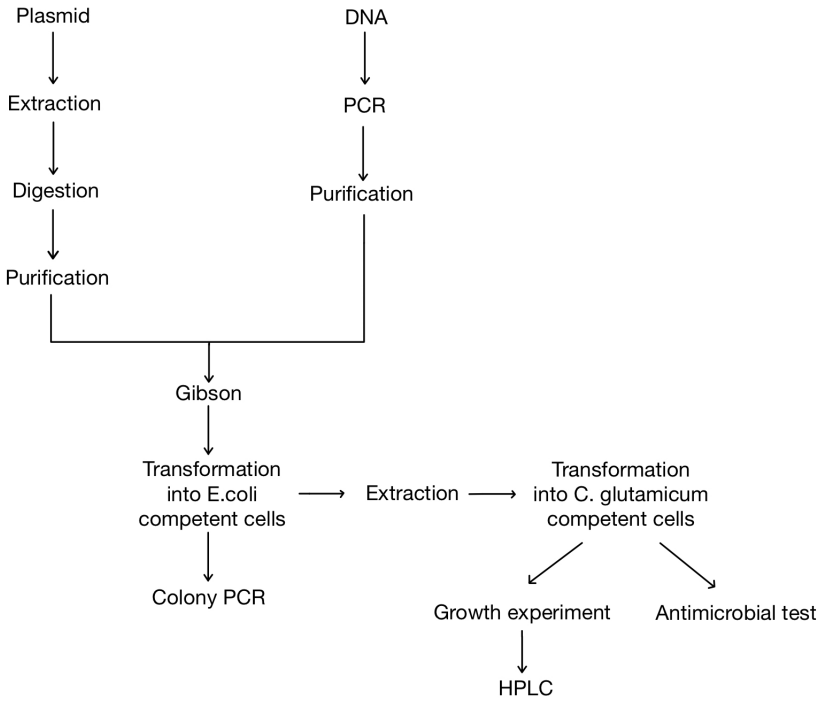

Figure 2.1: The methods used to construct plasmids and strains for growth experiments and antimicrobial tests are presented as a flow chart.

For the construction of strains utilized in the antimicrobial tests, the pVWEx1 plasmid with the gene inserts, *ribX* or *ribM*, were extracted from *E. coli* strains harboring them. The plasmids were each transformed into *C. glutamicum* wild-type strain, and a *C. glutamicum* strain harboring the riboflavin operon *riboCg*, before the antimicrobial tests were conducted.

2.2 Media, buffers and different solutions

Preparation of all cultural media, buffers, antibiotics, and salt solution utilized in this study thesis, are found in Appendix A.

2.3 Strains, plasmids and culture conditions

The plasmids utilized and constructed in this project are shown in Table 2.1. Constructed by Dr. Pérez-García, the plasmids pVWEx1-*ribM*, and pVWEx1-*ribX* were utilized in the antimicrobial test. The plasmid, pVWEx1 was modified to contain either the genes *rosABC*, the genes *rosABC-ribM*, or the genes *ribF-rosABC-ribM*. Several attempts without luck were made to construct the plasmid harboring the genes *ribF-rosABC*. The modified plasmids, pVWEx1-*rosABC*, pVWEx1-*rosABC-ribM*, pVWEx1-*ribF-rosABC* and pVWEx1-*ribF-rosABC-ribM* are shown in Figure 2.2.

Table 2.1: The name, description, and source of the plasmids used in this work.

Plasmid name	Description	Source
pVWEx1	KanR, C. glutamicum/E. coli shuttle plasmid (Ptac, lacI, pBL1 OriVCg)	Peters-Wendisch et al. (2001) [62]
pVWEx1-*rosAB*	Recombinant plasmid of pVWEx1 containing the genes *rosAB*	Rudberg's study [1]
pVWEx1-*rosABC*	Recombinant plasmid of pVWEx1 containing the genes *rosABC*	This work
pVWEx1-*rosABC-ribM*	Recombinant plasmid of pVWEx1 containing the genes *rosABC-ribM*	This work
pVWEx1-*ribF-rosABC-ribM*	Recombinant plasmid of pVWEx1 containing the genes *ribF-rosABC-ribM*	This work
pVWEx1-*ribM*	Recombinant plasmid of pVWEx1 containing the genes *ribM*	Pérez-García
pVWEx1-*ribX*	Recombinant plasmid of pVWEx1 containing the genes *ribX*	Pérez-García

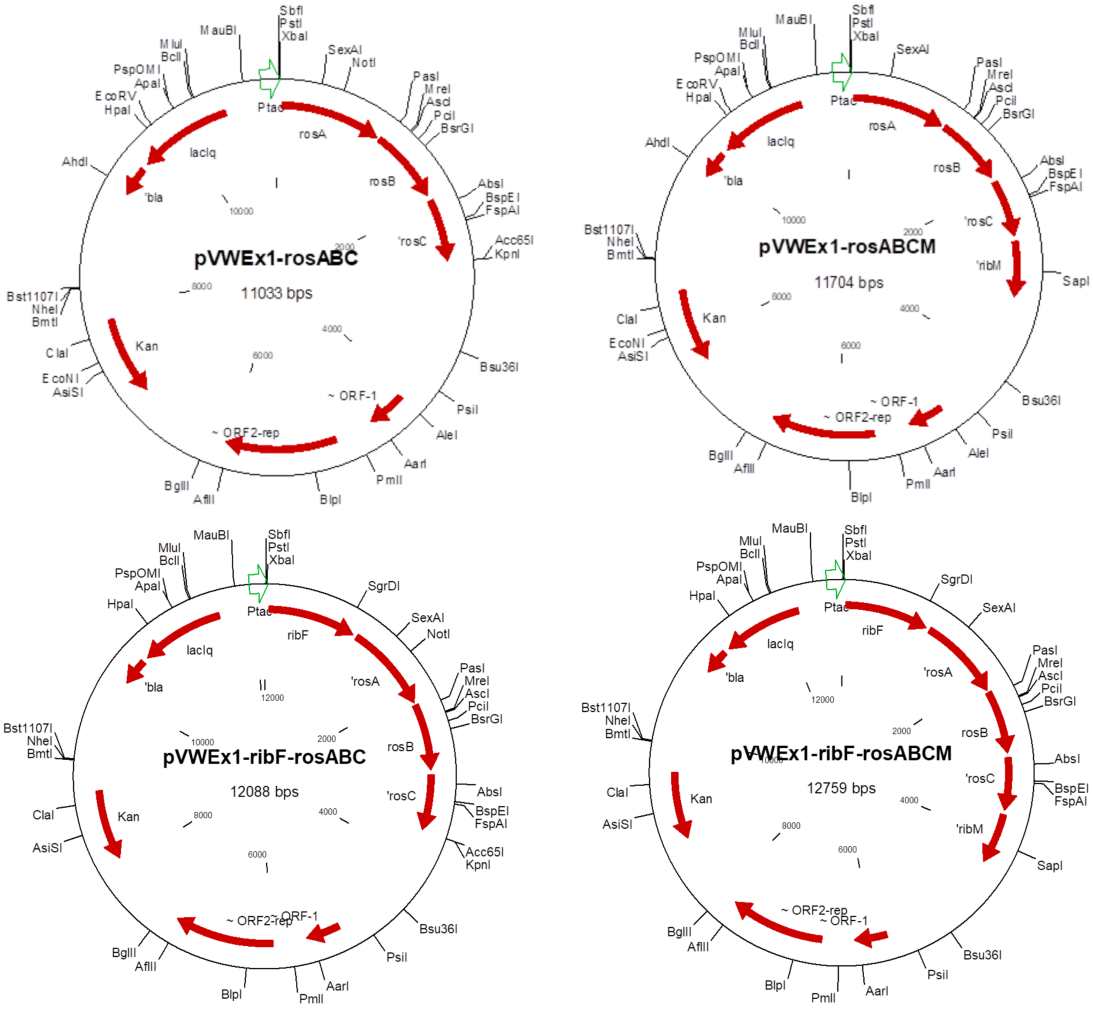

Figure 2.2: To the top left and right, are pVWEx1-*rosABC* and pVWEx1-*rosABC-ribM* illustrated, respectively. On the bottom left, pVWEx1-*ribF-rosABC* is illustrated, and to the bottom right, pVWEx1-*ribF-rosABC-ribM* is illustrated. The green arrow represents the IPTG inducible promotor, P_{tac}. The genes are represented by red arrows. Among the genes is the gene sequence for kanamycin resistance and the inserted genes, *ribF*, *rosA*, *rosB*, *rosC*, and *ribM*.

The length of pVWEx1-*rosABC*, pVWEx1-*rosABC-ribM*, pVWEx1-*ribF-rosABC*, and pVWEx1-*ribF-rosABC-ribM* in Figure 2.2 are 11 kb, 12 kb, 12 kb, and 13 kb, respectively. The tac promotor (P_{tac}) made the inserted genes inducible when isopropyl-β-D-1-thiogalactopyranoside (IPTG) was added. After the tac promotor, there is a multiple cloning site where DNA fragments can be inserted. To make the strains containing the pVWEx1 plasmids selective in growth media, the plasmids were made resistant to kanamycin by containing the gene *Kan*. To stop the transcription of the genes, a terminator sequence was located after *rosC* in pVWEx1-*rosABC* and pVWEx1-*ribF-rosABC*, and after *ribM* in pVWEx1-*rosABC-ribM* and pVWEx1-*ribF-rosABC-ribM*. The terminator sequence is not shown.

Table 2.2 shows the strains utilized and produced in this research. The cloning host was *E. coli* DHSα and the working horse for roseoflavin production was a strain of *C. glutmicum* constitutive overexpressing the riboflavin operon. The plasmids pVWEx1, pVWEx1-*rosABC*, pVWEx1-*rosABC-ribM*, and pVWEx1-*ribF-rosABC-ribM* were transformed into *C. glutamicum* cells

which already overexpressed the riboflavin operon by containing the plasmid, pSym-*riboCg*. The transformation constructed the strains *Cg*(pSym-*riboCg*)(pVWEx1), *Cg*(pSym-*riboCg*)(pVWEx1-*rosABC*), *Cg*(pSym-*riboCg*)(pVWEx1-*rosABC-ribM*), and *Cg*(pSym-*riboCg*)(pVWEx1-*ribF-rosABC-ribM*). Hereafter will the strains *Cg*(pSym-*riboCg*)(pVWEx1), *Cg*(pSym-*riboCg*)(pVWEx1-*rosABC*), *Cg*(pSym-*riboCg*)(pVWEx1-*rosABC-ribM*), and *Cg*(pSym-*riboCg*)(pVWEx1-*ribF-rosABC-ribM*) be referred to as Roseo0, Roseo1, Roseo2, and Roseo3. The plasmids pVWEx1, pVWEx1-*ribM*, and pVWEx1-*ribX* were each transformed into *C. glutamicum* wild-type and *C. glutamicum* strains harboring the *riboCg* operon. From the transformation, the strains *Cg*(pVWEx1), *Cg*(pVWEx1-*ribM*), *Cg*(pVWEx1-*ribX*), *Cg*(pSym-*riboCg*)(pVWEx1), *Cg*(pSym-*riboCg*)(pVWEx1-*ribM*), and *Cg*(pSym-*riboCg*)(pVWEx1-*ribX*), were constructed. The strains are further referred to as Transport0, Transport1, Transport2, Transport3, Transport4, and Transport5.

Table 2.2: The names, descriptions, and sources of the strains utilized in this work. The most used strains have been given abbreviated names.

Strains name	Abbreviated name	Description	Source
Corynebacterium glutamicum	Cg	Wild-type strain ATCC 13032, auxotrophic for biotin	Abe et al. (1967)[63]
Cg(pECXT-Psyn-*ribGCAH*)	Cg(pSym-riboCg)	*C. glutamicum* containing the plasmid (pECXT-Psyn-*ribGCAH*) further named (pSym-*riboCg*)	Pérez-García et al. (2022)[5]
Escherichia coli DHSα		DH5α Strain: Δ lacU169 (σ 80*lacZ* Δ M15), *supE*44, *hsdR*17, *recA*1, *endA*1, *gyrA*96, *thi* − 1, *relA*1	Hanahan (1983)[5]
E. coli(pVWEx1-*rosABC*)		*E. coli* harboring the plasmid (pVWEx1-*rosABC*)	This work
E. coli(pVWEx1-*rosABC-ribM*)		*E. coli* harboring the plasmid (pVWEx1-*rosABC-ribM*)	This work
E. coli(pVWEx1-*ribF-rosABC-ribM*)		*E. coli* harboring the plasmid (pVWEx1-*ribF-rosABC-ribM*)	This work
Cg(pSym-*riboCg*)(pVWEx1)	Roseo0/Transport3	*C. glutamicum* harboring the plasmids (pSym-*riboCg*) and (pVWEx1)	This work
Cg(pSym-*riboCg*)(pVWEx1-*rosABC*)	Roseo1	*C. glutamicum* harboring the plasmids (pSym-*riboCg*) and (pVWEx1-*rosABC*)	This work
Cg(pSym-*riboCg*)(pVWEx1-*rosABC-ribM*)	Roseo2	*C. glutamicum* harboring the plasmids (pSym-*riboCg*) and (pVWEx1-*rosABC-ribM*)	This work
Cg(pSym-*riboCg*)(pVWEx1-*ribF-rosABC-ribM*)	Roseo3	*C. glutamicum* harboring the plasmids (pSym-*riboCg*) and (pVWEx1-*ribF-rosABC-ribM*)	This work
Cg(pSym-*riboCg*)(pVWEx1-*rosAB*)	Roseo4	*C. glutamicum* harboring the plasmids (pSym-*riboCg*) and (pVWEx1-*rosAB*)	Rudberg's study[1]
Cg(pSym-*riboCg*)(pVWEx1-*rosAB-ribM*)	Roseo5	*C. glutamicum* harboring the plasmids (pSym-*riboCg*) and (pVWEx1-*rosAB-ribM*)	Rudberg's study[1]
E. coli(pVWEx1-*ribM*)		*E. coli* harboring the plasmid (pVWEx1-*ribM*)	Pérez-García (To be published)
E. coli(pVWEx1-*ribX*)		*E. coli* harboring the plasmid (pVWEx1-*ribX*)	Pérez-García (To be published)
Cg(pVWEx1)	Transport0	*C. glutamicum* harboring the plasmid (pVWEx1)	This work
Cg(pVWEx1-*ribM*)	Transport1	*C. glutamicum* harboring the plasmid (pVWEx1-*ribM*)	This work
Cg(pVWEx1-*ribX*)	Transport2	*C. glutamicum* harboring the plasmid (pVWEx1-*ribX*)	This work
Cg(pSym-*riboCg*)(pVWEx1-*ribM*)	Transport4	*C. glutamicum* harboring the plasmids (pSym-*riboCg*) and (pVWEx1-*ribM*)	This work
Cg(pSym-*riboCg*)(pVWEx1-*ribX*)	Transport5	*C. glutamicum* harboring the plasmids (pSym-*riboCg*) and (pVWEx1-*ribX*)	This work

E. coli strains were routinely grown overnight at 37°C on lysogeny broth (LB) agar plates or in liquid LB media. Strains of *C. glutamicum* were frequently grown at 30°C overnight in brain heart infusion (BHI) or on 2TY agar plates. During growth experiments, *C. glutamicum* strains were grown in CGVII minimal medium. Here, the *C. glutamicum* strains were inoculated to an optical density (OD) of 1, with OD measurements taken at a wavelength of 600 nm. The OD measurements are further explained in subsubsection 2.7.3. For growth experiments, glucose was

used as the carbon source at a concentration of 1%. Cultivation of *C. glutamicum* strains in liquid media, during the growth experiments, were performed in shake flasks at a speed of 155 rpm at 30 °C, and the incubator was set accordingly.

When growing the strains containing pVWEx1- or pSym- plasmids, the antibiotics kanamycin (12.5 µL/mL of media) or tetracyclin (12.5 µL/mL of media) were added to the growth media. For strains containing both plasmids, both antibiotics were added. The pVWEx1 plasmids provide resistance to kanamycin, while the pSym plasmids provide resistance to tetracycline, thereby enabling the selection and growth of strains containing these plasmids in the culture media.

2.4 Molecular cloning

2.4.1 Primers

To amplify the genes *rosA*, *rosB*, *rosC*, *ribM*, and *ribF* from the constructed plasmid pVWEx1-*rosAB*, the constructed plasmid pVWEx1-*rosABC-ribM*, genomic DNA of *S. davawensis*, and genomic DNA of *C. glutamicum*, the primers in Table 2.3 were used. The genomic DNA of *S. davawensis* (with DSM number, 101723) was ordered from the company DSMZ [64], and the genomic DNA of *C. glutamicum* was extracted by Dr. Pérez-García. The software Clone Manager V9 was utilized to create the primers. Before use, the primers were resuspended to 100 µL and diluted in a ratio of 1:10.

Table 2.3: The genes *rosAB*, *rosC*, *ribM*, and *ribX* were amplified from *S. davawensis* by the primers shown. Parts of the primers colored black represent overlapping sequences. Red-colored parts represent the ribosomal binding site and the blue-colored parts represent the annealing sequence. The parts colored green represent the linker sequences where genes were cloned together. The annealing temperatures are also shown.

Genes/ inserts	Template DNA	Primer name	Primer sequence 5'->3'	Annealing Temp. [°C]
rosAB	pVWEx1-*rosAB*	rosABC1	AGCTTGCATGCCTGCAGGTCGACTCTAGAGGAAAGGAGGCCCTTCAGATGCGGCCGGAACCGACCGAGC	64
		rosABC2	GAAAGCTCTCGCGTCCGTCACTCACCTGAAGGGCCTCCTTTCGGGGCGTTCGAATCAGCCGAGTTGGCTCTCCTCGAC	64
rosC1	*S. davawensis*	rosABC3	GGTCGAGGAGAGCCAACTCGGCTGATTCGAACGCCCCGAAAGGAGGCCCTTCAGGTGAGTGACGGACGCGAGAGCTTTC	64
		rosABC4	CAGTGAATTCGAGCTCGGTACCCGGGGATCTCAGATCACGTCGGACGGGGCCGCG	64
rosC2	*S. davawensis*	rosABCM1	AGGCCTCGGAGTTGAGCCAGTTCACCTGAAGGGCCTCCTTTCGGGGCGTTCGAATCAGATCACGTCGGACGGGGCCGCG	64
ribM	*S. davawensis*	rosABCM2	CGCGGCCCCGTCCGACGTGATCTGATTCGAACGCCCCGAAAGGAGGCCCTTCAGGTGAACTGGCTCAACTCCGAGGCC	71
		rosABCM3	CAGTGAATTCGAGCTCGGTACCCGGGGATCTCACGCGGGCGCTCCTTCCAGGACG	71
ribF	*C. glutamicum*	ribF-Fw	GCATGCCTGCAGGTCGACTCTAGAGGAAAGGAGGCCCTTCAGGTGGATATTTGGAGTGGACTAG	55
		ribF-Rv	TCGGTCGGTTCCGGCCGCATCTGAAGGGCCTCCTTTCGGGGCGTTCGAATTAAGCGCTGGGCTGGGTGTCG	55
rosABC	pVWEx1-*rosABC*	rosABC-Fv	ACACCCAGCCCAGCGCTTAATTCGAACGCCCCGAAAGGAGGCCCTTCAGATGCGGCCGGAACCGACCGAGC	70
		rosABC-Rv	AATTCGAGCTCGGTACCCGGGGATCTCAGATCACGTCGGACGGGGCC	70
rosABCM	pVWEx1-*rosABC-ribM*	rosABCM-Fv	ACACCCAGCCCAGCGCTTAATTCGAACGCCCCGAAAGGAGGCCCTTCAGATGCGGCCGGAACCGACCGAGC	70
		rosABCM-Rv	AATTCGAGCTCGGTACCCGGGGATCTCACGCGGGCGCTCCTTCCAGG	70

To amplify the genes *rosAB* from pVWEx1-*rosAB*, the primers rosABC1 and rosABC2 were used as forward and backward primers, respectively. *rosC* and *ribM* were amplified from the genomic DNA of *S. davawensis*. The primers rosABC3 and rosABC4 were used to amplify *rosC* for later construction of the pVWEx1-*rosABC* plasmid. To amplify *rosC* for the construction of the pVWEx1-*rosABCM* plasmid, the primers rosABC3 and rosABCM1 were used. The *ribM* gene was amplified by the use of the forward primer rosABCM2 and the backward primer rosABCM3. From genomic DNA of *C. glutamicum* *ribF* was amplified. *ribF* was amplified with ribF-Fw and rib-Rv as the forward and backward primer, respectively. From the constructed plasmids pVWEx1-*rosABC* and pVWEx1-*rosABC-ribM*, the genes *rosABC* and *rosABC-ribM* were amplified with the primers rosABC-Fv and rosABC-Rw, and rosABCM-Fv and rosABCM-Rw, respectively.

For colony PCR, general primes were used to amplify all the inserted genes as one unit. The general primers are listed in Table 2.4.

Table 2.4: The general primer sequence, name, and belonging annealing temperature used in colony PCR are listed.

Genes/ inserts	Primer name	Primer sequence 5'->3'	Annealing Temp. [°C]
rosABC	X1-Fw	CATCATAACGGTTCTGGC	57
rosABCM	X1-Rv	ATCTTCTCTCATCCGCCA	57

2.4.2 Polymerase chain reaction

Polymerase chain reaction (PCR) was used to amplify the genes *rosAB* from the plasmid pVWEx1-*rosAB*, *rosABC* from pVWEx1-*rosABC*, *rosABC-ribM* from pVWEx1-*rosABC-ribM*, *ribF* from the DNA of *C. glutamicum*, and the genes *rosC*, and *ribM* from the double-stranded DNA of *S. davawensis*. Each PCR solution contained the components in Table 2.5. For the gene amplification, the CloneAmp^{TM} HiFi PCR Premix Protocol-At-A-Glance [65] was followed and the machine Mastercycler nexus GX2 from Eppendorf AG was used. The thermal conditions for the PCR of the genes *rosAB*, *rosC*, *ribM*, *ribF*, *rosABC*, and *rosABC-ribM* are shown in Table 2.6, Table 2.7, Table 2.8, Table 2.9, Table 2.10, and Table 2.11 respectively. The annealing and extension steps varied for the genes.

Table 2.5: Components with corresponding volume in the PCR solutions.

Components	Volume [µL]
Deionized water	10.5
ClonAmp HiFi PCR Premix	12.5
Upstream primer	0.5
Downstream primer	0.5
DNA	1.0
Total volume	25.0

Table 2.6: Thermal conditions, cycles and the different steps for the HiFi Premix containing the genes *rosAB* [65].

Steps	Temperature [°C]	Time	Cycles
Denaturation	98	10 sec.	
Annealing	55	5 sec.	30-35
Extension	72	11 sec	

Table 2.7: Thermal conditions, cycles and the different steps for the HiFi Premix containing the genes *rosC* [65].

Steps	Temperature [°C]	Time	Cycles
Denaturation	98	10 sec.	
Annealing	50	15 sec.	30-35
Extension	72	6 sec.	

Table 2.8: Thermal conditions, cycles and the different steps for the HiFi Premix containing the genes *ribM* [65].

Steps	Temperature [°C]	Time	Cycles
Denaturation	98	10 sec.	
Annealing	60	5 sec.	30-35
Extension	72	5 sec.	

Table 2.9: Thermal conditions, cycles, and the different steps for the HiFi Premix containing the genes *ribF* [65].

Steps	Temperature [°C]	Time	Cycles
Denaturation	98	10 sec.	
Annealing	55	5 sec.	30-35
Extension	72	7 sec.	

Table 2.10: Thermal conditions, cycles and the different steps for the HiFi Premix containing the genes *rosABC* [65]. It was tried multiple different annealing temperatures, without luck, for the amplification.

Steps	Temperature [°C]	Time	Cycles
Denaturation	98	10 sec.	
Annealing	55/55/60/50	5/15/5/25 sec.	30-35
Extension	72	13 sec.	

Table 2.11: Thermal conditions, cycles and the different steps for the HiFi Premix containing the genes *rosABC-ribM* [65].

Steps	Temperature [°C]	Time	Cycles
Denaturation	98	10 sec.	
Annealing	60	5 sec.	30-35
Extension	72	17 sec.	

2.4.3 DNA isolation through extraction

From the bacterial culture of *E.coli*(pVWEx1), pVWEx1 plasmids were separated from the cells with extraction. The plasmid kit, ZR Plasmid Miniprep- Classic form ZYMO RESEARCH was used for the extraction, and the protocol [66] was followed. For the washing step, 20 µL of water was used instead of 30 µL DNA elution buffer. The bacterial culture was prepared the day before the extraction and contained LB medium (10 mL), kanamycin (5 µL), and *E.coli*(pVWEx1). The bacterial culture was incubated overnight at 37°C and 225 rpm. In addition, extraction of pVWEx1 plasmid with the different inserts was carried out.

2.4.4 Plasmid digestion

Digestion was used to linearize the circular plasmids. The digestion mix of 50 µL contained water, the extracted plasmids, CutSmart buffer, and BamHI-HF restriction enzyme. It was digested in a 37°C hot tube for 1.5 hours. The different amounts of components depended on the concentration of the extracted plasmids. Gel electrophoresis was used after the digestion to see if the cut was clear.

2.4.5 DNA purification

To purify the digested plasmids and the genes *rosA*, *rosB*, *rosC*, *ribM*, and *ribF* from similar DNA sequences and impurities, the QIAquick PCR purification Kit was used and the protocol was followed [67]. Instead of using Buffer EB for cleaning, 20 µL of water was used.

2.4.6 Gibson Assembly

Gibson Assembly is a cloning procedure allowing clonings of two or more fragments at the same time [68]. The Gibson method requires fewer steps than earlier methods, and restriction enzymes are unnecessary. The gene fragments in the Gibson method are designed by the user and contain overlapping homologous ends, which allows the gene fragments to attach to each other to form plasmids in one single round of cloning [68]. The Gibson Assembly® HiFi 1-Step Kit [68] was used, the protocol was followed, and the machine Mastercycler nexus GX2 from Eppendorf AG was used. The amount, size, and concentration of DNA fragments combined with the Gibson Assembly® Master Mix to produce the plasmids pVWEx1-*rosABC*, pVWEx1-*rosABC-ribM*, and pVWEx1-*ribF-rosABC-ribM* are shown in Table 2.12. The thermal conditions are shown in Table 2.13.

Table 2.12: Size, concentration, and volume of DNA fragments utilized in the Gibson procedure to produce the plasmids, pVWEx1-*rosABC*, pVWEx1-*rosABC-ribM*, and pVWEx1-*ribF-rosABC-ribM*. The volumes of the DNA fragments and deionized water were mixed with Gibson master mix.

Plasmids produced	DNA fragment	Size [bp]	Concentration [ng/µL]	Volume needed [µL]
pVWEx1-*rosABC*	pVWEx1	8396	48.3	2.07
	rosAB	1948	63.5	0.37
	rosC	735	48.5	0.19
Deionized water	-	-	-	2.38
pVWEx1-*rosABC-ribM*	pVWEx1	8396	48.3	2.07
	rosAB	1948	63.5	0.37
	rosC	877	38.3	0.25
	ribM	726	50.1	0.18
Deionized water	-	-	-	2.31
pVWEx1-*ribF-rosABCM-ribM*	pVWEx1	8396	22.0	4.55
	rosF	1117	75.5	0.18
	rosABC-ribM	3290	91.9	0.43
Deionized water	-	-	-	0

Table 2.13: Thermal condition for Gibson Assembly.

Temperature [°C]	Time [Min]
50	60
4	Infinite

2.4.7 Transformation of *E. coli* chemically competent cells

The plasmids were transformed into *E. coli* competent cells. *E. coli* competent cells were defrosted on ice and 10 µL of the Gibson solution, containing the plasmids, was added. The cell solution was incubated on ice for 10 minutes before heat shock at 42°C for 1.5 minutes. The cells were placed back on ice for 1 minute before 0.5 mL LB media was added and the cells were incubated at 37°C and 350 rpm for 1 hour. 100 µL of the cell solution was plated out on a 2TY agar plate containing kanamycin. The rest of the solution was centrifuged, the supernatant discarded, the cells were resuspended, and plated out on another plate. At 37°C, the plates were incubated overnight.

2.4.8 Colony PCR

Colony PCR was used to amplify the gene clusters, *rosABC*, *rosABC-ribM*, and *ribF-rosABC-ribM*, to control if the transformation of pVWEx1-*rosABC*, pVWEx1-*rosABC-ribM*, and pVWEx1-*ribF-rosABC-ribM* into *E. coli* competent cells went as anticipated. The colony PCR solution contained the components in Table 2.14. 24 small eppendorf tubes were used for each colony PCR. The thermal conditions used for the Mastercycler nexus GX2 machine, from Eppendorf AG, are shown in Table 2.15. The GoTaq® DNA Polymerase protocol [69] was used.

Table 2.14: Components with the corresponding volume in the colony PCR solutions.

Components	Volume [µL]
Deionized water	18.3
GoTax buffer	5.0
dNTPs	0.5
Upstream primer	0.5
Downstream primer	0.5
G2 GoTaq Polymerase	0.2
E. coli cells with pVWEx1-*rosABC*, pVWEx1-*rosABC-ribM*, or pVWEx1-*ribF-rosABC-ribM* from plate	-
Total volume	25.0

Table 2.15: Thermal conditions, time, and cycles used for the different steps in colony PCR are shown [69].

Steps	Temperature [°C]	Time [Min]	Cycles
Initial denaturation	95	10	1
Denaturation	95	1	25-35
Annealing	57	1	25-35
Extension	72	1 Min/kB	25-35
Extension	72	5	1
Soak	4	Infinite	1

2.4.9 Gel electrophoresis

To control that the digestion, PCR, and colony PCR went as anticipated, gel electrophoresis was used. Thermo Scientific™ GeneRuler 1 kb Plus DNA Ladder [70] and the sample was loaded into different wells in a solidified gel. The net charge of DNA is negative, leading the DNA to migrate towards the anode when an electric field is switched on, resulting in the separation of different DNA fragments. The conditions to create the electrical field were 100V and 400 mA. The recipe for the solidified gel is found in Appendix A. Depending on the length of the gel, the run time was 30 minutes for colony PCR and 37 minutes for PCR and digestion.

2.4.10 Sanger sequencing

To validate the accuracy of the molecular cloning process, sequencing analysis was utilized. Isolated expression plasmids from the cloning hosts were subjected to sequencing using the Eurofins Genomics LightRun tubes sequencing service. The specified requirements were followed: For sequencing, 5 µL of primer with a concentration of 5 µM was combined with 5 µL of purified template DNA. The purified template DNA had a concentration ranging from 50-100 ng/µL. The obtained sequencing results were then compared with the template sequence in silico using Clone Manager V9, a bioinformatics tool for scientific and educational purposes. Table 2.16 lists the template DNA and primers utilized in the samples sent to Eurofins Genomics LightRun tubes sequencing

service. The primers utilized are explained in subsubsection 2.4.1, and the primer rosAB3 is from Rudberg's study [1]. From colony PCR, two colonies in well 3 and well 18 were expected to contain pVWEx1-*rosABC*, and the colonies are marked in Table 2.16.

Table 2.16: DNA templates and primers sent to sequencing.

DNA tamplate	Primers
pVWEx1-*rosABC-ribM*	rosABC1
pVWEx1-*rosABC-ribM*	rosAB3 [1]
pVWEx1-*rosABC-ribM*	rosABC3
pVWEx1-*rosABC-ribM*	rosABCM3
pVWEx1-*rosABC-ribM*	X1-Fw
pVWEx1-*rosABC-ribM*	X1-Rv
Colony in well 3: pVWEx1-*rosABC*	rosABC3
Colony in well 3: pVWEx1-*rosABC*	rosAB3 [1]
Colony in well 3: pVWEx1-*rosABC*	X1-Fw
Colony in well 3: pVWEx1-*rosABC*	X1-Rv
Colony in well 18: pVWEx1-*rosABC*	rosABC1
Colony in well 18: pVWEx1-*rosABC*	rosAB3 [1]
Colony in well 18: pVWEx1-*rosABC*	X1-Fw
Colony in well 18: pVWEx1-*rosABC*	X1-Rv
pVWEx1-*ribF-rosABC-ribM*	ribF-FW
pVWEx1-*ribF-rosABC-ribM*	rosABCM-Rv
pVWEx1-*ribF-rosABC-ribM*	X1-Fw
pVWEx1-*ribF-rosABC-ribM*	X1-Rv

2.4.11 Microvolume spectrophotometer

The Nanodrop- Microvolume Spectrophotometer [71] was used to find the concentration and purity of the solution after extraction and purification.

2.5 Preparation of *C. glutamicum* electrocompetent cells

C. glutamicum-(pSym-*riboCg*) competent cells were prepared under sterile conditions. 5 mL BHI media containing 2.5 µL tetracycline was inoculated with *C. glutamicum*-(pSym-*riboCg*) overnight at 30°C. pSym-*riboCg* was the plasmid containing the ribCg operon. Into two flasks, 50 mL BHIS, and 2 mL of the overnight culture were added, and incubated at 30°C, for 2-4 hours, until the OD was measured to 0.6. 15 µL ampicillin (5 mg/mL) was added and incubated at 30°C for 1.5 hours in both flasks. Two falcon tubes were put on ice, the flask solution was transferred to the falcon tubes, and the falcon tubes were centrifuged at 4000 rpm for 7 min at 4°C. The supernatant was discarded before the cells were resuspended with 30 mL EPB1- buffer, and centrifuged with the same conditions. The last step was repeated two times. After the last centrifugation, 750 µL EPB2-buffer was transferred two one of the falcon tubes and the cells were resuspended. The resuspended solution was transferred to the second falcon tube, and the cells were resuspended. This made up the *C. glutamicum* competent cell solution. In 9-11 sterile Eppendorf tubes, 150 µL of the *C. glutamicum* competent cell solution was transferred and frozen at -80°C. Competent cells of *C. glutamicum* wild-type was prepared similar as for *C. glutamicum*-(pSym-*riboCg*), except that tetracycline was not added.

2.6 Transformation of *C. glutamicum* competent cells

C. glutamicum competent cells were defrosted on ice, and 1 mL BHIS medium was heated to 46°C. The competent cells were mixed with 800 ng of plasmids and transferred to an electroporation cuvette on ice. Electroporation was run after 5 minutes to create temporary pores in the cell membrane. The pores made it possible for plasmids to pass through the membrane and into the cells [72]. The electroporation was run with one single pulse at 200 Ω, 2.5 Kv, and 25 Fv, and the machine Geno Pulser Xcell from BIO RAD was used. The competent cell solution and preheated BHIS were mixed and incubated for 6 minutes at 46°C. The new solution was incubated at 30°C for 1 hour in a thermo-mixer. The cells were centrifuged for 3 minutes at 6000 rpm, and the supernatant was discarded. The cells were resuspended and plated out on selective media. The plates were incubated for 1-2 days at 30°C.

2.7 Growth experiments

Two growth experiments were carried out for the constructed strains of *C. glutamicum*. For the first growth experiment (Growth experiment 1), the growth curves of the constructed strains Roseo0, Roseo1, and Roseo2 were found. In the second growth experiment (Growth experiment 2), the growth curve of the newly constructed strain Roseo3, together with Roseo0, Roseo1, Roseo2, and the constructed strains, Roseo4 and Roseo5 from Rudberg's study [1], were found. The genes were induced in the exponential phase, six hours after the start of both growth experiments, based on the finding from Rudberg's study [1] that the highest roseoflavin production occurred under these conditions. Roseo0 harbored the empty plasmid, pVWEx1, and was used as a control strain in the growth experiments to enable a comparative assessment of growth and product yield between the other alternative strains.

2.7.1 Preculture preparation

For each of the different *C. glutamicum* strains, preculture was prepared in one sterile 500 mL flask with baffles. The components in the preculture are shown in Table 2.17. The *C. glutamicum* strain in Table 2.17 was either Roseo0, Roseo1, Roseo2, Roseo3, Roseo4 or Roseo5. Each strain was transferred from a plate to one flask, and the flask was inoculated overnight at 175 rpm and 30°C.

Table 2.17: Components with corresponding volume in the precultures for the growth experiments.

Components	Volume
2TY	50 mL
Tetracycline	25 µL
Kanamycin	25 µL
C. glutamicum strain	
Total volume	50 mL

2.7.2 Media preparation for growth experiments

For each of the strains Roseo0, Roseo1, and Roseo2 in Growth experiment 1 three parallels were carried out. For one parallel, 25 mL of selective media was prepared in one 250 mL flask with baffles. Hence, a total of nine flasks were used. The selective media was prepared according

to Table 2.18. Ten times the amount of 25 mL of selective media was prepared and mixed in one 500 mL flask before 25 mL of the selective media was transferred to each of the nine 250 mL flasks. PCA was added to the solution right before the selective media was used, and IPTG was added after 6 hours of the growth experiment. For Growth experiment 2, with the 6 strains Roseo0, Roseo1, Roseo2, Roseo3, Roseo4, and Roseo5, a total of 18 flasks were used, as three parallels were carried out for each strain. Twenty times the amount of 25 mL of selective media was prepared and 25 mL was transferred to each of the 18 flasks. PCA was not added since it was oxidized, and IPTG was added after 6 hours.

Table 2.18: Components and corresponding volume used in the preparation of selective media for Growth experiment 1 and Growth experiment 2.

Components	Amount x1 [mL]	Amount x10 [mL]	Amount x20 [mL]
CGXII	20.0000	200.000	400.00
C-S (glucose 40%)	0.6250	6.250	12.60
Biotein	0.0250	0.250	0.50
PCA	0.0250	0.250	-
TES	0.0250	0.250	0.50
IPTG	0.0250	0.250	0.50
Kanamycin	0.0125	0.125	0.25
Tetracyclin	0.0125	0.125	0.25
Water	4.2500	42.500	85.50
Total volume of media:	25.0000	250.000	500.00

Table 2.18 describes the distinct functions of the selective media components, whereby CGXII served as a saline solution that supported the growth of *C. glutamicum*. C-S acted as a glucose-derived carbon source that facilitated cellular growth. Biotin is a vitamin that plays vital roles in the synthesis of lipids and central metabolism in cells [73] [74]. Additionally, the trace element solution (TES) contained different cofactors for intracellular reactions within the cells [75]. The gene expression within the constructed plasmids was triggered by the use of IPTG (Isopropyl-β-D-1-thiogalactopyranoside).

2.7.3 Optical density measurements

The spectrophotometer, WPA CO 8000 Biowave Cell Density Meter from Biochrom Ltd [76], was used to measure the optical density (OD) of the precultures of Roseo0, Roseo1, Roseo2, Roseo3, Roseo4, and Roseo5 in Growth experiment 1 and Growth experiment 2. Cells from the precultures were transferred to flasks with 25 mL of selective media. The initial volume of precultures transferred was computed by considering the expected final OD of 1 in each flask. To achieve an OD of 1 in each flask, the precultures were diluted in a ratio of 1:40, and OD measurements of the precultures were carried out at the wavelength of 600 nm. The equation,

$$C_i \cdot V_i = C_f \cdot V_f. \tag{2.1}$$

was used to calculate the right initial volume, V_i, knowing the final concentration, C_f, final volume, V_f, and the measured initial concentration, C_i, by the spectrophotometer. C_f was equivalent to an OD of 1 and V_f was the final volume of 25 mL. The measured initial concentration multiplied with the dilution factor, and the calculated initial volume, V_i, are found in Appendix B in Table B.1 and Table B.2.

The predetermined initial volumes of the three distinct precultures in Growth experiment 1, and the six distinct precultures i Growth experiment 2, were distributed equally into three falcon tubes each. The cells in the falcon tubes were cleansed through centrifugation (5 min, 4500 rpm), decantation of supernatant, resuspension, followed by the addition of CGXII (20 mL). The cells were then subjected to another round of centrifugation with similar conditions. The supernatant was removed, the cells in each falcon tube were resuspended and transferred to one 250 mL flask with 25 mL of selective media.

To find the growth curves and final biomass of the different *C. glutamicum* strains, ODs were measured every second hour for 10 hours. The measurements started right after the cleaned cells from the precultures were inoculated to the selective media. The day after, two measurements were taken after 22 hours and after 24 hours. For Growth experiment 2, ODs were additionally measured after 72 hours. The values of the OD measurements are given in Appendix B, and the calculations of the growth rate, biomass, and biomass yield are given in Appendix C.

2.8 High-performance liquid chromatography (HPLC)

To measure the concentration of roseoflavin and riboflavin during the growth experiment, high-performance liquid chromatography (HPLC) was utilized. It is a separation technique, which separates the compounds present in solutions due to the molecular structure and properties [77]. During the growth experiment, HPLC samples were taken from the flasks before the genes were induced after 6 hours, and after the genes were induced after 24 hours and 72 hours. From each of the growth experiment flasks, 1 mL of cell solution was transferred to an Eppendorf tube and centrifuged 10 minutes at 13300 rpm. The supernatant was collected after centrifugation in a new Eppendorf tube. 1 mL of 15% of trichloroacetic acid was added to 0.5 mL of supernatant and the solution was agitated for 1 minute. The solution was incubated for 20 minutes at 25°C before the solution was centrifuged for 20 minutes at 4°C and 7830 rpm. To HPLC vials, 1 mL of supernatant was transferred and 150 µL of 2M K_3PO_4 was added to adjust the pH. Before the HPLC measurements started, the samples were vortexed. For the HPLC measurements and the quantification of roseoflavin and riboflavin, a 25°C prewarmed 75 mm × 4.6 mm Symmetry C18 Column 3.5 µm column was used. For detection, a Agilent 1260 FLD (Germany) fluorescence detector with emission and excitation wavelengths of 520 and 370 nm was used, respectively. A mobile phase consisting of a 5 mM solution of ammonium acetate and methanol in a 3:1 ratio, with a pH of 6.0, was used at a flow rate of 0.8 mL/min in the HPLC. The roseoflavin and riboflavin concentration were calculated from the HPLC measurements and are found in Appendix D.

2.9 Antimicrobial tests

Antimicrobial tests were carried out to see how different strains of *C. glutamicum* harboring different transporter proteins grew on different concentrations of roseoflavin, and to investigate the properties of the transporter proteins. *ribM* and *ribX* were the genes encoding the transporter proteins. From subsection 2.2 the strains Transport0, Transport1, Transport2, Transport3, Transport4, and Transport5 were used in the antimicrobial tests. The study investigated the impact of the *ribM* gene on the growth of *C. glutamicum* by examining whether it facilitated the export of roseoflavin and whether *ribM* encoded an antiporter or a uniporter. *ribX* encodes a riboflavin importer protein, found in the genome of *C. glutamicum*, and the antimicrobial test investigated how

ribX effects *C. glutamicum* growth on different roseoflavin concentrations. Three different antimicrobial tests were carried out. The first antimicrobial test contained complex media of 2TY, and the strains Transport0 and Transport1, harboring the plasmids, pVWEx1 and pVWEx1-*ribM*, respectively. The second antimicrobial test was carried out in CGVXII selective media (selective media) investigating Transport0, Transport1, and Transport2 harboring pVWEx1-*ribX*. In the final antimicrobial test, selective media was used. The antimicrobial test was applied to the strains Transport3, Transport4, and Transport5, all harboring pSym-*riboCg*, and either pVWEx1, pVWEx1-*ribM*, or pVWEx1-*ribMX*, respectively. Further are the antimicrobial tests referred to as Antimicrobial test 1, Antimicrobial test 2, and Antimicrobial test 3.

2.9.1 Preparation of strains and preculture

To construct the strains, the plasmids pVWEx1, pVWEx1-*ribM* and pVWEx1-*ribX* were extracted from different *E. coli* strains. Afterward, the plasmids were transformed into Cg and Cg(pSym-*riboCg*) competent cells, as explained in subsection 2.6. For Antimicrobial test 1, a precultures of 5.0 mL 2TY, 2.5 µL of kanamycin, and Transport0 from a plate was prepared in a falcon tube and mixed overnight at 30°C and 225 rpm. Similar was a preculture of Transport1 prepared. Precultures for Antimicrobial test 2 containing either Transport0, Transport1, or Transport2 were prepared the same way. Additionally, was 2.5 µL of tetracycline added to the precultures of Transport3, Transport4, and Transport5 in the preparation of the precultures in Antimicrobial test 3, due to the pSym-*riboCg* plasmid. When 2TY was used as the growth media, 300 µL of precultures were mixed with 7.5 mL of 2TY and 3.75 µL of kanamycin. For the antimicrobial tests where selective media was utilized, the precultures were washed. The precultures were centrifuged 5 minutes at 4500 rpm, the supernatant was removed and the cells were resuspended in 5 mL of CGVXII (containing no carbon source). The solution was centrifuged with the same conditions, the supernatant was discarded and 5 mL of CGVXII (containing no carbon source) was added. 300 µL of the washed cells in CGVXII was mixed with 7,5 mL of CGVXII selective media. The CGVXII selective media is found in Table 2.18. For Antimicrobial test 3, ODs of the precultures were measured before the cells were washed, and equal amount of cells was washed to get similar ODs for all parallels and strains in the test. The selective media used in Antimicrobial test 2 and Antimicrobial test 3 contained 0.5% of glucose. The selective media was prepared according to Table 2.19.

Table 2.19: Components and corresponding volume used in the preparation of selective media for Antimicrobial test 2 and Antimicrobial test 3.

	Antimicrobial test 2		**Antimicrobial test 3**	
Components	**Amount x1 [mL]**	**Amount x 2 [mL]**	**Amount x1 [mL]**	**Amount x 2 [mL]**
CGXII	20.000	40.000	20.000	40.000
C-S (glucose 40%)	0.313	0.625	0.313	0.625
Biotein	0.025	0.050	0.025	0.050
TES	0.025	0.050	0.025	0.050
IPTG	0.025	0.050	0.025	0.050
Kanamycin	0.013	0.025	0.013	0.025
Tetracyclin	-	-	0.013	0.025
Water	4.600	9.200	4.588	9.175
Total volume of media:	25.000	50.000	25.000	50.000

2.9.2 Preparation of plate and measurements

Plate 1 and Plate 2 were used in the antimicrobial tests illustrated in Figure 2.3 to the left and right, respectively. Different roseoflavin concentrations and strains were applied in the different wells on the plates. Only Plate 1 was utilized for Antimicrobial test 1. The plate for Antimicrobial test 1 was prepared the following way: 160 µL of 2TY was added to the first 7 wells in column 1. 100 µL of 2TY was added to the rest of the columns from row A to G marked yellow in Figure 2.3. In the first 7 wells in column 1, 40 µL of 0.5 g/L roseoflavin was transferred to a final volume of 200 µL and mixed thoroughly. From the first well in row A, 100 µL was transferred to the second well in row A, and mixed thoroughly. The transfer of 100 µL from a well to the next well with a higher column number, and thorough mixing, continued in row A until column 11. When 100 µL was transferred to well 11 and thoroughly mixed, 100 µL was discarded from the well leaving well 12 to only contain 2TY. This created a dilution series of roseoflavin concentration in a ratio of 1:2 from one well to another throughout row A, where A1 had the highest concentration of 0.1 g/L. The dilution of 1:2 made the concentration in A2 decrease by half the concentration. From row B to G, the dilution series of roseoflavin concentrations was repeated. In row A to C 100 µL of Transport0 was added, and in row D to F, 100 µL of Transport1 was added. In row G, 100 µL of 2TY was added to each well creating a blank row with different roseoflavin concentrations and no cells.

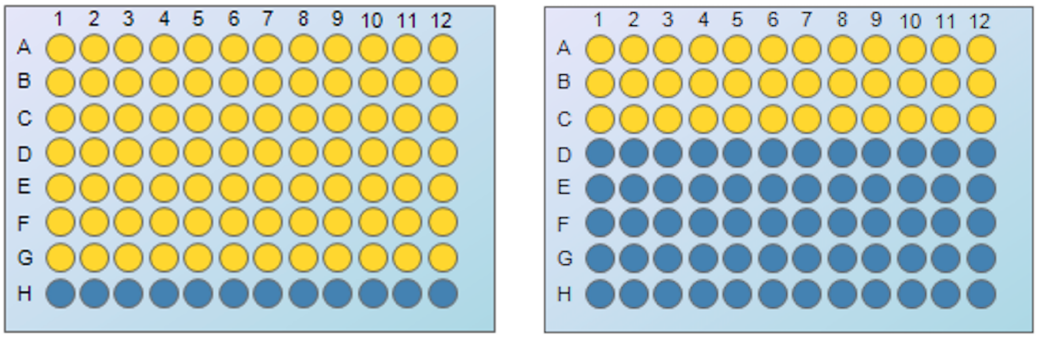

Figure 2.3: Plates used for OD measurements during the antimicrobial test. Yellow color marks the well used, and blue wells were not used wells. Plate 1 is to the left, and Plate 2 is to the right.

For Antimicrobial test 2 and Antimicrobial test 3, Plate 1 was prepared similarly as for Antimicrobial test 1, only 2TY was replaced with CGVXII selective media. In addition, three strains were tested instead of two. Hence, Plate 2 was additionally used for both tests. In Plate 1 for Antimicrobial test 2, Transport0 was inoculated in row A to C and Transport1 in row D to F. In Plate 2, Transport2 was inoculated in row A to C. For Antimicrobial test 3, Transport3 was inoculated in row A to C on Plate 1, and Transport4 was inoculated in row D to F. Transport5 was inoculated in row A to C on Plate 2 of the test.

To collect the OD measurement of the strains, a TECAN machine from Noax Lab AS was used. ODs were measured at a wavelength of 600 nm. 15 seconds of orbital shaking at 432 rpm of the plates were performed before the ODs were measured. The plates were of the brand Greiner 96 Flat Transparent, and the measurements were collected without the lids of the plates. Measurements were collected after 24 hours when the strains were assumed to have reached the stationary phase. The raw data and the final biomass calculations are displayed in Appendix F. Picture of the plates

after 24 hours are shown in Figure 2.4, displaying the dilution series of roseoflavin.

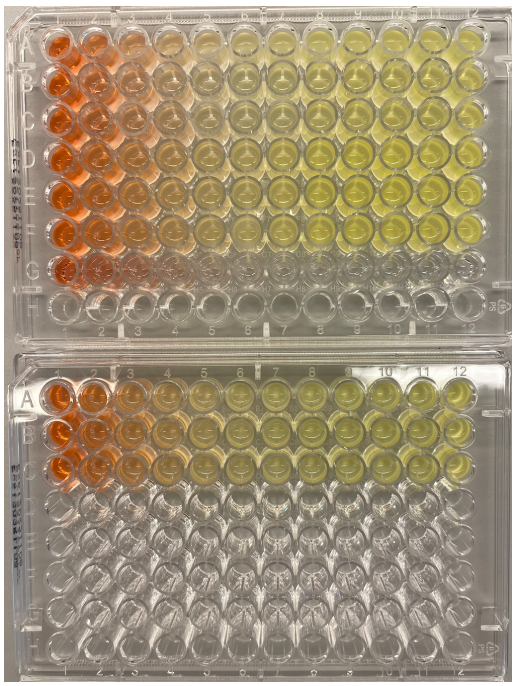

Figure 2.4: Plates after 24 hours. The plates were used in the OD measurements during the antimicrobial tests. The roseoflavin dilution series are seen.

3 Results

In this chapter constructed strains of *C. glutamicum* for optimized roseoflavin production were analyzed before the strains were evaluated through flask fermentation in growth experiments. Collected samples from the growth experiments were evaluated through HPLC analysis, and the HPLC results are presented as the roseoflavin- and riboflavin titers produces by each strain. The constructed strains Cg(pSym-*riboCg*)(pVWEx1), Cg(pSym-*riboCg*)(pVWEx1-*rosABC*), Cg(pSym-*riboCg*)(pVWEx1-*rosABC-ribM*), and Cg(pSym-*riboCg*)(pVWEx1-*ribF-rosABC-ribM*) are named here Roseo0, Roseo1, Roseo2 and Roseo3, respectively. The strains from Rudberg's study [1] are Cg(pSym-*riboCg*)(pVWEx1-*rosAB*) named Roseo4 and Cg(pSym-*riboCg*)(pVWEx1-*rosAB-ribM*) named Roseo5. The results look into the effect of overexpressing the genes *ribM*, *rosC*, and *ribF* for the newly constructed strains for optimized roseoflavin production in comparison to the strains from Rudberg's study [1]. Further are the results from the antimicrobial tests, investigating the toxicity of roseoflavin and the properties of the transporter proteins encoded by *ribM* and *ribX*, presented. Here, the strains utilized were Cg(pVWEx1), Cg(pVWEx1-*ribM*), Cg(pVWEx1-*ribX*), Cg(pSym-*riboCg*)(pVWEx1), Cg(pSym-*riboCg*)(pVWEx1-*ribM*), and Cg-(pSym-*riboCg*)(pVWEx1-*ribX*), and referred to as Transport0, Transport1, Transport2, Transport3, Transport4, and Transport5, respectively.

3.1 Construction of the strains Roseo1 and Roseo2 containing gene inserts from the roseoflavin biosynthesis pathway

In order to create the strains Roseo1 and Roseo2, the vectors pVWEx1-*rosABC* and pVWEx1-*rosABC-ribM* were constructed. For constructing the vectors, the genes *rosA*, *rosB*, *rosC*, and *rosM* were amplified either from the pVWEx1-*rosAB* plasmid, constructed in Rudberg's study [1], or the genomic DNA of *S. davawensis*. Gel electrophoresis was performed to verify the presence of these genes. Figure 3.1 show the gel pictures of the amplified genes. Displayed in **A**: Well 1 shows a specific band for the genes *rosAB*, and well 2 and well 3 display unspecified bands for *rosC*1 and *rosC*2, respectively. Displayed in **B**: The gene *rosC*1 is shown in well 1, and the gene was used in the construction of pVWEx1-*rosABC*. Displayed in **C**: The gene *rosC*2 for the construction of pVWEx1-*rosABC-ribM* are shown in well 1. Displayed in **D**: The presence of *ribM* is confirmed in well 5. The length of the amplified genes was 1984 bp for *rosAB*, 753 bp for *rosC*1, 777 bp for *rosC*2, and 726 bp for *ribM*. To identify the genes, the Thermo Scientific^{TM} GeneRuler 1 kb Plus DNA Ladder [70], was used as a size marker to identify the lengths of the DNA fragments.

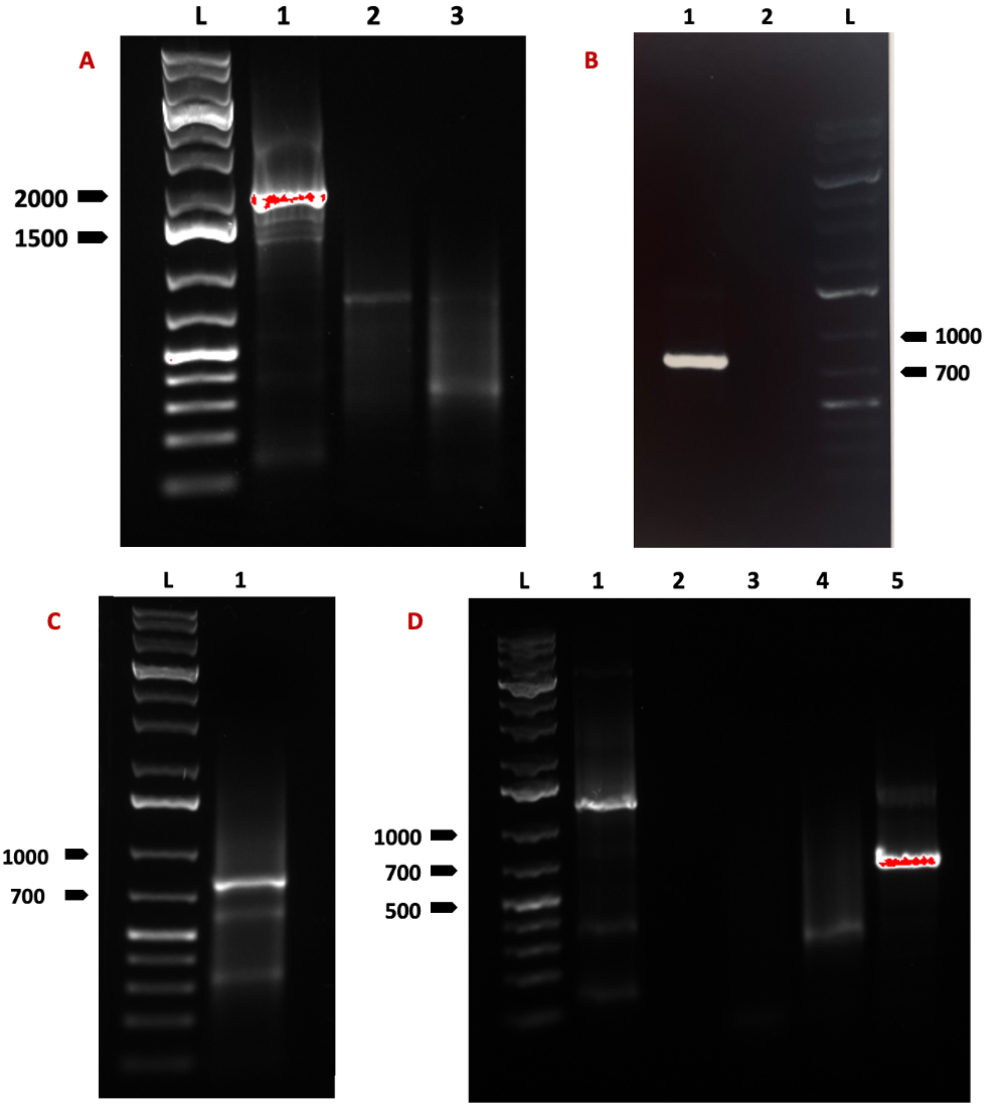

Figure 3.1: Gel electrophoresis displayed in **A**: A specific band for *rosAB* of 1948 bp are shown in well 1. The genes *rosC*1 and *rosC*2 are shown as unspecified bands in wells 2 and 3, respectively. Gel electrophoresis displayed in **B**: A specific band for *rosC*1 of 753 bp in well 1. Gel electrophoresis displayed in **C**: A specific band for *rosC*2 of 777 bp. Gel electrophoresis displayed in **D**: A specific band for *ribM* of 726 bp in well 5. The 1 kb plus ladder (L) is shown next to the samples.

In order to validate the successful construction of the plasmids, pVWEx1-*rosABC*, and pVWEx1-*rosABC-ribM* after cloning and transformation into *E. coli*, the target genes *rosABC* and *rosABC-ribM* were amplified through colony PCR. The resulting DNA fragments were then analyzed using gel electrophoresis for verification purposes. The gel images depicting the amplified genes, *rosABC*, and *rosABC-ribM*, are illustrated in Figure 3.2. Display in **A**: Indication of an unspecific band of *rosABC*, with a size of 2701 bp, is shown in wells 3 (at the red arrow) and 18. However, it is worth noting a potential issue with the ladder used as the size marker. Display in **B**: An unspecified band of *rosABC-ribM*, with a size of 3451 bp is shown in well 23.

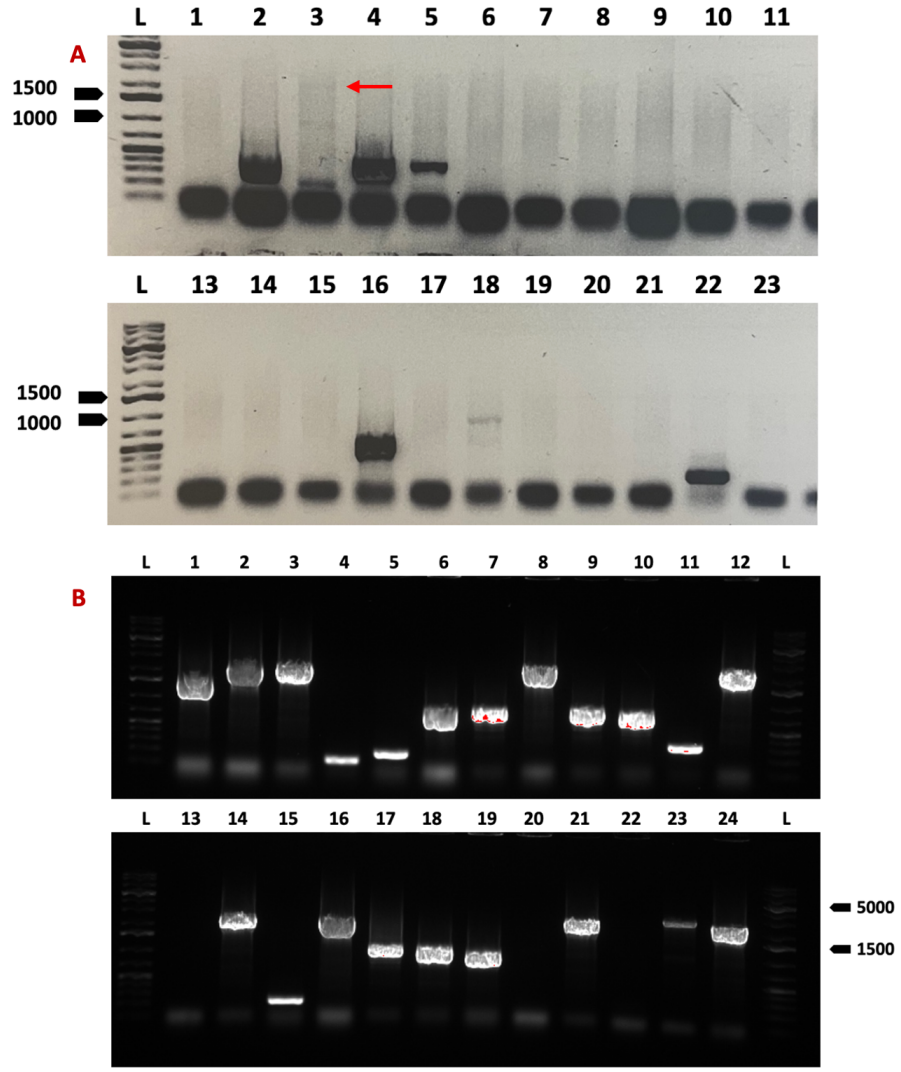

Figure 3.2: Gel electrophoresis displayed in **A**: Indications of *rosABC* of 2701 bp are shown in well 3 and well 18. The 1 kb plus ladder (L) was suspected of being wrong and is shown next to the samples. Gel electrophoresis displayed in **B**: In well 23, an unspecific band of *rosABC-ribM* of 3451 bp is shown. The 1 kb plus ladder is shown next to the samples.

To verify the construction of the plasmids pVWEx1-*rosABC* and pVWEx1-*rosABC-ribM*, and to confirm the presence of the genes *rosABC* in wells 3 and 18, and *rosABC-ribM* in well 23, two distinct tests were conducted. The first test was a PCR amplification test. Here, the gene *rosC* was amplified from colonies 3 and 18 which were assumed to contain the pVWEx1-*rosABC* plasmids. In addition, the *ribM* gene was amplified from colony 23 presumed to contain pVWEx1-*rosABC-ribM* plasmids. The gel images depicting the amplified genes from the PCR test are displayed in Figure 3.3. Second, a digestion test was conducted. Specific restriction enzymes were used to digest the pVWEx1-*rosABC* and pVWEx1-*rosABC-ribM*, and the resulting fragments were compared to the expected fragments listed in Table 3.1. The digestion test was performed on the pVWEx1-*rosABC* plasmids from colonies 3 and 18, as well as the pVWEx1-*rosABC-ribM* plasmids from colony 23. The gel images depicting the results from the digestion tests are shown in Figure 3.4.

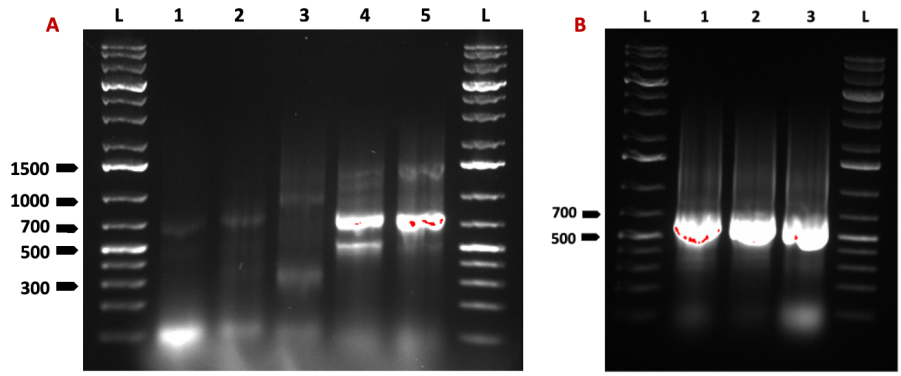

Figure 3.3: Gel electrophoresis displayed in **A**: Unspecific bands for *rosC* of 752 bp are shown in well 4 and well 5. *rosC* was amplified from pVWEx1-*rosABC* from colony 3 and 18 from the colony PCR, showing the band in well 4 and well 5, respectively. Gel electrophoresis displayed in **B**: *ribM* of 726 bp are shown in well 3. The 1 kb plus ladder is shown next to the samples.

In Figure 3.3 bands above 700 bp are shown in well 4 and well 5 displayed in **A**. The observed bands indicate the successful amplification of the *rosC* gene. Specifically, the band in well 4 corresponds to the amplification of *rosC* from the pVWEx1-*rosABC* plasmid from colony 3, whereas the band in well 5 corresponds to the amplification Displayed in **B**, a band above 700 bp is observed in well 3. The band indicates that *ribM* had been successfully amplified from colony 23 containing the pVWEx1-*rosABC-ribM* plasmids from the colony PCR.

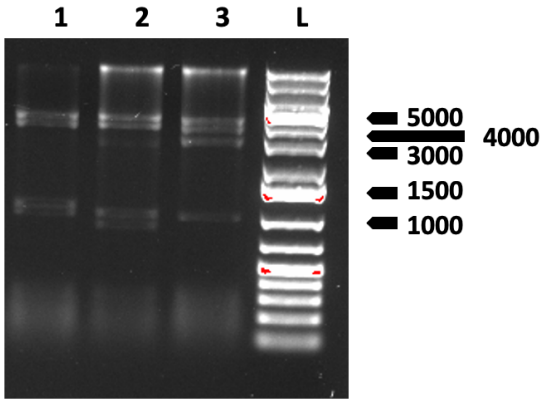

Figure 3.4: Gel electrophoresis of digested pVWEx1-*rosABC* plasmids in well 1 and 2, and digested pVWEx1-*rosABC-ribM* plasmids in well 3. All plasmids were digested with the restriction enzyme HindIII. The 1 kb plus ladder is shown next to the samples.

Table 3.1: The plasmids pVWEx1-*rosABC* and pVWEx1-*rosABC-ribM*, the restriction enzyme HindIII, and the expected fragments cut by the restriction enzyme are displayed.

Plasmids	**Restriction enzyme**	**Length of expected fragments in bps**
PVWEx1-*rosABC*	HindIII	3700, 3400, 2600, 1030
PVWEx1-*rosABCM*	HindIII	3700, 3400, 3300, 1000, 300

The gel electrophoresis results of the digestion test depicted in Figure 3.4 reveal the presence of four bands in well 3 for the digested pVWEx1-*rosABC-ribM* plasmid. Three of these bands fall within the range of 3000-4500 bp, while one band measures 1000 bp. Upon comparison

with the ladder bands, the results are inconclusive according to Table 3.1. Therefore, it could not be determined if the construction of pVWEx1-*rosABC-ribM* was successful. The digested samples from colonies 3 and 18 exhibits four and five bands in wells 1 and 2, respectively. The lengths of these bands are 4000 bp and between 1000 and 1500 bp. However, in relation to the expected fragment lengths listed in Table 3.1, the results remain inconclusive, making it difficult to ascertain the successful production of pVWEx1-*rosABC*. Due to the inconclusive findings from the digestion test, colonies from well 3 and well 18, assumed to contain pVWEx1-rosABC were subjected to sequencing analysis, subsubsection 2.4.10. Additionally, was the colony from well 23, assumed to contain pVWEx1-*rosABC-ribM*, sent to sequencing. The sequencing results confirmed that the colony in well 3 harbored pVWEx1-*rosABC*, while the colony in well 23 harbored pVWEx1-*rosABC-ribM*.

3.2 Evaluation of the behavior of roseoflavin producing *C. glutamicum* strains in Growth experiment 1

The performance and behavior of *C. glutamicum* strains were evaluated during flask fermentation in Growth experiment 1 shown in Figure 3.5. The strains Roseo0 (blue), Roseo1 (yellow), and Roseo2 (red) showed similar behavior in terms of growth with 1% of glucose as the sole carbon source. All strains entered the exponential phase from the beginning, coinciding with the inoculation of the initial strains at an OD_{600} of 1. After the genes were induced after 6 hours, the trends of the exponential phase did not change. All strains had depleted glucose after 22 hours, showing a decrease in the graphs from the 22^{nd} to the 24^{th} hour. From the steepness of the exponential phase, the growth rate in Table 3.2, of the strains were found to be similar due to the standard deviations. The exponential phase is defined from the 2^{nd} to 10^{th} hour. The growth rate of Roseo0 was found to be 0.308 ± 0.023 μ^{-1}, whereas the growth rate was 0.283 ± 0.006 μ^{-1} for Roseo1 and 0.280 ± 0.022 μ^{-1} for Roseo2. As for the final biomass yield, Roseo0 had a final biomass yield of 0.420 ± 0.029 g/g, Roseo1 had a final biomass yield of 0.488 ± 0.050 g/g, and Roseo2 had a final biomass yield of 0.456 ± 0.012 g/g. Here, the standard deviations are overlapping, making the final biomass yields equal for all strains.

Table 3.2: Growth rate, biomass and biomass yield for Roseo0, Roseo1 and Roseo2.

Strain name	Growth rate [μ^{-1}]	Biomass [g/L]	Biomass yield [g/g]
Roseo0	0.308 ± 0.023	4.20 ± 0.29	0.420 ± 0.029
Roseo1	0.283 ± 0.006	4.88 ± 0.50	0.488 ± 0.050
Roseo2	0.280 ± 0.022	4.56 ± 0.12	0.456 ± 0.012

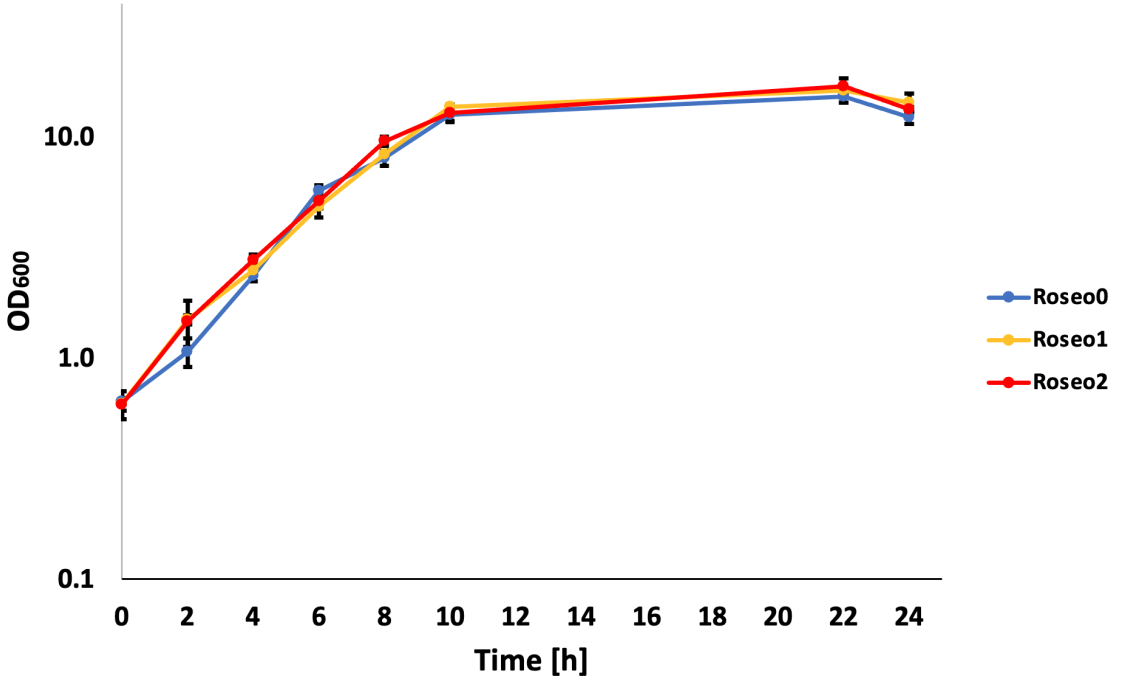

Figure 3.5: Growth experiment 1 was performed for the strains Roseo0 in blue, Roseo1 in yellow, and Roseo2 in red. The genes were induced after 6 hours. The x-axis displays the time in hours, and the y-axis display OD_{600} data given in a logarithmic scale. Means and standard deviations of the triplicates are shown.

3.3 Roseoflavin and riboflavin production in flask fermentation of different *C. glutamicum* strains in Growth experiment 1

In order to quantify the levels of roseoflavin and riboflavin produced by Roseo0, Roseo1, and Roseo2 in Growth experiment 1, samples were collected at 6, 24, and 72 hours for the HPLC analysis. The highest titer of roseoflavin was achieved by Roseo2 at 72 hours, as displayed in Table 3.3 and Figure 3.6. The roseoflavin titer of Roseo2 was 1.4 folds higher than for Roseo1 and had a titer of 0.045 ± 0.001 g/L. Roseo1 yielded the second highest titer of 0.033 ± 0.002 g/L. In Figure 3.6, the roseoflavin titers of Roseo2 obtained from the samples collected after 24 and 72 hours are both higher than the titers achieved by Roseo1, indicating higher production of roseoflavin in strains overexpressing *ribM*.

Regarding the riboflavin titers in Table 3.3, Roseo1 had the highest titers of 0.099 ± 0.006 from the sample collected after 72 hours. However, standard deviations made the highest riboflavin titer overlap with the third highest titer of 0.090 ± 0.006 collected at 24 hours for strain Roseo1. It was 1.1 fold higher than the second highest riboflavin titer of 0.090 ± 0.002, belonging to Roseo2 at 72 hours. The riboflavin titers from Table 3.3 are displayed as histograms in Figure 3.7. The histogram illustrate higher riboflavin titers for Roseo1 than for Roseo2. It is worth noticing that higher roseoflavin titers in Figure 3.6 coincide with lower riboflavin titers in Figure 3.7, as riboflavin serves as the precursor for roseoflavin biosynthesis. However, Figure 3.7 displays that the riboflavin titers produced by Roseo1 and Roseo2 are higher than the titer produced by the control strain Roseo0, which is a contradiction to the expectations.

Table 3.3: Titers of roseoflavin and riboflavin in Growth experiment 1. The titers are from samples collected from Roseo0, Roseo1, and Roseo2, after 6 hours, 24 hours, and 72 hours.

Time sample was collected [h]	Strains	Titer of roseoflavin [g/L]	Titer of riboflavin [g/L]
6	Roseo0	0.000 ± 0.000	0.018 ± 0.001
24	Roseo0	0.000 ± 0.000	0.062 ± 0.003
72	Roseo0	0.000 ± 0.000	0.067 ± 0.002
6	Roseo1	0.006 ± 0.001	0.025 ± 0.001
24	Roseo1	0.026 ± 0.001	0.090 ± 0.006
72	Roseo1	0.033 ± 0.002	0.099 ± 0.006
6	Roseo2	0.003 ± 0.001	0.020 ± 0.001
24	Roseo2	0.044 ± 0.002	0.086 ± 0.003
72	Roseo2	0.045 ± 0.001	0.090 ± 0.002

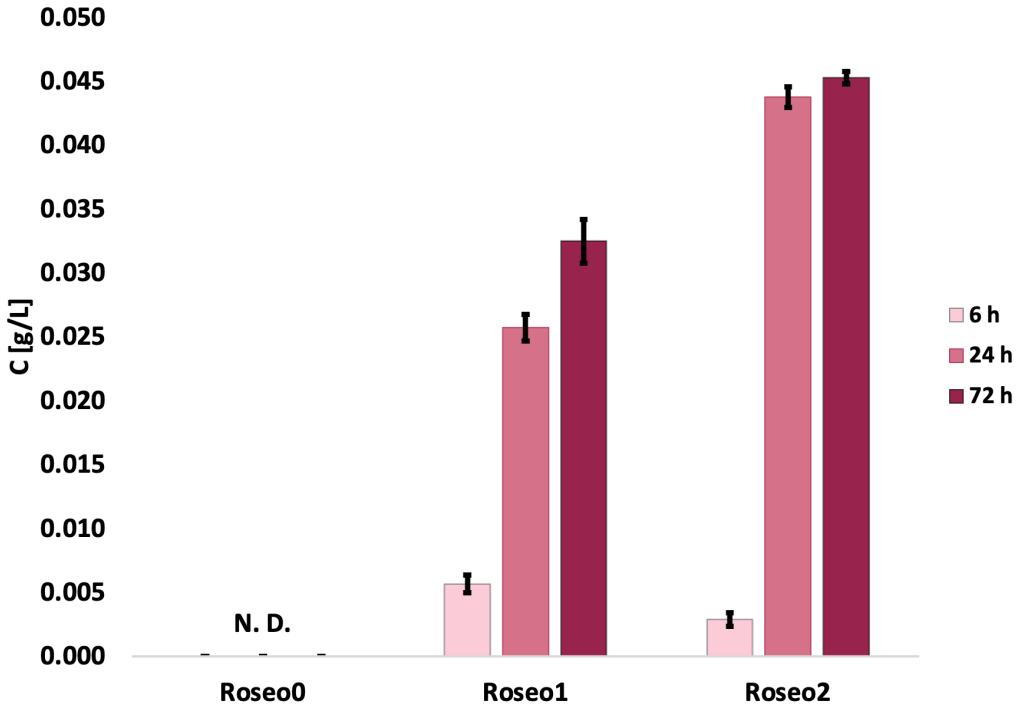

Figure 3.6: Titers of roseoflavin produced by Roseo0, Roseo1 and Roseo2. Titers from samples collected after 6 hours are light pink, samples collected after 24 hours are pink, and samples collected after 72 hours are dark pink. N. D means not detected. The triplicate means and standard deviations are shown. Y-axis shows the titers in g/L.

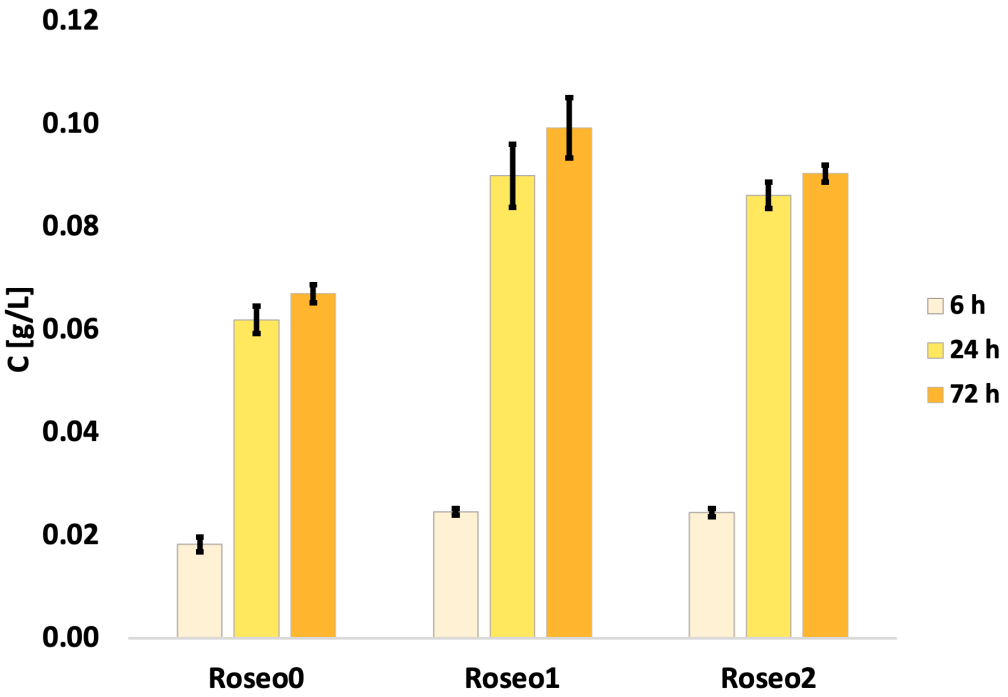

Figure 3.7: Titers of riboflavin produced by Roseo0, Roseo1 and Roseo2. Titers from samples collected after 6 hours are light yellow, samples collected after 24 hours are yellow, and samples collected after 72 hours are dark yellow. The triplicate means and standard deviations are shown. Y-axis shows the titers in g/L.

The roseoflavin titers obtained by the strain Roseo4 and Roseo5 in Rudberg's study [1] are presented in Table 3.4. Comparing the highest titer in Growth experiment 1 of Roseo2 with the titer achieved in Rudberg's study [1], Roseo4 and Roseo5 had a 6.5 fold and an 8.9 fold higher titer, respectively. The titer of Roseo4 was 0.296 ± 0.026 g/L and the titer of Roseo5 was 0.401 ± 0.008 g/L, achieved after 72 hours.

To show the different roseoflavin titers yielded by the strains in the two studies, the titers are displayed as histograms in Figure 3.8. The titer was higher for *ribM* overproducing strains, compared to strains without the gene. These results suggest that Roseo2 produced more roseoflavin than Roseo1, and Roseo5 produced more roseoflavin than Roseo4. Overproduction of *rosC* suggested that the roseoflavin titers of Roseo1 and Roseo2 were less than for Roseo4 and Roseo5.

Table 3.4: Titers of roseoflavin and riboflavin from Rudberg's study [1]. The titers are from samples collected from Roseo4, and Roseo5, after 6 hours, 24 hours, and 72 hours.

Time sample was collected [h]	Strains	Titer of roseoflavin [g/L]
6	Roseo4	0.000 ± 0.000
24	Roseo4	0.039 ± 0.002
72	Roseo4	0.296 ± 0.026
6	Roseo5	0.013 ± 0.003
24	Roseo5	0.210 ± 0.007
72	Roseo5	0.401 ± 0.008

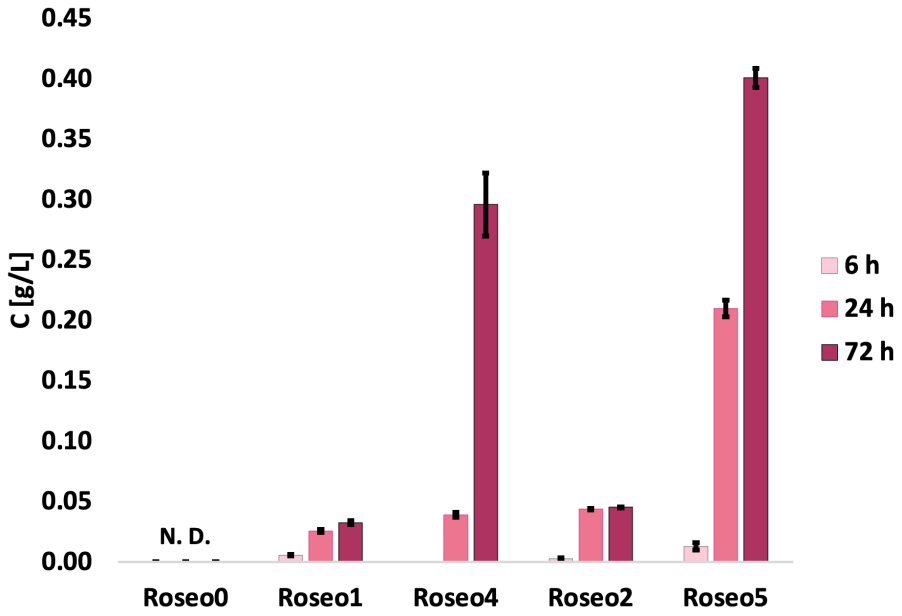

Figure 3.8: Titers of roseoflavin produced by Roseo0, Roseo1, Roseo2, Roseo4 and Roseo5. Roseo4 and Roseo5 show the values from Rudberg's study[1]. Titers from samples collected after 6 hours are light pink, samples collected after 24 hours are pink, and samples collected after 72 hours are dark pink. N. D means not detected. The triplicate means and standard deviations are shown. Y-axis shows the titers in g/L.

3.4 Connecting the riboflavin and roseoflavin pathways via expression of *ribF* gene

To construct the plasmids pVWEx1-*ribF-rosABC* and pVWEx1-*ribF-rosABC-ribM*, the genes *ribF* was amplified from the genomic DNA of *C. glutamicum*. Additionally, the genes *rosABC* and *rosABC-ribM* were amplified from the plasmids, pVWEx1-*rosABC*, and pVWEx1-*rosABC-ribM*, which were present in Roseo1 and Roseo2, respectively. Gel electrophoresis images of the amplified genes are shown in Figure 3.9. In **A**, a saturated band of *ribF* with a size of 1117 bp is observed. In **B**, a weak band of *rosABC* with a size of 2619 bp is displayed at the red arrow. Despite multiple attempts, it was not possible to obtain a saturated band for *rosABC* with the primers utilized. In **C** a saturated band of *rosABC-ribM* with a size of 3290 bp is displayed. Due to the challenges encountered in amplifying *rosABC*, further work focused on the cloning and construction of pVWEx1-*ribF-rosABC-ribM* in Roseo3.

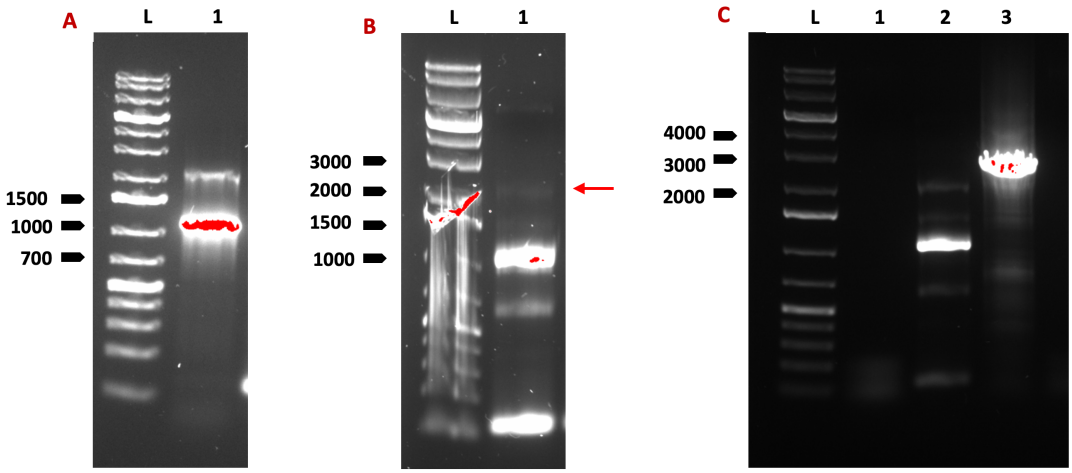

Figure 3.9: Gel electrophoresis displayed in **A**: A saturated band for *ribF* of 1117 bp are shown in well 1. Gel electrophoresis displayed in **B**: Several unspecific bands are shown in well 1. The weak band for *rosABC* of 2619 bp is shown at the red arrow. Gel electrophoresis displayed in **C**: A saturated specific band for *rosABC-ribM* of 3290 bp is shown in well 3. The 1 kb plus ladder (L) is shown next to the samples.

To verify the cloning of pVWEx1-*ribF-rosABC-ribM*, colony PCR was performed to amplify the genes *ribF-rosABC-ribM*. The gel electrophoresis results are presented in Figure 3.10. In well 9, an unspecific band with a size of 4407 bp is observed for *ribF-rosABC-ribM*.

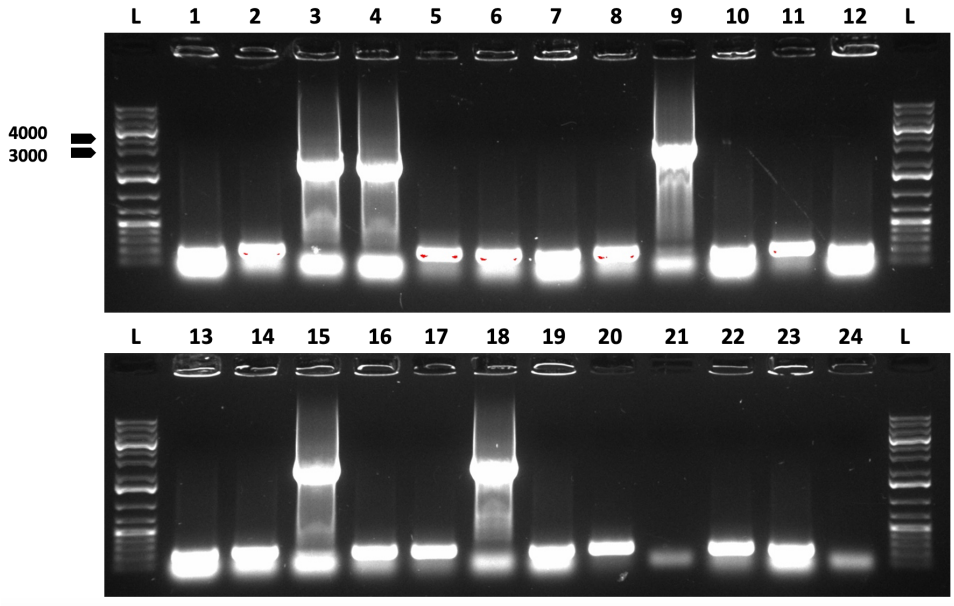

Figure 3.10: Indications of *ribF-rosABC-ribM* of 4407 bp are shown in well 9. The 1 kb plus ladder (L) is displayed next to the samples.

To confirm the presence of the pVWEx1-*ribF-rosABC-ribM* plasmid in the colony from well 9 in Figure 3.10, a PCR amplification test was conducted. Here the genes *ribF*, *ribM*, *rosABC*, and *rosABC-ribM* were amplified and the gel electrophoresis image is displayed in Figure 3.11. *ribF* are displayed in well 1 with the size of 1117 bp, *ribM* are displayed in well 2 with the size of 726 bp, *rosABC* are displayed in well 3 with the size of 3290 bp, and *rosABC-ribM* are displayed in well 4 with the size of 4407 bp.

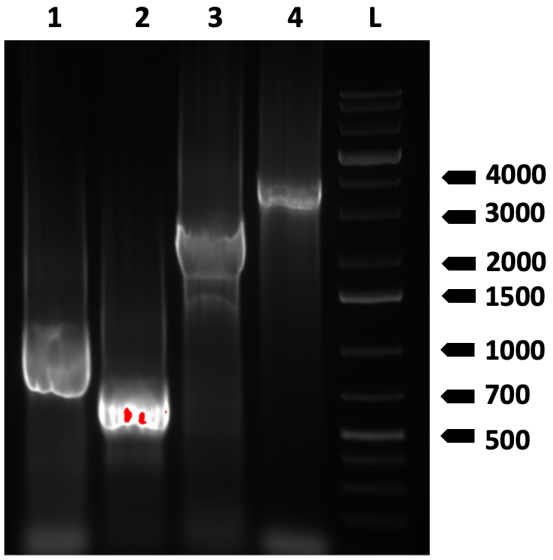

Figure 3.11: Unspecific bands for *ribF* of 1117 bp, *ribM* of 726 bp, *rosABC-ribM* of 3290, and *ribF-rosABC-ribM* of 4407 bp are shown in well 1, well 2, well 3, and well 4, respectively. All genes were amplified from pVWEx1-*ribF-rosABC-ribM* from the colony in well 9 displayed in the gel picture of the colony PCR. The 1 kb plus ladder is shown next to the samples.

The PCR amplification test from well 9 in Figure 3.10 was assumed to contain the pVWEx1-*ribF-rosABC-ribM* plasmid. However, in order to obtain conclusive evidence, the plasmid was subjected to sequencing analysis. The sequencing results revealed that the pVWEx1-*ribF-rosABC-ribM* plasmid was incomplete. Instead, it was determined that the plasmid contained the genes ribF, ribM, and most likely the genes rosAB. Due to the presence of *ribF*, the plasmid pVWEx1-*ribF-rosAB-ribM* was transformed into *C. glutamicum*, and is further named Roseo3.

3.5 Evaluation of the behavior of all constructed roseoflavin producing *C. glutamicum* strains in Growth experiment 2

Growth experiment 2, was performed by flask fermentation to analyze the behavior of the newly constructed strain Roseo3 and the effect of overexpressing the *ribF* gene. In addition, all constructed strains in both Rudberg's study [1] and this Master's were evaluated. Figure 3.12 shows the growth curves in Growth experiment 2 at two different time intervals. On top is an excerpt of the measurements collected until the 24^{th} hour, and on the bottom is the whole time interval until the 72^{th} hour. The trends in Figure 3.12 display that Roseo0 initiated a lag phase the two first hours, before it entered the exponential phase, from the 2^{nd} to the 10^{th} hour. After, it entered the stationary phase. Similarly, Roseo4 and Roseo5 both entered the stationary phase at the 10^{th} hour. Conversely, they initiated the exponential phase immediately after cell inoculation. The trends of Roseo1 and Roseo2 are similar. Both strains were in the lag phase until the 6^{th} hour, when they initiated exponential growth. From the measurements collected at the 22^{nd} and 24^{th} hours, the curves show that Roseo1 and Roseo2 were in the stationary phase. The trends of Roseo3 is unclear, due to high standard deviations. The strain was slow growing and stayed long in the lag phase. First after the measurement at the 22^{nd} hour, the strain was in the exponential phase.

From the steepness of the exponential phase, the growth rates in Table 3.5 were found. Due to standard deviations, the growth rates 0.225 ± 0.026 μ^{-1} and 0.207 ± 0.014 μ^{-1} were found similar for Roseo1 and Roseo2, respectively. For the same reason, the growth rates, 0.256 ± 0.030 μ^{-1} and 0.274 ± 0.014 μ^{-1}, of Roseo4 and Roseo5 were similar, respectively. Roseo0 achieved the highest growth rate, 0.325 ± 0.020 μ^{-1}. High standard deviations were calculated for the biomass yield, giving overlapping biomass yields. The highest biomass yield of 0.651 ± 0.088 g/g, achieved by Roseo2 overlapped with the biomass of Roseo1 of 0.592 ± 0.148 g/g. In addition, the biomass yield of Roseo1 overlaps with Roseo0, Roseo3, and Roseo5, with the biomass yields of 0.502 ± 0.023 g/g, 0.478 ± 0.040 g/g, and 0.434 ± 0.096 g/g, respectively.

Table 3.5: Growth rate, biomass and biomass yield for Roseo0, Roseo1, Roseo2, Roseo3, Roseo4, and Roseo5.

Strain name	Growth rate [μ^{-1}]	Biomass [g/L]	Biomass yield [g/g]
Roseo0	0.325 ± 0.020	5.02 ± 0.23	0.502 ± 0.023
Roseo1	0.225 ± 0.026	5.92 ± 1.48	0.592 ± 0.148
Roseo2	0.207 ± 0.014	6.51 ± 0.88	0.651 ± 0.088
Roseo3	0.114 ± 0.119	4.78 ± 0.40	0.478 ± 0.040
Roseo4	0.256 ± 0.030	3.36 ± 0.82	0.336 ± 0.082
Roseo5	0.274 ± 0.014	4.34 ± 0.96	0.434 ± 0.096

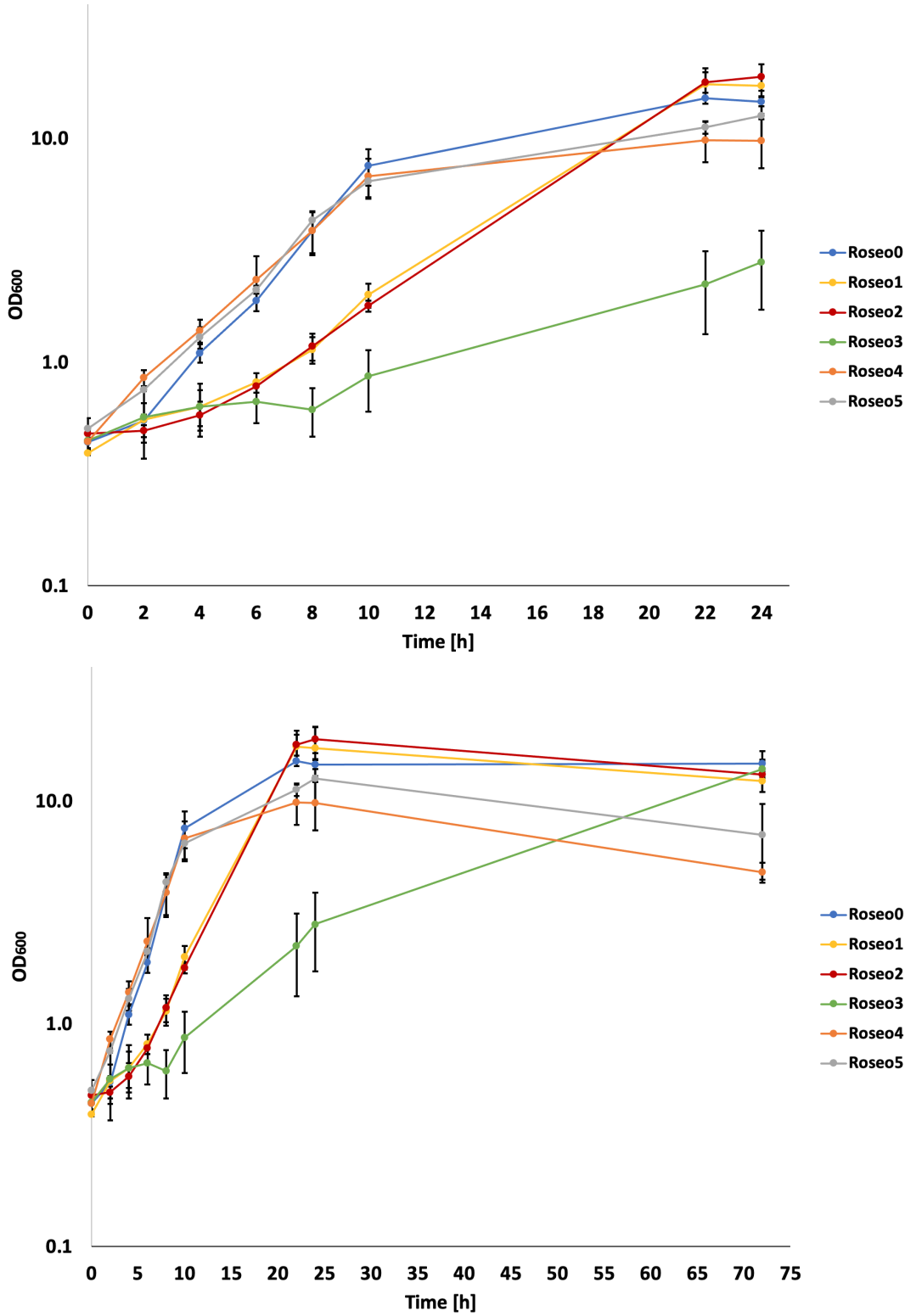

Figure 3.12: Growth experiment 2 was performed for the strains Roseo0 in blue, Roseo1 in yellow, Roseo2 in red, Roseo3 in green, Roseo4 in orange, and Roseo5 in grey. The genes were induced after 6 hours. The x-axis displays the time in hours, and the y-axis display OD_{600} data given in a logarithmic scale. Means and standard deviations of the triplicates are shown.

3.6 Roseoflavin and riboflavin production in flask fermentation of different *C. glutamicum* strains in Growth experiment 2

Similar to Growth experiment 1, samples for HPLC were collected after 6, 24, and 72 hours for Growth experiment 2 to analyze the titers of roseoflavin and riboflavin. Table 3.6 presents the measured roseoflavin and riboflavin titers achieved by all strains. To show the trends of the roseoflavin and riboflavin titers, histograms of the titers are displayed in Figure 3.13 and Figure 3.14, respectively. Roseo3 exhibited the highest roseoflavin titer of 4.065 ± 0.901 g/L in the sample collected at 72 hours. The titer was 3.0 fold higher than the second highest titer of 1.349 ± 0.322 g/L and 5.7 higher than the third highest titer of 0.719 ± 0.156 g/L produced by Roseo5 and Roseo4 after 72 hours, respectively.

The three highest riboflavin titers were produced by Roseo3, Roseo4, and Roseo5, and the titers are overlapping due to the standard deviations. The titers are 0.193 ± 0.031 g/L, 0.181 ± 0.002 g/L, and 0.171 ± 0.014 g/L, respectively. For Roseo3, the riboflavin titer was 1.6 higher than Roseo1 and 1.9 fold higher than Roseo2. The final riboflavin titer of Roseo1 and Roseo2 were 0.123 ± 0.003 g/L, and 0.103 ± 0.002 g/L, respectively.

All strains were constructed using competent cells of the *C. glutamicum* riboflavin overproducing strain, Cg(pSym-*riboCg*). As the maximum riboflavin titer Cg(pSym-*riboCg*) produces is 0.6 g/L [5], and roseoflavin is derived from riboflavin, it is impossible to measure roseoflavin titers as high as 4.065 ± 0.137 g/L. The too high roseoflavin titers will be discussed later in the Discussion, section 4.

Observed from Figure 3.13 and Figure 3.14, Roseo3, Roseo4 and Roseo5, producing the highest roseoflavin titers, also produces the highest riboflavin titers. An explanation is antimetabolite-resistance, further explained in the Discussion, section 4.

Table 3.6: Titers of roseoflavin and riboflavin in Growth experiment 2. The roseoflavin titers are from samples collected from Roseo0, Roseo1, Roseo2, Roseo3, Roseo4, and Roseo5 after 6 hours, 24 hours, and 72 hours.

Time sample was collected [h]	Strains	Concentration of roseoflavin [g/L]	Concentration of riboflavin [g/L]
6	Roseo0	0.000 ± 0.000	0.006 ± 0.002
24	Roseo0	0.000 ± 0.000	0.070 ± 0.001
72	Roseo0	0.000 ± 0.000	0.076 ± 0.002
6	Roseo1	0.000 ± 0.000	0.005 ± 0.000
24	Roseo1	0.014 ± 0.001	0.109 ± 0.002
72	Roseo1	0.000 ± 0.000	0.123 ± 0.003
6	Roseo2	0.000 ± 0.000	0.005 ± 0.000
24	Roseo2	0.048 ± 0.016	0.084 ± 0.003
72	Roseo2	0.082 ± 0.011	0.103 ± 0.002
6	Roseo3	0.041 ± 0.013	0.030 ± 0.007
24	Roseo3	0.677 ± 0.137	0.093 ± 0.016
72	Roseo3	4.065 ± 0.901	0.193 ± 0.031
6	Roseo4	0.014 ± 0.002	0.011 ± 0.001
24	Roseo4	0.069 ± 0.003	0.096 ± 0.005
72	Roseo4	0.719 ± 0.156	0.181 ± 0.002
6	Roseo5	0.011 ± 0.002	0.008 ± 0.000
24	Roseo5	0.142 ± 0.020	0.076 ± 0.003
72	Roseo5	1.349 ± 0.322	0.171 ± 0.014

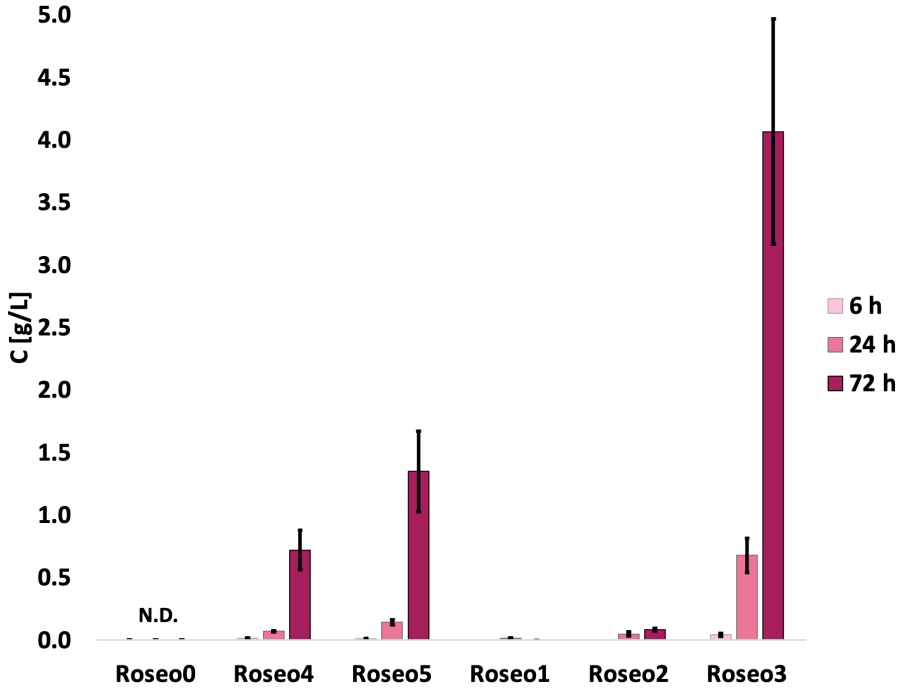

Figure 3.13: Titers of roseoflavin produced by Roseo0, Roseo1, Roseo2, Roseo3, Roseo4 and Roseo5. Roseo4 and Roseo5 show the values from Rudberg's study [1]. Titers from samples collected after 6 hours are light pink, samples collected after 24 hours are pink, and samples collected after 72 hours are dark pink. N. D means not detected. The triplicate means and standard deviations are shown. Y-axis shows the titers in g/L.

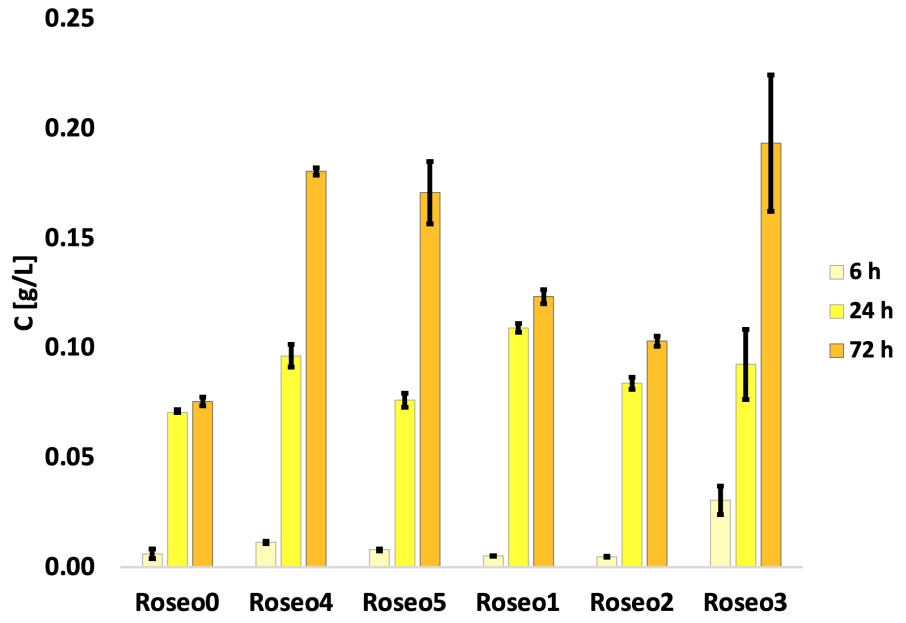

Figure 3.14: Titers of riboflavin produced by Roseo0, Roseo1, Roseo2, Roseo3, Roseo4 and Roseo5. Roseo4 and Roseo5 show the values from Rudberg's study [1]. Titers from samples collected after 6 hours are light yellow, samples collected after 24 hours are yellow, and samples collected after 72 hours are dark yellow. N. D means not detected. The triplicate means and standard deviations are shown. Y-axis shows the titers in g/L.

3.7 Antimicrobial tests exploring the transporter proteins *ribM* and *ribX* in *C. glutamicum* strains

3.7.1 Antimicrobial test 1

The performance of *C. glutamicum* overexpressing *ribM* was studied in nutrient and vitamin-rich complex media of 2TY [78] with varying concentrations of roseoflavin. All roseoflavin in the test is from the supplemented roseoflavin. In Figure 3.15, the final biomass of Transport1 exceeds the final biomass for Transport0 for each of the different dilutions of roseoflavin, indicating it coding for an exporter protein of roseoflavin. The trend in the histogram shows that as the roseoflavin concentrations decrease, the final biomass of Transport0 and Transport1 increases. From the roseoflavin dilution of 1:64 and higher, the final biomass for Transport1 is stable at 0.38 g/L, due to the standard deviations, observed in Table 3.7. Half the stable biomass is defined as the inhibitory constant, giving the inhibitory constant of 0.19 g/L. Transport1 achieved this biomass at a roseoflavin dilution of 1:2, with a biomass of 0.23 ± 0.01 g/L. The critical level of roseoflavin is 0.05 g/L, which corresponds to a roseoflavin dilution of 1:2. Hence, to support the growth of Transport1, roseoflavin concentrations must be maintained below 0.05 g/L. Because of the standard deviations, Transport1 cultivated in the absence of roseoflavin (0 in Figure 3.15) exhibits a biomass of 0.42 ± 0.02 g/L, which is similar to the biomass of Transport1 grown on the dilutions 1:128 and 1:512. However, the highest biomass is of those strains.

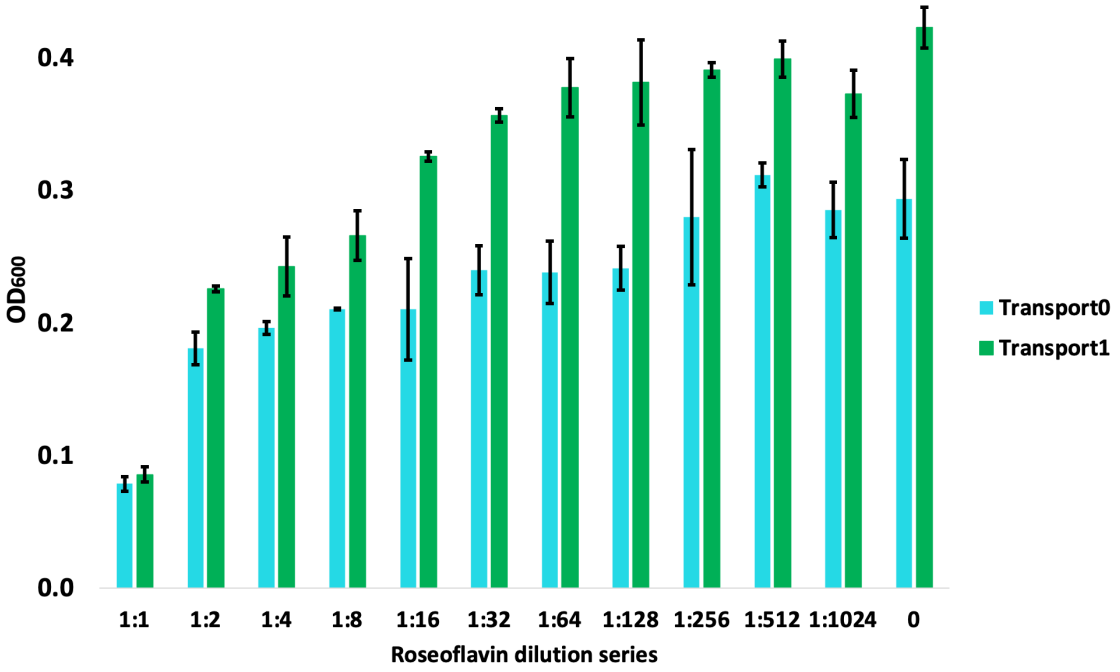

Figure 3.15: The final biomasses of Transport0 and Transport1 growing on different roseoflavin concentrations in Antimicrobial test 1 are displayed. In turquoise is Transport0 and in green is Transport1. Along the x-axis are the dilution series of roseoflavin, starting on a roseoflavin concentration of 0.1 g/L. The growth media used was 2TY complex media. The y-axis display OD_{600} data. Means and standard deviations of the triplicates are shown.

Table 3.7: Final biomasses for Transport0 and Transport1 calculated from the measurements after 24 hours in Antimicrobial test 1.

Dilution series	Transport0 Biomass [g/L]	Transport1 Biomass [g/L]
1:1	0.08 ± 0.01	0.09 ± 0.01
1:2	0.18 ± 0.01	0.23 ± 0.00
1:4	0.20 ± 0.01	0.24 ± 0.02
1:8	0.21 ± 0.00	0.27 ± 0.02
1:16	0.21 ± 0.04	0.33 ± 0.00
1:32	0.24 ± 0.02	0.36 ± 0.01
1:64	0.24 ± 0.02	0.38 ± 0.02
1:128	0.24 ± 0.02	0.38 ± 0.03
1:256	0.28 ± 0.05	0.39 ± 0.01
1:512	0.31 ± 0.01	0.40 ± 0.01
1:1024	0.29 ± 0.02	0.37 ± 0.02
0	0.29 ± 0.03	0.42 ± 0.02

3.7.2 Antimicrobial test 2

The transporter protein encoded by *ribM*, which enhances the roseoflavin tolerance of Transport1 in Antimicrobial test 1, was further investigated in Antimicrobial test 2 to explore its properties. Transport0 and Transport1 were grown in CGVXII selective media, which lacks vitamins but provides essential nutrients for cell growth of *C. glutamicum*. The objective was to determine whether the transporter protein required vitamins for cell growth. If vitamins were necessary, it was hypothesized that *ribM* encoded an antiporter protein that simultaneously imported vitamins while exporting roseoflavin. Conversely, if the cells could grow without vitamins in minimal media, *ribM* was suspected to be a uniporter only responsible for roseoflavin export.

Additionally, was Transport2 constructed in Antimicrobial test 2. Transport2 overexpressed *ribX* from the genome of *C. glutamicum*, which was encoding another transporter protein with unknown properties. To clearer depict the trends of the final biomass from Antimicrobial test 2 in Figure 3.16, Transport1 and Transport2 were separately displayed with Transport0 in two histograms. The trends of Transport0, Transport1, and Transport2 show limited growth for all strains in all roseoflavin dilutions up to 1:128, with biomass fluctuating around 0.1 g/L. For all strains, the final biomass increased from the dilutions 1:256 and higher. Compared to Antimicrobial test 1, the absence of vitamins decreased the roseoflavin tolerance of the strains. Due to standard deviations, the biomass in Table 3.8 are similar for Transport0, Transport1, and Transport2. Only at the dilution 1:1024, the final biomass of 0.85 ± 0.03 g/L for Transport1 is 1.4 fold higher than 0.61 ± 0.04 g/L of Transport0. High standard deviations of Transport2 make the biomass of the strains not comparable at the 1:1024 dilution.

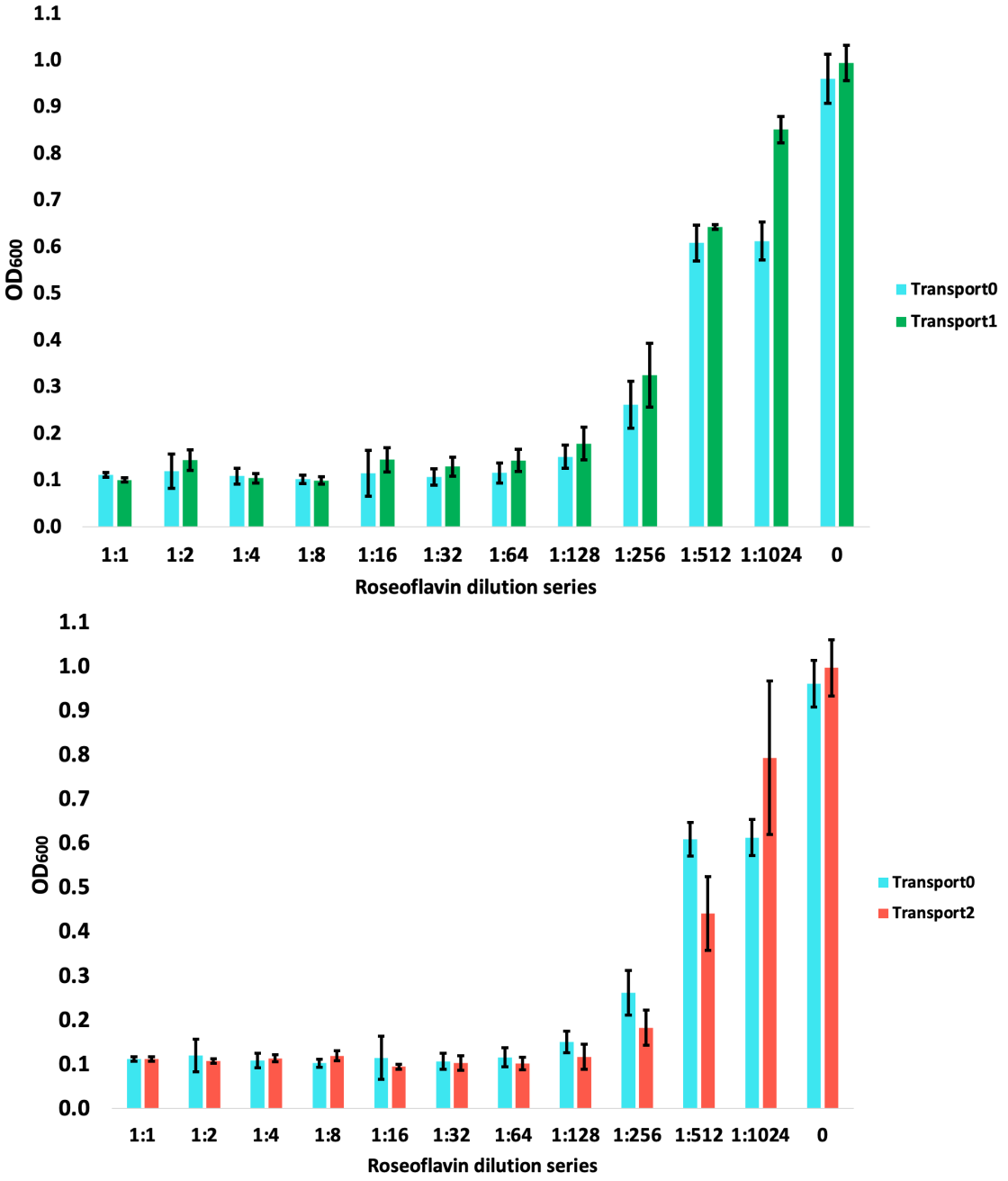

Figure 3.16: The final biomasses in Antimicrobial test 2 produced by Transport0, Transport1, and Transport2 growing on different roseoflavin concentrations are displayed. For better comparability, the control strain Transport0 in turquoise and Transport1 in green are shown on top, and the control strain Transport0 in turquoise and Transport2 in red are shown on the bottom. Along the x-axis are the dilution series of roseoflavin, starting on a roseoflavin concentration of 0.1 g/L. The growth media used was CGVXII selective media. The y-axis display OD_{600} data. Means and standard deviations of the triplicates are shown.

Table 3.8: Biomass for Transport0, Transport1, and Transport2 calculated from the measurements after 24 hours in Antimicrobial test 2.

Dilution series	Transport0 Biomass [g/L]	Transport1 Biomass [g/L]	Transport2 Biomass [g/L]
1:1	0.11 ± 0.01	0.10 ± 0.00	0.11 ± 0.01
1:2	0.12 ± 0.04	0.14 ± 0.02	0.11 ± 0.01
1:4	0.11 ± 0.02	0.10 ± 0.01	0.11 ± 0.01
1:8	0.10 ± 0.01	0.10 ± 0.01	0.12 ± 0.01
1:16	0.11 ± 0.05	0.14 ± 0.03	0.09 ± 0.01
1:32	0.11 ± 0.02	0.13 ± 0.02	0.10 ± 0.02
1:64	0.12 ± 0.02	0.14 ± 0.02	0.10 ± 0.01
1:128	0.15 ± 0.03	0.18 ± 0.04	0.12 ± 0.03
1:256	0.26 ± 0.05	0.32 ± 0.07	0.18 ± 0.04
1:512	0.61 ± 0.04	0.64 ± 0.01	0.44 ± 0.08
1:1024	0.61 ± 0.04	0.85 ± 0.03	0.79 ± 0.17
0	0.96 ± 0.05	0.99 ± 0.04	1.00 ± 0.06

3.7.3 Antimicrobial test 3

The decrease in roseoflavin tolerance observed in the absence of vitamins provided evidence that the transporter protein encoded by *ribM* functions as an antiporter. To further investigate the properties of *ribM* as an antiporter, and the properties of *ribX*, Antimicrobial test 3 was conducted. In this test, strains that overexpress the riboflavin operon *riboCg* were utilized to promote the production of riboflavin. The riboflavin-producing strains Transport3, Transport4, and Transport5 were constructed, where Transport3 served as the control strain, Transport4 harbored the *ribM* gene, and Transport5 harbored the *ribX* gene. Similar to Antimicrobial test 2, the strains were cultured in CGVXII selective media devoid of vitamins.

Figure 3.17 illustrates that all final biomass of Transport4 exceed all final biomasses of Transport3 and Transport5, while all final biomass of Transport3 is higher than all final biomass of Transport5. The trend observed in Transport4 shows a continuous increase in biomass from the 1:1 dilution up to a roseoflavin dilution of 1:32. After it stabilizes at a biomass of 0.84 g/L. The inhibitory constant, defined as half of the stable biomass, was determined to be 0.42 g/L. At the 1:2 dilution, Transport4 reaches the inhibitory constant, indicating a critical roseoflavin level of 0.05 g/L, considering the initial concentration of 0.1 g/L.

Table 3.9 presents the highest biomass of 0.86 ± 0.01 g/L achieved by Transport4 at a roseoflavin dilution of 1:256. For Transport3, the final biomass increases up to a roseoflavin dilution of 1:128. The high standard deviations observed for Transport5 result in similar final biomass values for the strains cultivated in dilutions ranging from 1:16 to 1:512.

The results suggested that *ribM* encodes an antiporter. Moreover, *ribX* decreased the roseoflavin tolerance indicating that roseoflavin was import into the cells. These findings will further be discussed in the forthcoming Discussion, section 4.

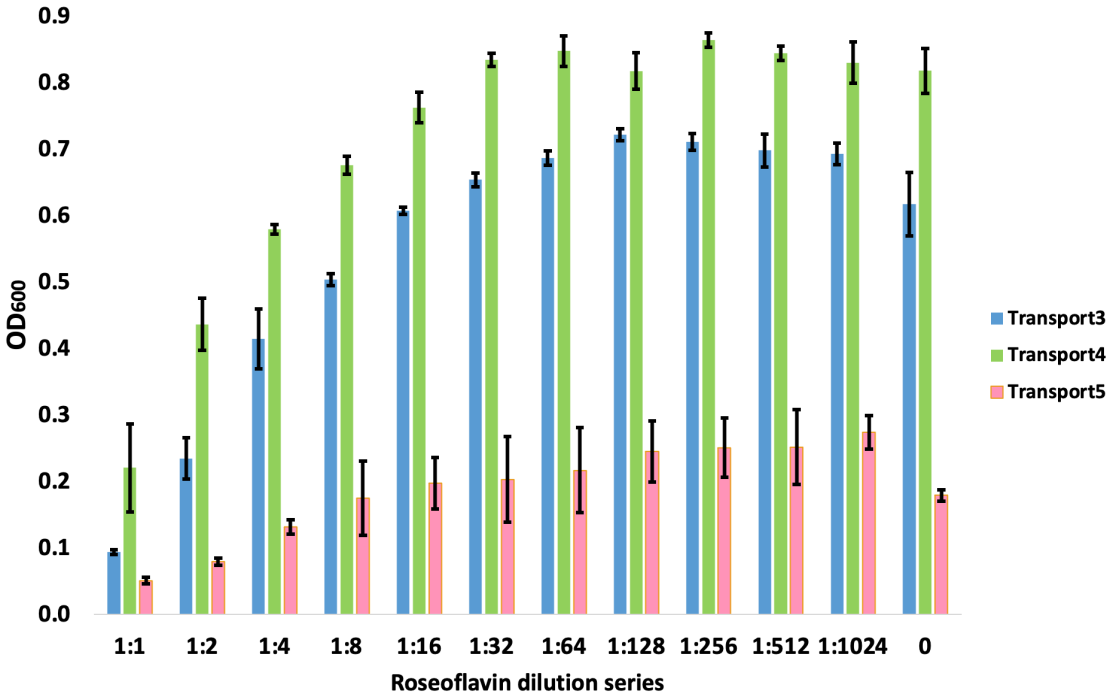

Figure 3.17: The final biomasses in Antimicrobial test 3 of Transport3, Transport4, and Transport5 growing on different roseoflavin concentrations are displayed. In blue is the control strain Transport3, in green is Transpor4, and in pink is Transport5. Along the x-axis are the dilution series of roseoflavin, starting on a roseoflavin concentration of 0.1 g/L. The growth media used was CGVXII selective media. The y-axis displays OD_{600} data given in a logarithmic scale. Means and standard deviations of the triplicates are shown.

Table 3.9: Biomasses for Transport3, Transport4, and Transport5 calculated from the measurements after 24 hours in Antimicrobial test 3.

Dilution series	Transport3 Biomass [g/L]	Transport4 Biomass [g/L]	Transport5 Biomass [g/L]
1:1	0.09 ± 0.00	0.22 ± 0.07	0.05 ± 0.01
1:2	0.23 ± 0.03	0.44 ± 0.04	0.08 ± 0.01
1:4	0.41 ± 0.04	0.58 ± 0.01	0.13 ± 0.01
1:8	0.50 ± 0.01	0.68 ± 0.01	0.18 ± 0.06
1:16	0.61 ± 0.01	0.76 ± 0.02	0.20 ± 0.04
1:32	0.65 ± 0.01	0.83 ± 0.01	0.20 ± 0.06
1:64	0.69 ± 0.01	0.85 ± 0.02	0.22 ± 0.06
1:128	0.72 ± 0.01	0.82 ± 0.03	0.25 ± 0.05
1:256	0.71 ± 0.01	0.86 ± 0.01	0.25 ± 0.05
1:512	0.70 ± 0.03	0.84 ± 0.01	0.25 ± 0.06
1:1024	0.69 ± 0.02	0.83 ± 0.03	0.27 ± 0.03
0	0.62 ± 0.05	0.82 ± 0.03	0.18 ± 0.01

4 Discussion

4.1 Assessment of roseoflavin production via microbial bioprocesses

Recently, *C. glutamicum* has been engineered for the production of riboflavin. In the study of Taniguchi and Wendisch (2015) [6], riboflavin was produced by overexpressing the *sigH* gene. *C. glutamicum* was engineered to utilize a mixture of mannose and xylose as the carbon sources, yielding the highest riboflavin titer of 0.027 g/L [36]. Another study by Pérez-García et al. (2022) [5], achieved a riboflavin titer of 1.291 g/L by overexpressing the riboflavin operon *riboCg*. The riboflavin production was achieved in combination with mannitol and glucose consumption from the sustainable feedstock of brown seaweed extract from *Laminaria hyperborea*. Riboflavin is the precursor of the antimicrobial compound roseoflavin, making antimicrobial fermentation of roseoflavin a possible production method [45]. The current production method is chemical synthesis [79]. The low molar yield of 5% makes the market price of roseoflavin high, depending on the supplier approximately 20-30 Eur per mg [45]. Hence, it is of great interest to study the possibility of roseoflavin production through fermentation. *S. davawensis* is a natural roseoflavin-producing bacteria, which contains the roseoflavin biosynthesis genes of *ribF*, *rosA*, *rosB*, and *rosC* in the bacterial genome. Mora-Lugo et al. (2019) [45] found out in their study that overexpression of the biosynthesis genes *rosAB* and *RFK* in *C. glutamicum* gave a maximum titer of 0.0007 g/L of roseoflavin. Additionally, a roseoflavin titer of 0.0014 g/L was obtained in *S. davawensis* overexpressing the endogenous genes *rosAB*. The roseoflavin titer of 0.0014 g/L was 78% higher than stains of *S. davawensis* not overexpressing the roseoflavin biosynthesis genes [45].

From Rudberg's study [1], roseoflavin biosynthesis genes *rosA* and *rosB* were tested, together with the transporter protein *ribM*, in a *C. glutamicum* riboflavin overproducing strain. In subsection 3.3 it was found that the *C. glutamicum* strain Roseo5 yielded the highest titer of 0.401 ± 0.008 g/L, 1.4 fold higher than the titer of Roseo4 and 286 fold higher than from the study of Mora-Lugo et al. In this Master's thesis, the maximum roseoflavin titer was obtained from Roseo3 containing all the genes in the roseoflavin biosynthesis pathway and a flavin transporter, seen in subsection 3.6. The roseoflavin titer of 4.065 ± 0.901 g/L was 10.1 fold higher than the highest titer in Rudberg's study [1] of Roseo5. This means that overexpressing *ribF* increased the titer by 914%. However, the high titers produced by Roseo3 in this study are possibly overestimated considering that the maximum riboflavin titer produced by Cg(pSym-*riboCg*), named CgRibo2 in the study of Pérez-García et al. (2022) [5], is 0.06 g/g. Therefore, as the strain CgRibo2 was utilized as a background for genetic engineering in this Master's thesis, and roseoflavin is derived from riboflavin, it is impossible to obtain a titer exceeding 0.06 g/g (0.6 g/L). Hence, the roseoflavin titers measured by means of HPLC must be a mixture of roseoflavin and another analyte with a similar retention time. As all obtained roseoflavin titers are likely affected by this unknown analyte, the absolute production values remain unknown.

The achieved riboflavin titers were not as anticipated, and did not meet the expected levels, subsection 3.3 and subsection 3.6. Despite using CgRibo2 [5], it was expected that the control strain, Roseo0, would exhibit similar riboflavin titers as CgRibo2, of 0.6 g/L in both growth experiments. Instead, a titer of 0.067 ± 0.002 g/L and 0.076 ± 0.002 g/L were obtained from Growth experiment 1 and Growth experiment 2, respectively. Thus, the observed riboflavin concentrations were 9.0 and 7.9 times lower than the expected values. Furthermore, Figure 3.7 and Figure 3.14 indicate

that all the other strains, namely Roseo1, Roseo2, Roseo3, Roseo4 and Roseo5, produced more riboflavin than Roseo0. Notably, the highest riboflavin titers were achieved by the strains Roseo3, Roseo4, and Roseo5, which additionally produce the highest roseoflavin titers. This finding is a contradiction to the assumption that riboflavin titers decrease as roseoflavin titers increase, due to roseoflavin being converted from riboflavin. A possible explanation is the presence of antimetabolite resistance in the strains [50]. This means that the strains are able to withstand the inhibitory effects of roseoflavin [50]. As a result, the trends in Figure 3.14 and Figure 3.13 display that when more roseoflavin is produced, the cells try to compensate and produce more riboflavin. In a related study by Dubey et al. (2021) [80], the authors investigated the impact of naturally occurring antimetabolites, namely L-thialysin and L-canavanine, shedding light on the effects of antimetabolites in strain engineering.

Similar methods for constructing the different *C. glutamicum* strains were conducted in the study by Mora-Lugo et al. (2019) [45] and our study. However, another shuttle plasmid pMKEx2, and the different gene insert *RFK* were utilized. Additionally, the *C. glutamicum* strains did not overexpress the riboflavin operon *riboCg*, which most likely affected the final roseoflavin titers in the two studies. The gene *RFK* encoding the human riboflavin kinase was used instead of *ribF* encoding the bifunctional riboflavin kinase/FAD synthetase of *C. glutamicum* [81] [45]. While *ribF* produces riboflavin-5' phosphate (RP) and processes RP further to FAD, *RFK* only produces RP due to it being a monofunctional enzyme [45] [82]. Additionally, the *C. glutamicum* genome naturally contains a bifunctional riboflavin kinase/FAD synthetase (GenBank WP_011014798.1) [81]. Hence, in this study, we explored roseoflavin production with and without the overexpression of *ribF* from the genome of *C. glutamicum*. It is worth mentioning that in the growth experiment conducted by Mora-Lugo et al., the *C. glutamicum* strains were cultivated in a minimal medium containing 4% glucose, allowing the strains to grow longer reaching higher biomass, whereas our study employed a medium with a glucose content of 1% [45]. As to determine the maximum expression level of roseoflavin biosynthetic genes, Northern Blot analysis was employed. Mora-Lugo et al. (2019) [45] found that the highest expression level was achieved when the genes were induced at 5 hours when the strains had reached the exponential phase. This support the findings in Rudberg's study [1] where optimal gene induction was in the exponential phase, after 6 hours [1]. For flask fermentation during growth experiments, all the strains in both studies were cultivated in minimal CGVXII media. The HPLC samples from the supernatant were collected after 18 hours in the study of Mora-Lugo et al. (2019) [45], whereas our study shows higher roseoflavin titers from HPLC samples collected after 72 hours in comparison to samples collected after 24 hours. An important difference in the studies is the result of increased roseoflavin production in all strains containing the *ribM* gene, where the study of Mora-Lugo et al. (2019) [45] obtained decreased roseoflavin titer in the *C. glutamicum* strain overexpressing the *ribM* gene. The roseoflavin titer of 0.0007 g/L decreased by 14% to 0.0006 g/L in the strain overexpressing *ribM*. Analysis of the remaining cell pellet indicated that less than 5% of the total produced roseoflavin remained. Hence, Mora-Lugo et al. (2019) [45] suggested that the export of roseoflavin was not primarily facilitated by the *ribM* gene, likely due to the hydrophobic isoalloxazine ring system present in roseoflavin. This ring system may enable roseoflavin to diffuse across the cytoplasmic membrane, leading to the detection of roseoflavin in the supernatants of *C. glutamicum* [45]. Another possible explanation based on our findings is that the strains did not overexpress any riboflavin operon. Our findings that *ribM* requires riboflavin import while exporting roseoflavin are explained later in the discussion, and

are a possible explanation why *ribM* did not increase the roseoflavin production in the study of Mora-Lugo et al. (2019) [45].

4.2 Closing the roseoflavin biosynthetic pathway via the expression of the *ribF* and *rosC* genes

Both studies of Mora-Lugo et al. (2019) [45] and our study, demonstrated increased roseoflavin production in strains where *RFK* or *ribF*, from *C. glutamicum*, was overexpressed. The genes encode enzymes involved in phosphorylating riboflavin to RP. While *ribF* produces RP and processes RP further to FAD, *RFK* only produces RP due to it being a monofunctional enzyme [45] [82]. Therefore, overexpression of *RFK* is expected to lead to higher RP levels, thereby benefiting the roseoflavin pathway [83] [84] [82].

A possible explanation for the presence of the unknown compound affecting our high roseoflavin titer of 4.065 ± 0.901 g/L obtained by Roseo3 may lie in the overexpression of *ribF* from *C. glutamicum*. As displayed in Figure 4.1, *ribF* converts RF to FAD which is not a part of the roseoflavin biosynthesis pathway [34]. Consequently, as FAD levels increase, the titers of roseoflavin decrease. To analyze this possibility, it would be necessary to obtain FAD standards and perform HPLC analysis, as the retention time of FAD is currently unknown to us.

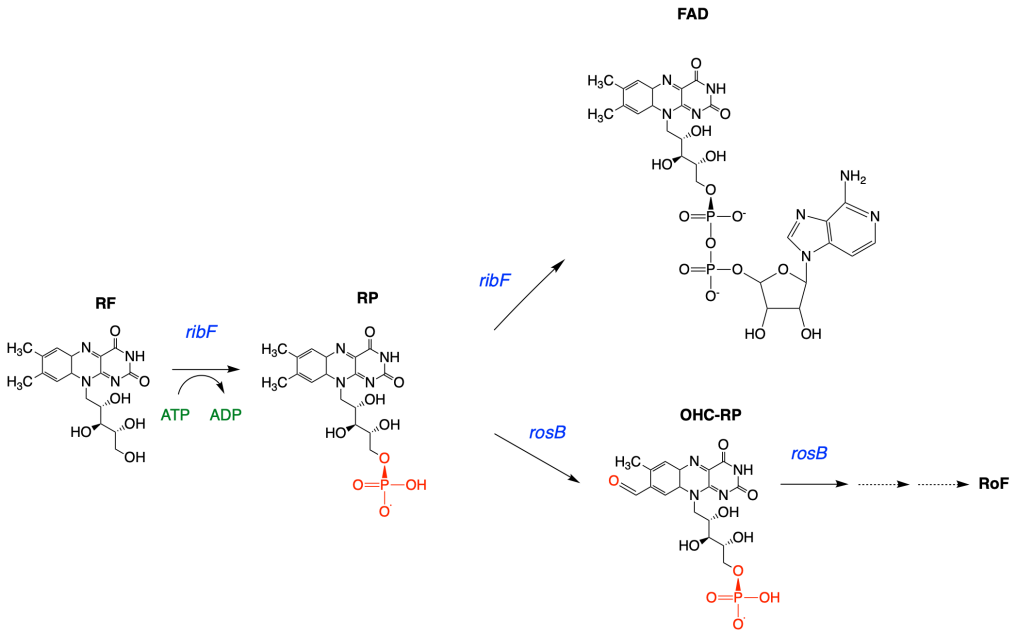

Figure 4.1: Biosynthetic pathway from riboflavin to either roseoflavin or FAD. The compounds are displayed in black bold writing, enzymes are displayed in blue. Red color display the molecular changes from riboflavin through the roseoflavin biosynthesis pathway. The abbreviated name, RF: Riboflavin, RP: FMN which is also called riboflavin-5´phosphate, FAD: Flavin adenine dinucleotide, and OHC-RF: 8-dimethyl-8-formyl FMN.

Furthermore, in the study of Pérez-García et al. (2022) [5], the detected riboflavin titer of Cg(pSym-*riboCg*) utilizing 1% of glucose, was found to be 0.6 g/L. Since both roseoflavin and FAD are products of riboflavin, the total amount of roseoflavin and FAD cannot exceed 0.6 g/L. Therefore, the unknown compound affecting the roseoflavin titer values in this study is likely another compound, and it cannot be any of the intermediates in the roseoflavin biosynthesis pathway. To find

the unknown compound, and to detect that roseoflavin was produced, nuclear magnetic resonance spectroscopy (NMR) should be conducted [85].

A multiple alignment analysis was carried out to look at the differences and similarities in the FASTA sequences of the three enzymes riboflavin kinase/FAD synthetase, riboflavin biosynthesis protein, and human riboflavin kinase, encoded by the three genes *ribF* from *C. glutamicum*, *ribF* from *S. davawensis*, and *RFK* synthetically constructed, respectively. In the GenBank riboflavin kinase/FAD synthetase is listed as WP_011014798.1 [81], riboflavin biosynthesis protein is listed as CCK27094.1 [86], and human riboflavin kinase is listed as QDM39061.1 [87]. The multiple alignment analysis is displayed in Figure 4.2

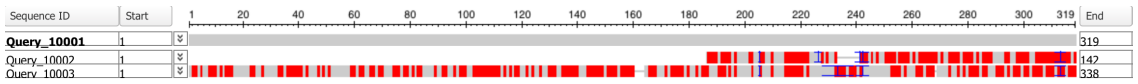

Figure 4.2: A multiple alignment analysis of *ribF* from the genome of *S. davawensis*, *ribF* from the genome of *C. glutamicum* and *RFK* synthetically constructed [88]. Query_10001 is Riboflavin biosynthesis protein RibF [*S. davawensis* JCM 4913] (GeneBank CCK27094.1), Query_10002 is riboflavin kinase [Synthetic construct] (GenBank QDM39061.1), and Query_10003 is bifunctional riboflavin kinase/FAD synthetase [*C. glutamicum*] (GenBank WP_011014798.1). Query_10001 was set as the anchor sequence and Query_10002 and Query_10003 were compared with Query_10001. Red color illustrates the differences in the sequences, whereas the grey color shows similarities.

In Figure 4.2, The FASTA sequence of *ribF* from *S. davawensis* was set as the anchor sequence. The comparison revealed variations, indicated by red regions, in both *ribF* from *C. glutamicum* and the synthetic construct of *RFK*, in contrast to the anchor sequence. Moreover, they all catalyze the enzymatic conversion of riboflavin to RP [45]. However, the alignment verifies that the FASTA sequences of the enzymes are different making it clear that further research should focus into overexpressing *RFK* instead of *ribF* from *C. glutamicum*. As *ribF* from the native roseoflavin producer *S. davawensis* has a different FASTA sequence than *ribF* from *C. glutamicum*, overexpressing *ribF* from *S. davawensis* should also be considered as a potential research direction.

The researchers Schneider et al. (2020) [53] discovered and identified the last unknown gene *rosC* (BN159_8033) in the roseoflavin biosynthetic pathway encoding an AFP phosphatase, Figure 1.5 *rosC* was discovered immediately downstream of *rosA* belonging to the same gene cluster of 10 genes as *rosA*. Through deletion of *rosC* in the genome of *S. davawensis*, reduced roseoflavin production was observed and AFP was not dephosphorylated [53]. Besides was *rosC* determined to be the fastest enzyme in the roseoflavin biosynthesis, (k_{cat} 31.3 ± 1.4 min^1) [53]. No previous study has investigated overexpressing of *rosC* for roseoflavin production. This Master's thesis showed decreased roseoflavin production in all strains harboring *rosC* expression, compared to strains without *rosC*. The results contradict the assumed prediction that *rosC* would optimize and increase the roseoflavin titers. The sequencing results, in subsection 3.1 and subsection 3.4 verified the correct gene sequences of Roseo1 and Rosoe2 and showed an inconclusive gene sequence of Roseo3. Hence, Roseo1 contained *rosABC*, Roseo2 contained *rosABC-ribM*, whereas Roseo3 missed *rosC*, and contained *ribF-rosAB-ribM*. In subsection 3.3 the roseoflavin titer of Roseo1 was measured to 0.033 ± 0.002 g/L, which was lower than 0.296 ± 0.026 g/L obtained by Roseo4 containing *rosAB*. Similarly, was the roseoflavin titers of 0.045 ± 0.001 g/L from Roseo2 lower than the titer of 0.401 ± 0.008 g/L from Roseo5 overexpressing *rosAB-ribM*. Rudberg's study [53] performed a BLASTp search of *rosC* (BN159_8033) in the genome of *C. glutamicum*, and uncovered a phosphoglycerate mutase/fructose-2,6-bisphosphatase and a histidine phosphatase protein

with the same catalytic function as AFP phosphatase has in *S. davawensis*. As *C. glutamicum* is able to convert AFP to AF, the roseoflavin biosynthetic pathway is fulfilled. However, in some cases, the gene order of the operon has an impact on the final product, as exemplified in the study of Goldbeck et al. (2021) [89]. Here, the order of the genes played a crucial role in the production of the antimicrobial compound the bacteriocin pediocin in *C. glutamicum* strains. The potential influence of gene order on production yield should not be overlooked, as rearranging the gene order in our study has the potential to improve roseoflavin production for strains containing *rosC*. Based on the discovery that *rosC* is located directly downstream of *rosA* [53], a proposed reordering of the genes could be *rosACB* instead of *rosABC*. Sometimes the gene expressions in a synthetic operon have to be modulated to achieve better production values as in the studies of Henke et al. (2016) [90] and Gießelmann et al. (2019) [91]. Henke et al. (2016) [90] balanced the expression of crtW and crtZ by using different ribosome binding sites, spacing, and translational start codon to produce the carotenoid astaxanthin [90]. As a result, a volumetric productivity of 0.0004 g/Lh was achieved. The research of Gießelmann et al. (2019) [91] achieved an ectoine titer of 65 g/L by using transcriptional balancing of the ectoine pathway taken from *Pseudomonas stutzeri* in *C. glutamicum* strains. 19 synthetic promotors and three linker elements were randomly combines for the purpose [91]. Therefore, different expressions of the genes in the roseoflavin biosynthetic pathway should be considered.

4.3 Insights on the transporter proteins encoded by *ribM* and *ribX*

The properties of the transporter proteins encoded by *ribM* and *ribX* have been investigated in the study by Schneider et al. (2021) [49]. Through deletion of the riboflavin biosynthetic operon *ribE1MAB5H* containing *ribM*, a second riboflavin transport system encoded by *ribXYZ* was found in the genome of *S. davawensis*. Hence, *ribXY* was discovered to be a riboflavin importer and not a roseoflavin transporter, which it previously was suspected of. The genes *ribXYZ* were encoding an ABC transporter, which is in the superfamily of membrane proteins that converts the energy gain from ATP hydrolysis into substrate export or import through the transmembrane [92]. Different parts of the transmembrane are encoded by *ribXYZ*, as explained in subsubsection 1.3.3. In the study, *ribM* was also found to be a riboflavin importer, and the transporter protein only protected the cells from roseoflavin in the presence of riboflavin. They concluded that *ribM* could not be a roseoflavin exporter since it did not protect cells in the absence of riboflavin. Riboflavin was suggested as being an agonist, accumulating and protecting the cells from roseoflavins toxic effects. Contrarily, in the study of Hemberger et al. (2011) [54], *ribM* was classified as a riboflavin/roseoflavin transporter and was proven to increase riboflavin uptake in *E. coli* and in *B. subtilis*. In this Master's thesis, the gene *ribM* from the genome of *S. davawensis* and *ribX* from the genome of *C. glutamicum* were overexpressed in different *C. glutamicum* strains. Through Antimicrobial test 1, subsubsection 3.7.1, carried out in vitamin-rich 2TY media, the strain Transport1 containing *ribM* was more tolerant of the different roseoflavin concentrations than the control strain Transport0. At the roseoflavin dilution of 1:64, Transport1 was stable, and the critical roseoflavin level was found to be 0.05 g/L. Due to better survival in a vitamin-rich media, *ribM* was suspected of being a roseoflavin exporter and a vitamin importer. Antimicrobial test 2, subsubsection 3.7.2, assayed the growth of Transport0, Transport1, and Transport2 strains in minimal media without vitamins, resulting in low roseoflavin tolerance for all the strains. Transport2 was constructed to contain the *ribX* gene and the growth of the strains, Transport0,

Transport1, and Transport2 in Antimicrobial 2, was equal for all the strains. Low roseoflavin tolerance and equal growth indicated that the transporter protein encoded by *ribM* required vitamins in order to export roseoflavin. Additionally, it is an indication that the vitamins were imported into the cytoplasm of the cells when roseoflavin was exported. Due to the findings in Antimicrobial test 2 and the findings by Schneider et al. (2021) [49], that *ribM* could not encode a roseoflavin exporter, it is suggested a hypothesis that *ribM* encodes an antiporter. An antiporter is a transmembrane protein transporting two molecules at the same time in opposite directions [93], meaning through cotransport, one molecule is imported to the cytoplasm and one molecule is exporter to the exterior of the cell. To further test the hypothesis, the strains Transport3, Transport4, and Transport5 were constructed and further tested in Antimicrobial test 3, subsubsection 3.7.3. In addition for the control strain Transport3 to contain the empty plasmid, Transport4 to overexpress *ribM*, and Transport5 to overexpress *ribX*, all strains were constructed to overexpress the riboflavin operon *riboCg*. The highest roseoflavin tolerance was observed in Transport4, followed by Transport3 and Transport5. The stable biomass measured for Transport4 was 0.84 g/L. The findings support the hypothesis that *ribM* is an antiporter exporting roseoflavin at the same time as riboflavin is imported. Additionally, the observed trends in the growth experiments revealed that strains overexpressing *ribM* exhibited higher roseoflavin titers compared to those without, supporting the proposed hypothesis. Another finding from Antimicrobial test 3 was the efficiency of the transporter protein encoded by *ribX* from the genome of *C. glutamicum*. Decreased roseoflavin tolerance in the riboflavin overproducing strain Transport5, suggested roseoflavin import into the cytoplasm. Roseoflavin import increased the toxic conditions, yielding less biomass. Similar structures of riboflavin and roseoflavin make riboflavin importers able to import roseoflavin [46] [2]. Comparing the roseoflavin tolerance of Transport5 to Transport2 in Antimicrobial test 2, the roseoflavin tolerance was higher for Transport5 which overproduces riboflavin. Hence, *ribX* from the genome of *C. glutamicum* was suspected of both being a riboflavin and roseoflavin importer in our study.

The tested *ribX* gene from the genome of *C. glutamicum*, differed from the *ribX* gene (BN159_7987) from the genome of *S. davawensis* utilized in the research of Schneider et al. (2021) [49]. The GenBank listed the FASTA sequence of *ribX* in *C. glutamicum* as QYO73792.1, encoding a putative membrane protein-C [94]. This gene is also associated with an ABC transporter where only ribX is known. The FASTA sequence of *ribX* (BN159_7987) from the genome of *S. davawensis* is denoted as CCK32366.1 and encode a binding-protein-dependent transport systems inner membrane component [95]. A multiple alignment analysis of the FASTA sequences was conducted to compare the sequences, and the resulting alignment is illustrated in Figure 4.3. Query_10001 is the putative membrane protein in *C. glutamicum*, and Query_10002 is the binding-protein-dependent transport systems inner membrane component in *S. davawensis*. Conserved amino acids are highlighted in red, while blue amino acids display the differences.

```
Query_10001  1    --------------------MTTNAPDGATNNINNAHSGAVGKPKVQLSDAEIQEYTAAFAGTTTTKPWEL-----EVTT  55
Query_10002  1    MFPRSATRDTSRSEADNQESVTADESESA-RSIGPEKSTGRQKSRRRSNGRGIGILAPLLLGLLLVALWDAVTRFGAVST  79

Query_10001  56   KFLKKIAWVAVVVIMAVHIFMGAVVDVDFTGAAVTFVDTLAFPALGIIFSVLVFLGLTRPRVRANEDGVEVRNFIGTRFY  135
Query_10002  80   FFLPTPYSIAKELVSQSQD--GFLLDY----LAQTVTESVAGSALGLAVALPLAYLIARNRVAAAALQPYVAASQAVPAV  153

Query_10001  136  PWVVIYGMSFPKGSSVARLELPDFEFVPMWAFQSRDGEDVVRAVATFRDLENKYMPED----------------------  193
Query_10002  154  ALAPLLALWFGYGLLPIAVLCALLVFFPI----------LVSTVVGLRQIDPDVMNAARVDGVGRVQMLRHIEWPLALPS  223

Query_10001       ------------------------------------------------------------------------
Query_10002  224  TLAGIRAGLTLSVTGAVVGEFVVGGDGLGQLLTVQRSEADTVGLFATLCVLTLLAACFYGLMLLLERWARW  294
```

Figure 4.3: Compared fasta sequences of *ribX* from the genome of *C. glutamicum* (on top) and *S. davawensis* (on the bottom), respectively [88]. Red color display conserved amino acids, blue are different residues, and grey residues contain gaps in the sequencing compaction. Query_10001 are the putative membrane protein, RibX-family [*C. glutamicum*], and Query_10002 is the riboflavin ABC transporter permease [*S. davawensis*].

In the research of Schneider et al. (2021) [49] both genes *ribXY*, being part of the ABC transporter genes *ribXYZ*, were investigated and expressed simultaneously in the findings which revealed that *ribXY* functions as a riboflavin importer. As this Master´s thesis only explores *ribX* from the genome of a different bacteria, and the FASTA sequences showed dissimilarities in the alignment, the trends displayed in Antimicrobial test 3 are not comparable with the results of Schneider et al.(2021) [49].

4.4 *C. glutamicum* resilience against antimicrobial agents.

Based on the research conducted by Mora-Lugo et al. (2019) [45], the study revealed that a recombinant strain of *S. davawensis* exhibited favorable characteristics for roseoflavin production. In comparison to both its wild-type strains and the recombinant *C. glutamicum* strains, the recombinant *S. davawensis* strain demonstrated a substantial increase in productivity. Notably, the overproduction of roseoflavin did not affect the growth of *S. davawensis* which can be attributed to the presence of specialized elements within its genetic makeup. These include a RoFMN-insensitive FMN riboswitch [96], a dedicated roseoflavin exporter [54] [97], and the enzymes *rosA* and *rosB* that serve as a protective system against toxic riboflavin analogs [98] [55] [45]. Nevertheless, in larger-scale industrial production, it is worth considering that *C. glutamicum* emerge as a favorable host for roseoflavin production due to its simpler cultivation requirements in contrast to the filamentous nature of *S. davawensis*. *S. davawensis* exhibits surface adhesion and forms aggregates, posing challenges for cultivation in vessels [45]. Consequently, processing the metabolites becomes challenging, making bacteria such as *C. glutamicum* more advantageous for industrial production. Additionally, Mora-Lugo et al. (2019) [45] observed *C. glutamicum* reached maximum roseoflavin titers faster compared to *S. davawensis*. After 1 day, the maximum roseoflavin level was reached in *C. glutamicum* whereas *S. davawensis* required a duration of 10 days. With the high repertoire of genetic engineering tools available for *C. glutamicum* [99] [10], it is a favorable bacteria to utilize. Contrary to the study of Mora-Lugo et al. (2019) [45], our research using *C. glutamicum* demonstrates considerable resilience against roseoflavin as an antimicrobial compound. The roseoflavin titer achieved by the *C. glutamicum* strain Roseo3 was higher than that of *C. glutamicum* strains in the study of Mora-Lugo et al. (2019) [45]. However, the high roseoflavin concentration in our study made the growth of Roseo3 slower as compared to the other strains in Growth experiment 2. However, after 72 hours the final biomass reached similar values as the other constructed strains,

displayed in Figure 3.12. Another antimicrobial compound studied as a novel production compound of *C. glutamicum*, is violacein. Violacein properties are antibacterial [18], antitumoral [19], antiviral [100], and antioxidant [101]. Fermentation of violacein in natural producers was limited and difficult on a large scale [102]. Hence, violacein production in *C. glutamicum* has been studied, due to *C. glutamicum* being used for the production of tryptophan, and tryptophan is the precursor of violacein. Hongnian et al. (2016) [10] found in their study the highest violacein titer and productivity ever reported. The violacein titer was 5.436 g/L and achieved in a bioreactor of 3 L [10]. This high titer together with our collected data indicates that *C. glutamicum* is a robust bacterial host for the production of antimicrobial compounds.

4.5 Outlook

Several avenues for further investigation can be pursued based on the findings of this study. Firstly, considering the observed toxicity of roseoflavin toward *C. glutamicum* cells, the RoFMN non-sensitive FMN riboswitch in the genome of *S. davawensis* can be investigated for implementation in roseoflavin producing *C. glutamicum* strains [45]. The toxicity of roseoflavin was seen in Growth experiment 2, due to the slow growth of the highest roseoflavin producer strain Roseo3. The high roseoflavin titer of 4.065 ± 0.901 g/L produced by Roseo3 was contaminated by an unknown compound which resulted in a masked titer. After further optimization of the method, and after the improvement in the roseoflavin titers, the production can be scaled up in bioreactors. *C. glutamicum* is a highly robust bacterium that is commonly employed in bioreactors for the synthesis of innovative compounds. Noteworthy achievements in terms of compound production have been reported in studies conducted by Rohles et al. (2016) [103], Pérez-García et al. (2017) [104], and Jorge et al. (2016) [105]. Specifically, these studies have demonstrated the successful generation of 28.0 g/L of 5-aminovalerate, 22.0 g/L of ectopine, and 63.2 g/L of gamma-aminobutyric acid (GABA), respectively. Moreover, the antimicrobial tests exploring the function of *ribM* revealed an inhibitory constant of 0.05 g/L roseoflavin. And the roseoflavin level should be kept below this level for growth in bioreactors.

The production of compounds can be enhanced through the application of evolutionary engineering. Adaptive Laboratory Evolution (ALE), a method that utilizes natural selection, allows for the optimization of a specific characteristic in a production strain without the need for prior knowledge of its genetic background [106]. This approach becomes more feasible when there are options available to enhance growth advantages [107]. For instance, the increased tolerance towards a particular compound, such as roseoflavin in our case, provides a significant advantage in optimizing the growth rate [108]. ALE has been successfully employed in various studies with *C. glutamicum*, including enhancing tolerance to higher temperatures [109], improving methanol utilization and wild-type growth rate [106], enhancing consumption of xylose and cellobiose, and increasing the production of ornithine and glutarate [110] [106]. Hence, ALE should be investigated to increase the roseoflavin titer and increase the roseoflavin tolerance of *C. glutamicum*.

The production method should further be optimized by expressing *ribF* from the genome of *S. davawensis* or the synthetically constructed *RFK* gene. As we saw the roseoflavin titer increased with the strain overexpressing *ribF*. However, *ribF* from *C. glutamicum* catalyzes the intermediate RB of the roseoflavin biosynthesis pathway to FAD, which may have affected the roseoflavin titer. *RFK* should in theory produce more RP, since *RFK* encodes the monofunctional enzyme

only producing RB [45]. Hence, overexpression of *RFK* should be a priority for further process optimization.

To fulfill the roseoflavin biosynthetic pathway and optimize the roseoflavin production, *rosC* encoding AFP phosphatase was overexpressed [53]. The finding of decreased roseoflavin production in strains overexpressing *rosC* was surprising. A BLAST search revealed native enzymes in *C. glutamicum* sharing up to 34% similarity with the protein encoded by *rosC*, making the roseoflavin biosynthetic pathway complete without the overexpression of *rosC*. This gene is located immediately downstream of *rosA* in the genome of *S. davawensis* [53]. As the *rosC* gene was difficult to amplify, an alternative approach could be to amplify *rosA* and *rosC* simultaneously from *S. davawensis* as one block [53]. Previous studies in *C. glutamicum* has discovered that gene order in synthetic operons play an important role in production yield [89] [91]. Therefore, is rearranging the gene order from *rosABC* to *rosACB* interesting for further research.

A main focus for investigation should involve identifying the unknown compound that elutes at the same retention time as roseoflavin and affects the measured roseoflavin titers. For this, NMR spectroscopy should be employed. With NMR analysis, the chemical structure of the unknown compound can be evaluated, leading to a better understanding of its role in the observed roseoflavin titers [85]. Additionally, an HPLC analysis of a FAD sample should be conducted. The analysis aims to determine whether the unknown compound could be FAD.

Furthermore, glucose serves as a native carbon source for common biotechnological microorganisms such as *B. subtilis* [111], *E. coli* [112], and *C. glutamicum* [113]. However, glucose in commonly used in human food industry, making the utilization of glucose for biobased metabolite production a competition [22]. Hence, other non-food sustainable carbon sources can be utilized, and sustainable feedstocks from agriculture, industrial waste, and seaweed are optional carbon sources that should be utilized [113]. Seaweed is a promising sustainable feedstock for *C. glutamicum* [5]. The advantages of seaweed biomass are that it provides a transition towards circular and low fossil carbon economies because of such as cultivation does not require arable land, minimal freshwater is needed for cultivation, and the composition contains fermentable carbohydrates [114] [5]. The research conducted by Pérez-García et al. (2022) demonstrated the potential of Norwegian brown seaweed *L. hyperborea* as a microbial substrate for *C. glutamicum*. Thus, coupling the genes responsible for roseoflavin production with specific *C. glutamicum* strains that utilize alternative feedstocks, such as the sugar alcohol mannitol or the glucose-based polymer laminarin derived from brown seaweed, hold promise for further optimization [5].

The antimicrobial tests examined the function of *ribX* from the genome of *C. glutamicum* as a transporter protein. *ribX* is a part of a ABC transporter, where *ribY* and *ribZ* remain unidentified. In the genome of *S. davawensis* the ABC transporter genes *ribXYZ* were found and investigated in the research of Schneider et al. (2021) [49]. Throughout our study, *ribX* was found to be a riboflavin and roseoflavin importer. Further antimicrobial tests can explore the genes *ribXYZ* from the genome of *S. davawensis*, to test their functions as both riboflavin and roseoflavin importers.

Lastly, the application of RNA sequencing can prove valuable in identifying secretion systems that could serve as potential metabolic targets for enhancing roseoflavin production. By elucidating the underlying mechanisms and pathways involved, this approach offers insights for maximizing the production of roseoflavin. In the research conducted by Pérez-García et al. (2019) [115],

they employed RNA sequencing to identify the proline permease ProP as a potential system for pipecolic acid uptake, thus demonstrating the practical application of this sequencing technique in their study.

5 Conclusion

This Master's thesis successfully reached production of roseoflavin using engineered strains of *C. glutamicum*. The overexpression of the *rosAB* genes from *S. davawensis* was sufficient for roseoflavin production in a riboflavin-producing *C. glutamicum* strain. Furthermore, co-expression of the *ribF* gene increases the roseoflavin titer, as did co-expression with the *ribM* gene. Additionally, overexpression of *ribM* reduced the toxicity of roseoflavin and was found through antimicrobial tests to be an antiporter co-transporting roseoflavin out of the cells while importing riboflavin. Moreover, it was indicated from the antimicrobial tests that *ribX*, from the genome of *C. glutamicum*, encodes a riboflavin importer. Due to the similar structures of roseoflavin and riboflavin, the transporter also functions as a roseoflavin importer, worsening the environment for cell growth. The antimicrobial tests obtained a roseoflavin inhibitory constant of 0.05 g/L.

The highest roseoflavin titer was obtained by the strain Roseo3, yielding the roseoflavin titer of 4.065 ± 0.9006 g/L. The high titer was obtained through optimization of the strains, and Roseo3 was constructed to overexpress the genes *ribF*, *rosAB*, and *ribM*. However, an unknown compound influenced that titer, making the exact value of pure roseoflavin unknown. Nevertheless, the production method of microbial fermentation for roseoflavin shows to be promising, and further optimization of the process will hopefully render it a viable alternative to the costly and energy-inefficient chemical synthesis. This study opens doors for future work on the production of roseoflavin by *C. glutamicum*, as well as in efforts for sustainable production by means of alternative feedstocks.

References

[1] Rudberg R. and Pérez-García F. *Production of Roseoflavin Using the Engineered Bacteria, Corynebacterium glutamicum*, 2022.

[2] Kißling L., Schneider C., Seibel K., Dorjjugder N., Busche T., Kalinowski J., and Mack M. *The roseoflavin producer Streptomyces davaonensis has a high catalytic capacity and specific genetic adaptations with regard to the biosynthesis of riboflavin*, 2020. URL https://sfamjournals.onlinelibrary.wiley.com/doi/10.1111/1462-2920.15066. Downloaded: 26.04.2023.

[3] ThermoFisher Sientific. *Raney Nickel Safety data sheet*, 2021. URL https://www.fishersci.fi/store/msds?partNumber=10172953&productDescription=500GR+Raney-Nickel2C+activated+catalyst2C+5025+slurry+in+watercountryCode=FIlanguage=en. Downloaded: 27.04.2023.

[4] MedChemExpress. *Roseoflavin*, 2022. URL https://www.medchemexpress.com/roseoflavin.html. Downloaded: 27.04.2023.

[5] Pérez-García F., Klein V. J., Brito L. F., and Brautset T. *From Brown Seaweed to a Sustainable Microbial Feedstock for the Production of Riboflavin*, 2022. URL https://www.frontiersin.org/articles/10.3389/fbioe.2022.863690/full Downloaded: 19.02.2023.

[6] Taniguchi H. and Wendisch V. F. Exploring the role of sigma factor gene expression on production by corynebacterium glutamicum: sigma factor h and fmn as example, 2015. URL https://pubmed.ncbi.nlm.nih.gov/26257719/. Downloaded: 06.06.2023.

[7] Wolf S., Becker J., Tsuge Y., Kawaguchi H., Kondo A., Marienhagen J., Bott M., Wendisch V. F., and Wittmann C. *Advances in metabolic engineering of Corynebacterium glutamicum to produce high-value active ingredients for food, feed, human health, and well-being*. https://doi.org/10.1042/EBC20200134, 2021. Downloaded: 29.03.2023.

[8] microbiology. *Corynebacterium glutamicum*, 2011. URL https://microbewiki.kenyon.edu/index.php/Corynebacterium_glutamicum. Downloaded: 29.03.2023.

[9] Tsuge M. H. and Elevated Y. *Elevated, non-proliferative temperatures change the profile of fermentationproducts in Corynebacterium glutamicum*. Appl Microbiol Biotechnol 105, 367–377 (2021)., 2020. URL https://doi.org/10.1007/s00253-020-11024-w. Downloaded: 29.03.2023.

[10] Sun H., Zhao D., Xiong B., Zhang C., and Bi C. *Engineering Corynebacterium glutamicum for violacein hyper production*, 2016. URL https://microbialcellfactories.biomedcentral.com/articles/10.1186/s12934-016-0545-0. Downloaded: 29.03.2023.

[11] Takeno S. Ikeda M. *Amino acid production by Corynebacterium glutamicum*. Yukawa H, Inui M, editors, 2013. Downloaded: 08.04.2023.

[12] Gopinath V. and Nampoothiri K. M. Corynebacterium glutamicum. In Batt C. A. and Tortorello M. L., editors, *Encyclopedia of Food Microbiology (Second Edition)*, pages 504–517. Academic Press, Oxford, second edition edition, 2014. ISBN 978-0-12-384733-1. doi:

https://doi.org/10.1016/B978-0-12-384730-0.00076-8. URL https://www.sciencedirect.com/science/article/pii/B9780123847300000768. Downloaded: 29.03.2023.

[13] Zahoor A., Lindner S. N., and Wendischa V. F. *Metabolic engineering of Corynebacterium glutamicum aimed at alternative carbon sources and new products*, 2012. URL https://www.ncbi.nlm.nih.gov/pmc/articles/PMC3962153/. Downloaded: 25.10.2022.

[14] Nešvera J. and Pátek M. Tools for genetic manipulations in corynebacterium glutamicum and their applications, 2011. URL https://pubmed.ncbi.nlm.nih.gov/21519933/. Downloaded: 11.06.2023.

[15] Bathe B., Kalinowski J., and Pühler A. A physical and genetic map of the corynebacterium glutamicum atcc, 2004. URL https://link.springer.com/article/10.1007/BF02173771. Downloaded: 11.06.2023.

[16] Krömer J. O., Sorgenfrei O., Klopprogge K., Heinzle E., and Wittmann C. In-depth profiling of lysine-producing corynebacterium glutamicum by combined analysis of the transcriptome, metabolome, and fluxome, 2004. URL https://www.ncbi.nlm.nih.gov/pmc/articles/PMC355958/. Downloaded: 11.06.2023.

[17] Becker J., Rohles C. M., and Wittmann C. *Metabolically engineered Corynebacterium glutamicum for bio-based production of chemicals, fuels, materials, and healthcare products*, 2018. URL https://pubmed.ncbi.nlm.nih.gov/30031852/. Downloaded: 29.03.2023.

[18] Choi S. Y., Kim S., Lyuck S., Kim S. B., and Mitchell R.J. High-level production of violacein by the newly isolated duganella violaceinigra str. ni28 and its impact on staphylococcus aureus, 2015. URL https://link.springer.com/content/pdf/10.1038/srep15598.pdf. Downloaded: 28.05.2023.

[19] Platt D., Amara S., Mehta T., Vercuyssee K., Myles E. L., Johnson T., and Tiriveedhi V. Violacein inhibits matrix metalloproteinase mediated cxcr4 expression: potential anti-tumor effect in cancer invasion and metastasis, 2014. URL https://www.sciencedirect.com/science/article/pii/S0006291X14019445. Downloaded: 28.05.2023.

[20] National Center for Biotechnology Information. *PubChem Compound Summary for CID 11053, Violacein*, 2023. URL https://pubchem.ncbi.nlm.nih.gov/compound/Violacein. Downloaded: 29.03.2023.

[21] Hoshino T. *Violacein and related tryptophan metabolites produced by Chromobacterium violaceum: biosynthetic mechanism and pathway for construction of violacein core*, 2011. URL https://link.springer.com/article/10.1007/s00253-011-3468-z. Downloaded: 06.04.2023.

[22] Zhang B., Jiang Y., Li Z., Wang F., and Wu X. Y. Recent progress on chemical production from non-food renewable feedstocks using corynebacterium glutamicum, 2020. URL https://www.frontiersin.org/articles/10.3389/fbioe.2020.606047/full. Downloaded: 11.06.2023.

[23] Bren A., Park J. O., Towbin B. D., Dekel E., Rabinowitz J. D., and Alon U. Glucose becomes one of the worst carbon sources for e.coli on poor nitrogen sources due to suboptimal

levels of camp, 2016. URL https://www.nature.com/articles/srep24834. Downloaded: 11.06.2023.

[24] Aggarwal R. K. and Narang A. Inducer exclusion, by itself, cannot account for the glucose-mediated lac repression of escherichia coli, 2021. URL https://www.cell.com/biophysj/pdf/S0006-3495(22)00045-5.pdf. Downloaded: 11.06.2023.

[25] Jurtshuk P. Bacterial metabolism, 1996. URL https://www.ncbi.nlm.nih.gov/books/NBK7919/. Downloaded: 11.06.2023.

[26] Powers H. J. *Riboflavin (vitamin B-2) and health*, 2003. URL https://academic.oup.com/ajcn/article/77/6/1352/4689829. Downloaded: 10.04.2023.

[27] Giancaspero T. A., Colella M., Brizio C., Difonzo G., Fiorino G. M., Leone P., Brandsch R., Bonomi F., Iametti S., and Barile M. *Remaining challenges in cellular flavin cofactor homeostasis and flavoprotein biogenesis*, 2019. URL https://www.researchgate.net/figure/FMN-and-FAD-synthesis-from-riboflavin-and-main-biological-functions\protect\@normalcr\relax-of-flavoenzymes-in_fig2_275771315. Downloaded: 10.04.2023.

[28] Shuang L., Hu W., Wang Z., and Chen T. *Production of riboflavin and related cofactors by biotechnological processes*, 2020. URL https://microbialcellfactories.biomedcentral.com/articles/10.1186/s12934-020-01302-7. Downloaded: 10.04.2023.

[29] Vabulas R. M. *Ferroptosis-Related Flavoproteins: Their Function and Stability*, 2021. URL https://www.ncbi.nlm.nih.gov/pmc/articles/PMC7796112/. Downloaded: 10.04.2023.

[30] National Institutes of Health (NIH). *Riboflavin*, 2022. URL https://ods.od.nih.gov/factsheets/Riboflavin-HealthProfessional/. Downloaded: 10.04.2023.

[31] Averianova L. A., Balabanova L. A., Son O. M., Podvolotskaya A. B., and Tekutyeva L. A. *Production of Vitamin B2 (Riboflavin) by Microorganisms: An Overview*, 2020. URL https://www.ncbi.nlm.nih.gov/pmc/articles/PMC7693651/. Downloaded: 10.04.2023.

[32] Schwechheimer S. K., Park E. Y., Revuelta J. L., Becker J., and Wittmann C. *Biotechnology of riboflavin*, 2016. URL https://link.springer.com/article/10.1007/s00253-015-7256-z. Downloaded: 10.04.2023.

[33] Hiltunen H. M., Illarivonov b., and Grimm B. *Arabidopsis RIBA Proteins: Two out of Three Isoforms Have Lost Their Bifunctional Activity in Riboflavin Biosynthesis*, 2012. URL https://www.researchgate.net/figure/Biosynthesis-of-riboflavin-Riboflavin-biosynthesis-is-initiated-by-the-enzymes-GTP_fig1_233829340. Downloaded: 20.04.2023.

[34] KEGG Pathway. *Riboflavin metabolism - Corynebacterium glutamicum ATCC 13032 (Bielefeld)*, 2021. URL https://www.genome.jp/kegg-bin/show_pathway?cgb00740. Downloaded: 19.04.2023.

[35] InterPro. *FAD synthetase-Overlapping homologous superfamilies*, 2020. URL https://www.ebi.ac.uk/interpro/entry/InterPro/IPR015864/. Downloaded: 19.04.2023.

[36] Pérez-García F., Burgardt A., Kallman D R., Wendisch V. F., and Bar N. *Dynamic Co-Cultivation Process of Corynebacterium glutamicum Strains for the Fermentative Production of Riboflavin*, 2021. URL https://www.mdpi.com/2311-5637/7/1/11/htm. Downloaded: 10.04.2023.

[37] Kovářová J. and Barrett M. P. *The Pentose Phosphate Pathway in Parasitic Trypanosomatids*, 2016. URL https://www.sciencedirect.com/science/article/pii/S1471492216300137#fig0015. Downloaded: 21.04.2023.

[38] Shi S., Chen T., Zhang Z., Chen X., and Zhao X. M. *Transcriptome analysis guided metabolic engineering of Bacillus subtilis for riboflavin production*, 2009. URL https://www.semanticscholar.org/paper/Transcriptome-analysis-guided-metabolic-engineering-Shi-Chen/2a443927bd69bfece476704a526da734420c9db3. Downloaded: 21.04.2023.

[39] Dasgupta B., Hirota Y., and Fujii Y. et al. *Targeting Energy Metabolism to Overcome Therapeutic Resistance of Glioblastoma and Tumor-associated Edema.*, 2021. URL https://www.ncbi.nlm.nih.gov/books/NBK570702/figure/Ch7-f0002/. Downloaded: 22.04.2023.

[40] Delarue M., Duclert-Savatier N., Miclet E., Haouz A., Giganti D., Ouazzani J., Lopez P., Nilges M., and Stoven V. Three dimensional structure and implications for the catalytic mechanism of 6-phosphogluconolactonase from trypanosoma brucei. *Journal of Molecular Biology*, 366(3):868–881, 2007. ISSN 0022-2836. doi: https://doi.org/10.1016/j.jmb.2006.11.063. URL https://www.sciencedirect.com/science/article/pii/S002228360601610X. Downloaded: 25.04.2023.

[41] Tazzini N. *GLYCOLYSIS: STEPS, ENZYMES, AND PRODUCTS*, 2018. URL https://www.tuscany-diet.net/2018/02/06/glycolysis/. Downloaded: 25.04.2023.

[42] Gerald Litwack. Chapter 10 - nucleic acids and molecular genetics. In Gerald Litwack, editor, *Human Biochemistry (Second Edition)*, pages 287–356. Academic Press, Boston, second edition edition, 2022. doi: https://doi.org/10.1016/B978-0-323-85718-5.00010-8. URL https://www.sciencedirect.com/science/article/pii/B9780323857185000108. Downloaded: 25.04.2023.

[43] nsturm. *Purine metabolism*, 2020. URL http://www2.csudh.edu/nsturm/CHEMXL153/PurineMetabolism.htm. Downloaded: 21.04.2023.

[44] Ahmad M., Wolberg A., and Kahwaji C. I. *GBiochemistry, Electron Transport Chain*, 2022. URL https://www.ncbi.nlm.nih.gov/books/NBK526105/. Downloaded: 26.04.2023.

[45] Mora-Lugo R., Stegmüller J., and Mack M. *Metabolic engineering of roseoflavin-overproducing microorganisms*, 2019. URL https://microbialcellfactories.biomedcentral.com/articles/10.1186/s12934-019-1181-2. Downloaded: 26.04.2023.

[46] Preciado A. G., Torres A. G., Merino E., Bonomi H. R., Goldbaum F. A., and Angulo V. A. G. *Extensive Identification of Bacterial Riboflavin Transporters and Their Distribution across Bacterial Species*, 2015. URL https://journals.plos.org/plosone/article?id=10.1371/journal.pone.0126124. Downloaded: 26.04.2023.

[47] Pedrolli D. B and Mack M. *Bacterial Flavin Mononucleotide Riboswitches as Targets for Flavin Analogs*, 2013. URL https://link.springer.com/protocol/10.1007/978-1-62703-730-3_13. Downloaded: 26.04.2023.

[48] Gutierrez-Preciado A., Torres A.G., Merino E., Bonomi H.R., Goldbaum F.A., and Garcia-Angulo V.A. Extensive identification of bacterial riboflavin transporters and their distribution across bacterial species., 2015. URL https://doi.org/10.1371/journal.pone.0126124. Downloaded: 03.05.2023.

[49] Schneider C. and Mack M. A second riboflavin import system is present in flavinogenic Streptomyces davaonensis and supports roseoflavin biosynthesis, 2021. URL https://onlinelibrary.wiley.com/doi/10.1111/mmi.14726. Downloaded: 03.05.2023.

[50] Lee E. R., Blount K. F., and Breaker R. R. *Roseoflavin is a natural antibacterial compound that binds to FMN riboswitches and regulates gene expression*, 2009. URL https://www.ncbi.nlm.nih.gov/pmc/articles/PMC5340298/. Downloaded: 27.04.2023.

[51] Fisher Sientific. *Material Safety Data Sheet Hydrazine anhydrous*, 2007. URL https://fscimage.fishersci.com/msds/11040.htm. Downloaded: 27.04.2023.

[52] Chemical Book. *Hydrazine*, 2016. URL https://www.chemicalbook.com/Price/HYDRAZINE.htm. Downloaded: 27.04.2023.

[53] Schneider C., Konjik K., Kisling L., and Mack M. *The novel phosphatase RosC catalyzes the last unknown step of roseoflavin biosynthesis in Streptomyces davaonensis*, 2020. URL https://onlinelibrary.wiley.com/doi/full/10.1111/mmi.14567. Downloaded: 30.04.2023.

[54] Hemberger S., Pedrolli D.B., Stolz J., Vogl C., Lehmann M., and Mack M. RibM from Streptomyces davawensis is a riboflavin/roseoflavin transporter and may be useful for the optimization of riboflavin production strains, 2011. URL https://bmcbiotechnol.biomedcentral.com/articles/10.1186/1472-6750-11-119. Downloaded: 24.05.2023.

[55] Konjik V., Brunle S., Demmer U., Vanselow A., Sandhoff R., Ermler U., and Mack M. The crystal structure of rosb: insights into the reaction mechanism of the first member of a family of flavodoxin-like enzymes, 2017. URL https://onlinelibrary.wiley.com/doi/abs/10.1002/anie.201610292. Downloaded: 28.05.2023.

[56] Rodionova I.A., Li X., Plymale A.E., Motamedchaboki K., Konopka A.E., and M.F. Romine. Genomic distribution of B-vitamin auxotrophy and uptake transporters in environmental bacteria from the Chloroflexi phylum., 2015. Downloaded: 11.05.2023.

[57] Jankowitsch F., Schwarz J., Ruckert C., Gust B., and Szczepanowski R. *hypothetical protein BN159.8033 [Streptomyces davaonensis JCM 4913]*, 2012. URL https://www.ncbi.nlm.nih.gov/protein/CCK32411.1. Downloaded: 03.05.2023.

[58] National Liberary of Medicine. *Q: What is the Expect (E) value?*, 2022. URL https://blast.ncbi.nlm.nih.gov/Blast.cgi?CMD=Web&PAGE_TYPE=BlastDocs&DOC_TYPE=FAQ. Downloaded: 03.05.2023.

[59] resources.qiagenbioinformatics.com. The E-value, 2022. URL https://resources.qiagenbioinformatics.com/manuals/clcgenomicsworkbench/650/_E_value.html Downloaded: 03.05.2023.

[60] Fungal Diversity Survey. Examining Your BLAST Results, 2022. URL https://fundis.org/component/sppagebuilder/41-examining-your-blast-results Downloaded: 03.05.2023.

[61] Vivek Thiruvettai. A Crash Course in BLAST Searching, 2022. URL https://bitesizebio.com/37866/crash-course-blast-searching/ Downloaded: 03.05.2023.

[62] P. G. Peters-Wendisch, B. Schiel, V. F. Wendisch, E. Katsoulidis, B. Möckeland, H. Sahm, and B. J. Eikmanns. *Pyruvate carboxylase is a major bottleneck for glutamate and lysine production by Corynebacterium glutamicum*, 2001. URL https://pubmed.ncbi.nlm.nih.gov/11321586/. Downloaded: 19.02.2023.

[63] Abe S., Takayama K.-I., and Kinoshita S. *Taxonomical Studies on Glutamic Acid-Producing Bacteria*, 1967. Downloaded: 15.03.2023.

[64] Leibniz institute DSMZ-German Collection of Microorganisms. Streptomyces davaonensis, 2018. URL https://www.dsmz.de/collection/catalogue/details/culture/DSM-101723. Downloaded: 06.06.2023.

[65] Clontech Laboratories and Inc. A Takara Bio Company. *CloneAmpTM HiFi PCR Premix Protocol-At-A-Glance*, 2012. URL https://www.takarabio.com/documents/UserManual/CloneAmpHiFiPCRPremixProtocol/CloneAmpHiFiPCRPremixProtocol-At-A-Glance_092612.pdf Downloaded: 02.02.2023.

[66] ZYMO RESEARCH. *ZR Plasmid MiniprepTM-Classic*, 2015. URL https://files.zymoresearch.com/protocols/_d4015_d4016_d4054_zr_plasmid_miniprep.pdf. Downloaded: 02.01.2023.

[67] QUIAGEN. *QIAquick® PCR Purification Kit*, 2018. URL https://www.qiagen.com/us/products/discovery-and-translational-research/dna-rna-purification/dna-purification/dna-clean-up/qiaquick-pcr-purification-kit/. Downloaded: 15.01.2023.

[68] SGIDNA. *Gibson assembly cloning guide*, 2017. URL https://www.biocat.com/bc/files/Gibson_Guide_V2_101417_web_version_8.5_x_11_FINAL.pdf. Downloaded: 24.02.2023.

[69] Promega. *GoTaq® DNA Polymerase (M300) Protocol*, 2018. URL https://no.promega.com/resources/protocols/product-information-sheets/g/gotaq-dna-polymerase-m300-protocol/. Downloaded: 10.02.2023.

[70] Thermo Fisher Scientific. *Thermo Scientific™ GeneRuler 1 kb Plus DNA Ladder*, 2021. URL https://www.fishersci.com/shop/products/fermentas-generuler-1kb-plus-dna-ladder/p-4529751 Downloaded: 10.02.2023.

[71] ThermoFisher. *NanoDrop One User Guide*, 2021. URL https://bionordika.no/application/files/3616/4560/9663/nanodrop-one-c-user-guide-EN_20211102_REV_DEC2021.pdf. Downloaded: 07.02.2023.

[72] ThermoFisher Scientific. *How electroporation works*, 2021. URL https://www.thermofisher.com/no/en/home/references/gibco-cell-culture-basics/transfection-basics/transfection-methods/electroporation.html. Downloaded: 19.02.2023.

[73] Cao Y., Duan z., and Shi Z. *Effect of biotin on transcription levels of key enzymes and glutamate efflux in glutamate fermentation by Corynebacterium glutamicum*, 2014. URL https://pubmed.ncbi.nlm.nih.gov/23990041/. Downloaded: 02.03.2023.

[74] Dasgupta A. *Chapter 2 - Biotin: Pharmacology, Pathophysiology, and Assessment of Biotin Status*, 2019. URL https://www.sciencedirect.com/science/article/pii/B9780128164297000022. Downloaded: 02.03.2023.

[75] Nimbalkar P. R., Khedkar M. A., Parulekar R. S., Chandgude V. K., Sonawane K. D., Chavan P. V., and Bankar S. B. *Role of Trace Elements as Cofactor: An Efficient Strategy toward Enhanced Biobutanol Production*, 2018. URL https://www.ncbi.nlm.nih.gov/pmc/articles/PMC6156106/. Downloaded: 03.03.2023.

[76] biochrom. Biochrom wpa range of colorimeters and spectrophotometers, 2022. URL http://www.biochrom.co.uk/product/20/biochrom-wpa-co8000-cell-density-meter.html. Downloaded: 03.03.2023.

[77] SHIMADZU. *What is HPLC (High Performance Liquid Chromatography)?*, 2022. URL https://www.shimadzu.com/an/service-support/technical-support/analysis-basics/basic/what_is_hplc.html. Downloaded: 14.03.2023.

[78] Merch. 2xYT medium, 2023. URL https://www.sigmaaldrich.com/NO/en/product/sigma/y1003. Downloaded: 19.05.2023.

[79] Otani S., Kasai S., and Matsui K. Isolation, chemical synthesis, and properties of roseoflavin, 1980. URL https://www.sciencedirect.com/science/article/abs/pii/0076687980664647. Downloaded: 24.05.2023.

[80] Dubey S., Majumder P., Penmatsa A., and Sardesai A. A. Topological analyses of the l-lysine exporter lyso reveal a critical role for a conserved pair of intramembrane solvent-exposed acidic residues, 2021. URL https://www.sciencedirect.com/science/article/pii/S0021925821009704. Downloaded: 07.06.2023.

[81] National Library of Medicine NIH. Multispecies: bifunctional riboflavin kinase/fad synthetase [corynebacterium], 2022. URL https://www.ncbi.nlm.nih.gov/protein/WP_011014798.1/. Downloaded: 26.05.2023.

[82] Ota T., Suzuki Y., Nishikawa T.and Otsuki T., Sugiyama T., Irie R., Wakamatsu A., Hayashi K., Sato H., and Sugano S. Rifk_human, 2004. URL https://www.uniprot.org/uniprotkb/Q969G6/entry. Downloaded: 26.05.2023.

[83] Pedrolli D. B., Nakanishi S., Barile M., Mansurova M., Carmona E. C., Lux A., Gärtner W., and Mack M. The antibiotics roseoflavin and 8-demethyl-8-amino-riboflavin from streptomyces davawensis are metabolized by human flavokinase and hu-

man fad synthetase, 2011. URL https://www.sciencedirect.com/science/article/pii/S0006295211006800?via%3Dihub. Downloaded: 27.05.2023.

[84] Anoz-Carbonell E. Rivero M., Polo V., Velázquez-Campoy A., and Medina M. Human riboflavin kinase: Species-specific traits in the biosynthesis of the fmn cofactor, 2020. URL https://faseb.onlinelibrary.wiley.com/doi/full/10.1096/fj.202000566R. Downloaded: 27.05.2023.

[85] Forskningsrådet. Nnp: Stor nytte av ny nmr-teknologi, 2020. URL https://www.forskningsradet.no/sok-om-finansiering/midler-fra-forskningsradet/infrastruktur/norsk-veikart-for-forskningsinfrastruktur/prosjektbeskrivelser/under-etableringi-drift/stor-nytte-av-ny-nmr-teknologi/. Downloaded: 01.06.2023.

[86] Jankowitsch, F., Schwarz J., Ruckert C., Gust B., Szczepanowski R., Blom J., Pelzer S., Kalinowski J., and Mack M. Riboflavin biosynthesis protein ribf [streptomyces davaonensis jcm 4913], 2012. URL https://www.ncbi.nlm.nih.gov/protein/CCK27094.1. Downloaded: 27.05.2023.

[87] Mora-Lugo R., Stegmuller J., and Mack M. riboflavin kinase [synthetic construct], 2019. URL https://www.ncbi.nlm.nih.gov/protein/QDM39061.1. Downloaded: 27.05.2023.

[88] COBALT National Librarly of Medicine. Constraint-based multiple alignment tool, 2023. URL https://www.ncbi.nlm.nih.gov/tools/cobalt/re_cobalt.cgi. Downloaded: 12.06.2023.

[89] Goldbeck O., Desef D. N., Ovchinnikov K. V., Perez-Garcia F., Christmann J., Sinner P., Crauwels P., Weixler D., Cao P., Becker J., Kohlstedt M., Kager J., Eikmanns B. J., Seibold G. M., Herwig C., Wittmann C., Bar N. S., Diep D. B., and Riedel C. U. Establishing recombinant production of pediocin pa-1 in corynebacterium glutamicum, 2021. URL https://pubmed.ncbi.nlm.nih.gov/34492380/. Downloaded: 31.05.2023.

[90] Henke N. A., Heider S. A. E., Peters-Wendisch P., and Wendisch V. F. Production of the marine carotenoid astaxanthin by metabolically engineered corynebacterium glutamicum, 2016. URL https://www.ncbi.nlm.nih.gov/pmc/articles/PMC4962014/. Downloaded: 07.06.2023.

[91] Gießelmann G., Dietrich D., Jungmann L., Kohlstedt M., Jeon E. J., Yim S. S., Sommer F., Zimmer D., Mühlhaus T., Schroda M., Jeong K. J., Becker J., and Wittmann C. Metabolic engineering of corynebacterium glutamicum for high-level ectoine production: Design, combinatorial assembly, and implementation of a transcriptionally balanced heterologous ectoine pathway, 2019. URL https://onlinelibrary.wiley.com/doi/full/10.1002/biot.201800417. Downloaded: 07.06.2023.

[92] Locher K. P. Structure and mechanism of atp-binding cassette transporters, 2008. URL https://www.ncbi.nlm.nih.gov/pmc/articles/PMC2674090/. Downloaded: 24.05.2023.

[93] Ferrol N. Membrane transporters, an overview of the arbuscular mycorrhizal fungal transportome, 2021. URL https://www.sciencedirect.com/science/article/abs/pii/B9780128199909000214. Downloaded: 25.05.2023.

[94] Linder M., Haak M., Botes A., Kalinowski J., and Ruckert C. putative membrane protein, ribx-family [corynebacterium glutamicum], 2021. URL https://www.ncbi.nlm.nih.gov/protein/QYO73792.1. Downloaded: 25.05.2023.

[95] Jankowitsch F., Schwarz J., Ruckert C., Gust B., Szczepanowski R., Blom J., Pelzer S., Kalinowski J., and Mack M. binding-protein-dependent transport systems inner membrane component [streptomyces davaonensis jcm 4913], 2012. URL https://www.ncbi.nlm.nih.gov/protein/408534192. Downloaded: 25.05.2023.

[96] Pedrolli D.B., Matern A., Wang J., Ester M., Siedler K., Breaker R., and Mack M. A highly specialized flavin mononucleotide riboswitch responds differently to similar ligands and confers roseoflavin resistance to streptomyces davawensis, 2012. URL https://academic.oup.com/nar/article/40/17/8662/2411739. Downloaded: 28.05.2023.

[97] Grill S., Busenbender S., Pfeiffer M., Kohler U., and Mack M. The bifunctional flavokinase/flavin adenine dinucleotide synthetase from streptomyces davawensis produces inactive flavin cofactors and is not involved in resistance to the antibiotic roseoflavin, 2008. URL https://doi.org/10.1128%2FJB.01586-07. Downloaded: 28.05.2023.

[98] Jankowitsch F., Kuhm C., Kellner R., Kalinowski J., Pelzer S., Macheroux P., and Mack M. A novel n,n-8-amino-8-demethyl-d-riboflavin dimethyltransferase (rosa) catalyzing the two terminal steps of roseoflavin biosynthesis in streptomyces davawensis, 2011. URL https://www.sciencedirect.com/science/article/pii/S0021925820506716?via%3Dihub. Downloaded: 28.05.2023.

[99] Vertes A. A., Inui M., and Yukawa H. Manipulating corynebacteria, from individual genes to chromosomes., 2005. URL https://journals.asm.org/doi/abs/10.1128/aem.71.12.7633-7642.2005. Downloaded: 28.05.2023.

[100] Andrighetti-Fröhner C., Antonio R., Creczynski-Pasa T., Barardi C., and Simões C. Cytotoxicity and potential antiviral evaluation of violacein produced by chromobacterium violaceum, 2003. URL https://www.scielo.br/j/mioc/a/YSMyCPsNmd7gq3WSCKhhnjL/abstract/?lang=en. Downloaded: 28.05.2023.

[101] Konzen M., De Marco D., Cordova CA. and. Vieira T. O., Antônio R. V., and Creczynski-Pasa T.B. Antioxidant properties of violacein: possible relation on its biological function, 2006. URL https://www.sciencedirect.com/science/article/pii/S0968089606007309. Downloaded: 28.05.2023.

[102] Mendes A., de Carvalho J., Duarte M.T., Durán N., and Bruns R. Factorial design and response surface optimization of crude violacein for chromobacterium violaceum production, 2001. URL https://link.springer.com/article/10.1023/A:1013734315525. Downloaded: 28.05.2023.

[103] Rohles C. M., Gießelmann G., Kohlstedt M., Wittmann C., and Becker J. Systems metabolic engineering of corynebacterium glutamicum for the production of the carbon-5 platform chemicals 5-aminovalerate and glutarate, 2016. URL https://microbialcellfactories.biomedcentral.com/articles/10.1186/s12934-016-0553-0. Downloaded: 08.06.2023.

[104] Pérez-García F., Ziert C., Risse J. M., and Wendisch V. F. Improved fermentative production of the compatible solute ectoine by corynebacterium glutamicum from glucose and alternative carbon sources, 2017. URL https://pubmed.ncbi.nlm.nih.gov/28478080/ Downloaded: 08.06.2023.

[105] Jorge J. M. P., Nguyen A. Q. D., Pérez-García F., Kind S., and Wendisch V. F. Improved fermentative production of gamma-aminobutyric acid via the putrescine route: Systems metabolic engineering for production from glucose, amino sugars, and xylose, 2016. URL https://pubmed.ncbi.nlm.nih.gov/27800627/ Downloaded: 08.06.2023.

[106] Prell C., Busche T., Rückert C., Nolte L., Brandenbusch C., and Wendisch V. F. Adaptive laboratory evolution accelerated glutarate production by corynebacterium glutamicum, 2021. URL https://link.springer.com/article/10.1186/s12934-021-01586-3 Downloaded: 13.06.2023.

[107] Sandberg T. E., Salazar M. J., Weng L. L., Palsson B. O., and Feist A. M. The emergence of adaptive laboratory evolution as an efficient tool for biological discovery and industrial biotechnology., 2019. URL https://doi.org/10.1016/j.ymben.2019.08.004. Downloaded: 13.06.2023.

[108] Portnoy V. A., Bezdan D., and Zengler K. Adaptive laboratory evolution—harnessing the power of biology for metabolic engineering., 2011. URL https://doi.org/10.1016/j.copbio.2011.03.007. Downloaded: 13.06.2023.

[109] Oide S., Gunji W., Moteki Y., Yamamoto S., Suda M., and Jojima T. Thermal and solvent stress cross-tolerance conferred to corynebacterium glutamicum by adaptive laboratory evolution., 2015. URL https://doi.org/10.1128/AEM.03973-14. Downloaded: 13.06.2023.

[110] Jiang L.-Y., Chen S.-G., Zhang Y.-Y., and Liu J.-Z. Metabolic evolution of corynebacterium glutamicum for increased production of l-ornithine, 2013. URL https://doi.org/10.1186/1472-6750-13-47. Downloaded: 13.06.2023.

[111] Fujita Y. Carbon catabolite control of the metabolic network in bacillus subtilis, 2009. URL https://www.jstage.jst.go.jp/article/bbb/73/2/73_80479/_article/-char/ja/. Downloaded: 28.05.2023.

[112] Bren A., Park J. O., Towbin B. D., Dekel E., Rabinowitz J. D., and Alon U. Glucose becomes one of the worst carbon sources for e.coli on poor nitrogen sources due to suboptimal levels of camp, 2016. URL https://link.springer.com/content/pdf/10.1038/srep24834.pdf Downloaded: 28.05.2023.

[113] Lindner S. N., Seibold G. M., Henrich A.and Krämer R., and Wendisch V. F. Phosphotransferase system-independent glucose utilization in corynebacterium glutamicum by inositol permeases and glucokinases, 2011. URL https://pubmed.ncbi.nlm.nih.gov/21478323/ Downloaded: 28.05.2023.

[114] Barbot Y. N, Al-Ghaili H., and Benz R. A review on the valorization of macroalgal wastes for biomethane production, 2016. URL https://www.mdpi.com/1660-3397/14/6/120. Downloaded: 27.05.2023.

[115] Pérez-García F., Brito L. F., and Wendisch V. F. Function of l-pipecolic acid as compatible solute in corynebacterium glutamicum as basis for its production under hyperosmolar conditions, 2019. URL https://pubmed.ncbi.nlm.nih.gov/30858843/. Downloaded: 08.06.2023.

Appendices

A Media-, buffer-, antibiotic-, salt solution- and gelRed- preparation

A.1 Media preparation

2TY media

2TY media was prepared by adding the components in Table A.1 to water while stirring. The antibiotic kanamycin (0.5 mL/L), was added to the 2TY media if the cells contained pVWEx1 plasmids, and the antibiotic tetracyclin (0.5 mL/L) was added if the cells contained pSym plasmids. The media was sterilized by autoclaving at 121°C for 15 min. 2TY agar plates were prepared by adding agar (15 g/L) to the 2TY media during preparation.

Table A.1: Chemicals with concentrations used in 2TY media.

Components	Concentration [g/L]	Volume [mL]/ Mass [g]
Deionized water		500 mL
Yeast extract	10.0	5.0 g
Tryptone	16.0	8.0 g
NaCl	5.0	2.5 g
Total volume		500 mL

LB media

LB media was prepared by adding the components in Table A.2 to water while stirring. The antibiotic kanamycin (0.5 mL/L), was added if cells contained pVWEx1 plasmids, and the antibiotic tetracyclin (0.5 mL/L) was added if the cells contained pSym plasmids. The media was sterilized by autoclaving at 121°C for 15 min. LB agar plates were prepared by adding agar (15 g/L) to the LB during the preparation.

Table A.2: Chemicals with concentrations used in LB media.

Components	Concentration [g/L]	Volume [mL]/ Mass [g]
Deionized water		500 mL
Yeast extract	5.0	2.5 g
Tryptone	8.0	4.0 g
NaCl	5.0	2.5 g
Total volume		500 mL

BHI media

LB media was prepared by adding the component in Table A.3 to water while stirring. The media was sterilized by autoclaving at 121°C for 15 min.

Table A.3: Chemical with concentration used in BHI media.

Components	Concentration [g/L]	Volume [mL]/ Mass [g]
Deionized water		400 mL
BHI	37.0	14.8 g
Total volume		400 mL

Sorbitol media

While stirring, sorbitol media was prepared by adding the component in Table A.4 to water. The media was sterilized by autoclaving at 121°C for 15 min.

Table A.4: Chemical with concentration used in Sorbitol media.

Components	Concentration [g/L]	Volume [mL]/ Mass [g]
Deionized water		100 mL
Sorbitol	455	45.5 g
Total volume		100 mL

A.1.1 BHIS media

BHIS media was prepared by mixing BHI media and sorbitol media in the ratio 1:5, four parts of BHI media and one part of sorbitol media.

A.2 Antibiotics preparation

Tetracyclin stock solution

Tetracyclin was diluted in ethanol (EtOH) to get the tetracyclin stock solution, Table A.5. The tetracyclin stock solution was sterilized by filtration and stored at -20°C.

Table A.5: Chemicals with concentrations used in tetracyclin stock solution.

Components	Concentration	Volume [mL]/ Mass [g]
Tetracyclin	10 g/L	0.1 g
EtOH	70 %	10 ml
Total volume		10 mL

Kanamycin stock solution

Kanamycin was diluted in EtOH to get the kanamycin stock solution, Table A.6. The kanamycin stock solution was sterilized by filtration and stored at -20°C.

Table A.6: Chemicals with concentrations used in kanamycin stock solution.

Components	Concentration	Volume [mL]/ Mass [g]
Kanamycin	50 g/L	0.5 g
EtOH	70 %	10 mL
Total volume		10 mL

A.3 Components in selective media

CGXII salt solution

CGXII media was prepared by adding the components in Table A.7 to water. pH was adjusted to 7 with KOH (1M) before the solution was sterilized by autoclaving at 121°C for 15 min.

Table A.7: Chemicals with concentrations used in CGXII salt solution.

Components	Concentration	Volume [mL]/ Mass [g]
Deionized water		400 mL
$(NH_4)_2SO_4$	10 g/L	5.0 g
KH_2PO_4	1 g/L	0.5 g
K_2HPO_4	1 g/L	0.5 g
UREA	5 g/L	2.5 g
MOPS	42 g/L	21.0 g
Ca-stock 1000X	1 mL/L	0.5 mL
Mg-stock 1000X	1 mL/L	0.5 mL
Total volume		400 mL

Ca-stock 1000X

The Ca-stock 1000X solution was prepared after Table A.8. The solution was sterilized by filtration.

Table A.8: Chemicals with concentrations used in Ca-stock 1000X solution.

Components	Concentration	Volume [mL]/ Mass [g]
Deionized water		10 mL
$CaCl_2$ x 2 H_2O	13.25 g/L	0.6625 g
Total volume		50 mL

Mg-stock 1000X

The Mg-stock 1000X solution was prepared after Table A.9. The solution was sterilized by filtration.

Table A.9: Chemicals with concentrations used in Mg-stock 1000X solution.

Components	Concentration	Volume [mL]/ Mass [g]
Deionized water		10 mL
$MgSO_4$ 7 H_2O	250 g/L	12.5 g
Total volume		50 mL

Biotin solution

The biotin solution was prepared after Table A.10. The solution was sterilized by filtration and stored at -20°C.

Table A.10: Chemicals with concentrations used in the biotin solution.

Components	Concentration	Volume [mL]/ Mass [g]
Biotin	0.2 g/L	0.002 g
NaOH	1 M	10 mL
Total volume		10 mL

Protocatechuic acid or 3,4-dihydroxybenzoic acid (PCA) solution

The PCA solution was prepared after Table A.11. The solution was sterilized by filtration and stored at -20°C.

Table A.11: Chemicals with concentrations used in the PCA solution.

Components	Concentration	Volume [mL]/ Mass [g]
PCA	30 g/L	0.3 g
NaOH	1 M	10 mL
Total volume		10 mL

Isopropyl β-D-1-thiogalactopyranoside (IPTG) solution

The IPTG solution was prepared after Table A.12. The solution was sterilized by filtration and stored at -20°C.

Table A.12: Chemicals with concentrations used in the IPTG solution.

Components	Concentration	Volume [mL]/ Mass [g]
Deionized water		10 mL
IPTG	238.31 g/L	2.38 g
Total volume		10 mL

Trace element solution

The trace element solution was papered after Table A.13. pH was adjusted to 1 with 0.5 M HCL. The solution was sterilized by filtration and stored at 4°C.

Table A.13: Chemicals with concentrations used in the trace element solution.

Components	Concentration [g/L]	Volume [mL]/ Mass [g]
(FeSO4) x7 H2O	16.40	1.640 g
MnSO4 x H2O	10.00	1.000 g
ZnSO4 x7 H2O	1.00	0.100 g
CuSO4 x5 H2O	0.31 6	0.031 g
$NiCl_2$ x6 H2O	0.02	0.002
Total volume		100 mL

Glucose stock solution 40%

The 40 % glucose stock solution was prepared following Table A.14.

Table A.14: Chemical with concentrations used in glucose stock.

Components	Concentration[g/L]	Volume [mL]/ Mass [g]
Deionized water		500 mL
Glucose	0.4	200 g
Total volume		500 mL

A.4 EPB buffers

The EPB buffers used in the production of competent cells were produced after the recipe in Table A.15 and Table A.16. NaOH (1 M) was used to adjust the pH to 7.2 before the media was sterilized by autoclaving.

Table A.15: Chemicals with concentrations used in EPB1 buffer.

Components	Concentration [g/L]	Volume [mL]/ Mass [g]
Deionized water		800.00 mL
HEPES	5.05	4.04 g
Glycerin	89 %	36.60 mL
Total volume		836.60 mL

Table A.16: Chemicals with concentrations used in EPB2 buffer.

Components	Concentration [g/L]	Volume [mL]/ Mass [g]
Deionized water		50.00 mL
HEPES	1.2	0.06 g
Glycerin	89 %	6.85 mL
Total volume		56.85 mL

A.5 GelRed

Agarose and Tris- Acetate- EDTA (1xTAE) in Table A.17 were mixed and dissolved by heating it in the microwave. GelRed was added. The solution was stored in a heating cabinet at 60° C.

Table A.17: Chemicals with concentrations used in gelRed.

Components	Volume [mL]/ Mass [g]
Agarose	3.2 g
1xTAE	400 mL
GelRed	20.0 µL
Total volume	400 mL

A.6 Ammonium acetate, solvent for HPLC

The ammonium acetate solvent used for the HPLC was prepared following Table A.18. pH of the solvent was adjusted to 6 by acetic acid before the solvent was filtrated.

Table A.18: Chemical with concentrations used in ammonium acetate solvent used in the HPLC.

Components	Concentration[g/L]	Volume [L]/ Mass [g]
Dionized water		1 L
Ammonium acetate	0.385	0.385 g
Total volume		1 L

B OD600 measurements- raw data from growth experiments

The initial concentrations after the measured ODs were multiplied with the dilution factor of 40, and initial volumes are shown for Growth experiment 1 in Table B.1 and Growth experiment 2 in Table B.2. The initial volumes were calculated using the equation Equation 2.1 in subsubsection 2.7.3.

Table B.1: Initial ODs and initial volumes for the precultures of Roseo0, Roseo1 and Roseo2 in Growth experiment 1 after the raw data was multiplied by the dilution factor 40.

Pre-cultures	**Roseo0**	**Roseo1**	**Roseo2**
Initial concentrations (C_i)	3.76	2.48	1.52
Initial volumes (V_i) [mL]	6.65	10.08	16.45

Table B.2: Initial ODs and initial volumes for the precultures of Roseo0, Roseo1, Roseo2, Roseo3, Roseo4 and Roseo5 in Growth experiment 2 after the raw data was multiplied by the dilution factor 40.

Pre-cultures	**Roseo0**	**Roseo1**	**Roseo2**	**Roseo3**	**Roseo4**	**Roseo5**
Initial concentrations (C_i)	8.72	3.64	2.60	3.80	1.60	2.04
Initial volumes (V_i) [mL]	2.87	6.87	9.62	6.58	15.63	12.25

The values of the OD measurements during Growth experiment 1 and Growth experiment 2 are shown in Table B.3, and Table B.4, respectively.

Table B.3: OD measurement values of independent triplicates of the strains Roseo0, Roseo1 and Roseo2 in Growth experiment 1. The time of the measurement during the growth experiment is given.

Time [h]	**Roseo0**			**Roseo1**			**Roseo2**		
	I	II	III	I	II	III	I	II	III
0	0.65	0.62	0.65	0.59	0.60	0.67	0.67	0.67	0.52
2	0.94	1.02	1.24	1.56	1.42	1.48	1.86	1.20	1.34
4	2.28	2.28	2.50	2.48	2.48	2.50	2.95	2.70	2.68
6	6.04	5.40	5.68	5.44	4.40	4.68	4.96	4.84	5.52
8	8.70	7.80	7.50	8.20	8.50	8.40	9.50	9.10	10.00
10	13.30	11.80	12.60	13.70	13.80	13.50	13.60	13.30	11.50
22	15.97	14.16	15.25	16.09	16.70	15.61	16.21	18.51	15.97
24	12.9	11.30	12.50	15.60	12.70	14.40	13.40	12.90	13.60

Table B.4: OD measurement values of independent triplicates of the strains Roseo0, Roseo1, Roseo2, Roseo3, Roseo4 and Roseo5 in Growth experiment 2. The time of the measurement during the growth experiment is given.

Time [h]	**Roseo0**			**Roseo1**			**Roseo2**		
	I	II	III	I	II	III	I	II	III
0	0.50	0.42	0.40	0.40	0.39	0.39	0.47	0.47	0.50
2	0.60	0.62	0.42	0.52	0.58	0.56	0.46	0.52	0.50
4	1.18	1.14	0.98	0.68	0.72	0.50	0.48	0.62	0.64
6	1.84	2.1	1.72	0.86	0.86	0.72	0.78	0.78	0.78
8	4.00	4.68	2.96	1.24	1.22	0.96	1.32	1.22	1.00
10	6.70	9.20	6.80	1.88	2.28	1.84	1.88	1.80	1.68
22	15.1	15.3	15.1	21.2	15.9	15.5	18.2	19.7	15.9
24	14.40	25.40	14.10	14.20	15.40	22.20	21.40	16.30	19.20
72	15.90	15.90	12.40	10.90	12.60	13.40	15.70	12.20	11.70
Time [h]	**Roseo3**			**Roseo4**			**Roseo5**		
	I	II	III	I	II	III	I	II	III
0	0.41	0.48	0.45	0.45	0.47	0.40	0.56	0.51	0.45
2	0.34	0.66	0.70	0.86	0.92	0.78	0.76	0.74	0.76
4	0.46	0.80	0.64	1.20	1.50	1.46	1.20	1.22	1.46
6	0.52	0.78	0.70	1.64	2.46	2.92	2.02	2.14	2.18
8	0.44	0.70	0.70	2.96	4.28	4.40	4.00	4.24	4.72
10	0.56	1.00	1.04	6.30	5.80	8.30	6.00	5.70	7.70
22	1.30	2.30	3.10	8.60	8.80	12.20	12.10	10.70	11.00
24	1.60	3.70	3.10	7.90	9.00	12.50	10.40	11.80	15.80
72	14.40	12.60	14.80	4.80	4.30	5.30	5.40	5.70	10.10

The average and standard deviation was calculated for the three triplicates of each strain in Table B.3 and Table B.4. The average, $\bar{x}$, was calculated using

$$\bar{x} = \sum_{i=1}^{N} \frac{x_i}{N}. \tag{B.1}$$

x_i represents a specific OD measurement i. For one strain at a specific time, N is the number of OD measurements. Hence, N is 3. To measure the spread of the measured values, the standard deviation, σ_x, was calculated,

$$\sigma_x = \sqrt{\frac{\sum(x_i - \bar{x})^2}{N}}. \tag{B.2}$$

In Table B.5 and Table B.6 the calculated averages and standard deviations are given for Growth experiment 1 and Growth experiment 2, respectively.

Table B.5: The average and standard deviation of the triplicate OD measurements carried out on the strains Roseo0, Roseo1, and Roseo2 in Growth experiment 1. The time the measurements were carried out is shown.

Time [h]	Roseo0	Roseo1	Roseo2
0	0.64 ± 0.02	0.62 ± 0.04	0.62 ± 0.09
2	1.07 ± 0.16	1.49 ± 0.07	1.47 ± 0.35
4	2.35 ± 0.13	2.49 ± 0.01	2.78 ± 0.15
6	5.71 ± 0.32	4.84 ± 0.54	5.11 ± 0.36
8	8.00 ± 0.62	8.30 ± 0.26	9.53 ± 0.45
10	12.56 ± 0.75	13.67 ± 0.15	12.80 ± 1.14
22	15.13 ± 0.91	16.13 ± 0.55	16.90 ± 0.55
24	12.23 ± 0.83	14.23 ± 1.46	13.30 ± 0.36

Table B.6: Average and standard deviation of the triplicate OD measurements carried out of the strains Roseo0, Roseo1, Roseo2, Roseo3, Roseo4, and Roseo5 in Growth experiment 2. The time the measurements were carried out is shown.

Time [h]	Roseo0	Roseo1	Roseo2
0	0.44 ± 0.05	0.39 ± 0.00	0.48 ± 0.02
2	0.55 ± 0.11	0.55 ± 0.03	0.49 ± 0.03
4	1.10 ± 0.10	0.63 ± 0.12	0.58 ± 0.09
6	1.89 ± 0.19	0.81 ± 0.08	0.78 ± 0.00
8	3.88 ± 0.87	1.14 ± 0.16	1.18 ± 0.16
10	7.56 ± 1.42	2.00 ± 0.24	1.79 ± 0.10
22	15.17 ± 0.12	17.53 ± 3.18	17.93 ± 1.91
24	14.63 ± 0.68	17.27 ± 4.31	18.97 ± 2.56
72	14.73 ± 2.02	12.3 ± 2.18	13.20 ± 2.18
Time [h]	**Roseo3**	**Roseo4**	**Roseo5**
0	0.45 ± 0.03	0.44 ± 0.04	0.50 ± 0.06
2	0.57 ± 0.20	0.85 ± 0.07	0.75 ± 0.01
4	0.63 ± 0.17	1.39 ± 0.16	1.29 ± 0.15
6	0.67 ± 0.13	2.34 ± 0.65	2.11 ± 0.08
8	0.61 ± 0.15	3.88 ± 0.80	4.32 ± 0.37
10	0.87 ± 0.27	6.80 ± 1.32	6.47 ± 1.08
22	2.23 ± 0.90	9.87 ± 2.03	11.27 ± 0.74
24	2.80 ± 1.08	9.80 ± 2.40	12.67 ± 2.80
72	13.93 ± 1.17	4.80 ± 0.50	7.07 ± 2.63

For the growth curves in Figure 3.5 in subsection 3.2, the values in Table B.5 are the plotted values, and for the growth curves in Figure 3.12 in subsection 3.5, the values in Table B.6 are the plotted values. The y-axis values are the average OD measurement values of the strains and the x-axis values are the time of the measurements.

C Growth rates, biomass and biomass yields

To find the growth rate of Roseo0, Roseo1, and Roseo2 in Growth experiment 1, the OD values in Table B.5 of the exponential phase were converted to logarithmic values and plotted against the time. Similarly, was the values in Table B.6 for Roseo0, Roseo1, Roseo2, Roseo3, Roseo4, and Roseo5 in Growth experiment 2 converted to logaritimic values. From the slope of each graph, the growth rate was found. The OD values in the exponential phase were defined from the 2^{nd} to the 10^{th} hour in Growth experiment 1. In Growth experiment 2, the exponential phase varied. To convert the OD values to logarithmic values the equation Equation C.1 was used.

$$\mathrm{y} = \log(\mathrm{OD}(t)) \tag{C.1}$$

y is the logarithmic values, and OD(t) is the measured OD values at time t, where t varied from the 2^{nd} to the 10^{th} hour in Growth experiment 1. t varied in Growth experiment 2. In Figure C.1 and Table C.1 the graphs and equations for each graph are shown for Growth experiment 1, respectively. For growth experiment 2, the graphs and equations are displayed in Figure C.2 and Table C.2. The value before the x in each equation is the slope value, which also is the growth rate.

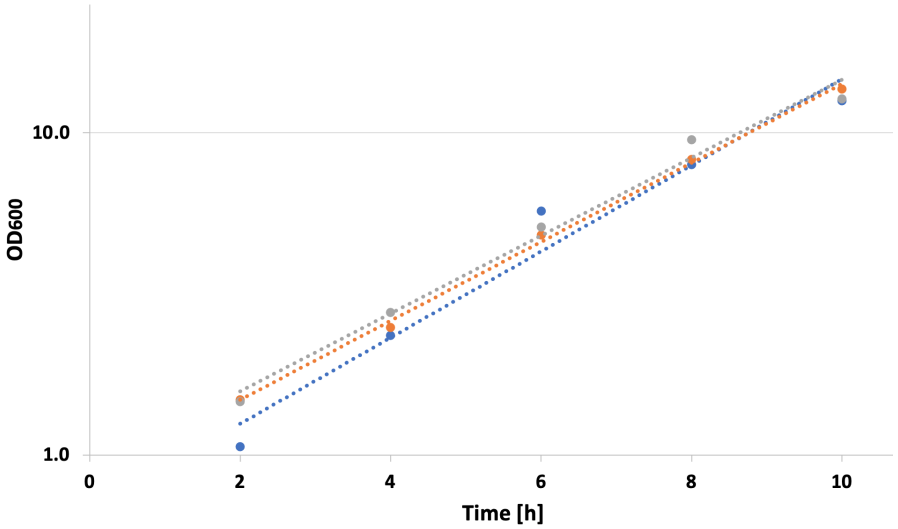

Figure C.1: The average logarithmic values of the OD measurements are plotted against time for Growth experiment 1. The equation for Roseo0 in blue is $\mathrm{y} = 0.68\mathrm{e}^{0.31x}$, the equation for Roseo1 in orange is $\mathrm{y} = 0.84\mathrm{e}^{0.28x}$ and the equation for Roseo2 in grey is $\mathrm{y} = 0.90\mathrm{e}^{0.28x}$.

Table C.1: The equation for the average logarithmic value for Roseo0, Roseo1 and Roso2 in Growth experiment 1. The growth rate is the slope value before x in each equation.

Roseo0	Roseo1	Roseo2
$\mathrm{y} = 0.68\mathrm{e}^{0.31x}$	$\mathrm{y} = 0.84\mathrm{e}^{0.28x}$	$\mathrm{y} = 0.90\mathrm{e}^{0.28x}$

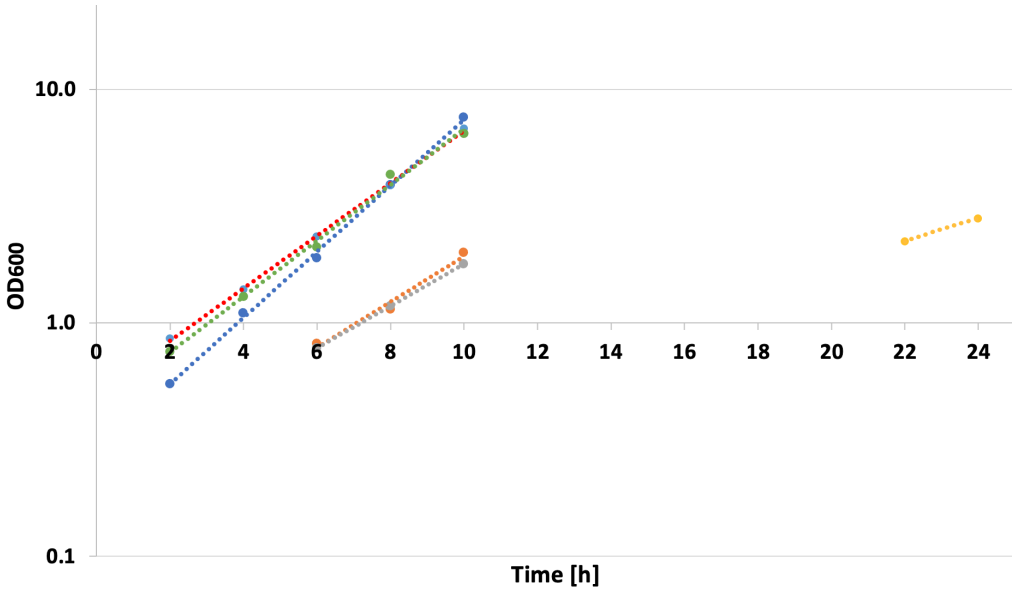

Figure C.2: The average logarithmic values of the OD measurements are plotted against time in Growth experiment 2. The equation for Roseo0 in blue is $y = 0.29e^{0.33x}$. The equation for Roseo1 in orange is $y = 0.29e^{0.22x}$. The equation for Roseo2 in grey is $y = 0.26e^{0.21x}$. The equation for Roseo3 in yellow is $y = 0.19e^{0.11x}$. The equation for Roseo4 in red is $y = 0.50e^{0.26x}$. The equation for Roseo5 in green is $y = 0.43e^{0.28x}$.

Table C.2: The equation for the average logarithmic value for Roseo0, Roseo1, Roso2, Roseo3, Roseo4, and Roseo5 in Growth experiment 2. The growth rate is the slope value before x in each equation.

Roseo0	**Roseo1**	**Roseo2**	**Roseo3**	**Roseo4**	**Roseo5**
$y = 0.29e^{0.33x}$	$y = 0.29e^{0.22x}$	$y = 0.26e^{0.21x}$	$y = 0.19e^{0.11x}$	$y = 0.50e^{0.26x}$	$y = 0.43e^{0.28x}$

The OD values measured at the 24^{th} hour in Table B.3 were used to calculate the biomass and biomass yield for both growth experiments. An exception was the strain Roseo3 in Growth experiment 2, due to slow growth. Here, the final biomass and biomass yield were calculated after the 72^{nd} hour. The final biomass of the strains was reached when the cells had reached stationary phase at the 24^{th} or the 72^{nd} hour. The average, $\bar{\text{OD}}_{600(24h)}$, of the OD values for each triplicates were calculated,

$$\bar{\text{OD}}_{600(24h)} = \sum_{i=1}^{N} \frac{\text{OD}_{600(24h)i}}{N}. \tag{C.2}$$

$\text{OD}_{600(24h)i}$ represents a specific OD measurement i at the 24^{th} or the 72^{nd} hour. N is the number of OD measurements at a specific time for one strain, making N equal to 3, due to 3 triplicates. The biomass was calculated by multiplying the average, $\bar{\text{OD}}_{600(24h)}$, with a correlation factor,

$$\text{Biomass} = \text{Correlation factor} \cdot \bar{\text{OD}}_{600(24h)}. \tag{C.3}$$

The correlation factor was 0.343, found by Dr. Pérez-García[5]. The biomass yield was calculated from equation,

$$\text{Biomass yield} = \frac{\text{Biomass}}{\text{C}_{\text{glucose}}}. \tag{C.4}$$

1% of glucose was utilized during the two growth experiments, equalling 10 g/L, as the concentration of glucose, $C_{glucose}$.

D HPLC calculations

To find the retention time of roseoflavin and riboflavin, 5 standards with known titers of each compound were analyzed with HPLC. From the chromatogram of the HPLC standards, the heights of the peaks were plotted against the known titers of the roseoflavin and riboflavin standards, shown in Figure D.1 and Figure D.2. To calculate the roseoflavin and riboflavin titers in the samples, collected during Growth experiment 1, the slope of the graphs in Figure D.1 were used together with the heights of the peaks of the samples chromatograms. For the samples in Growth experiment 2, the slope of the graphs in Figure D.2 were used. Table D.1 and Table D.2 show the titer and heights of the chromatogram of the standards used for samples collected during Growth experiment 1 and Growth experiment 2, respectively.

Table D.1: The heights of the peaks and titers of the roseoflavin and riboflavin standards used for samples collected in Growth experiment 1.

$C_{Roseoflavin}$ [g/L]	$H_{Roseoflavin}$ [EU]	$C_{Riboflavin}$ [g/L]	$H_{Riboflavin}$ [EU]
0.500	4360	0.00500	181274
0.250	2404	0.00250	86779
0.125	1428	0.00125	43490
0.063	650	0.00063	21843
0.000	-	0.00000	-

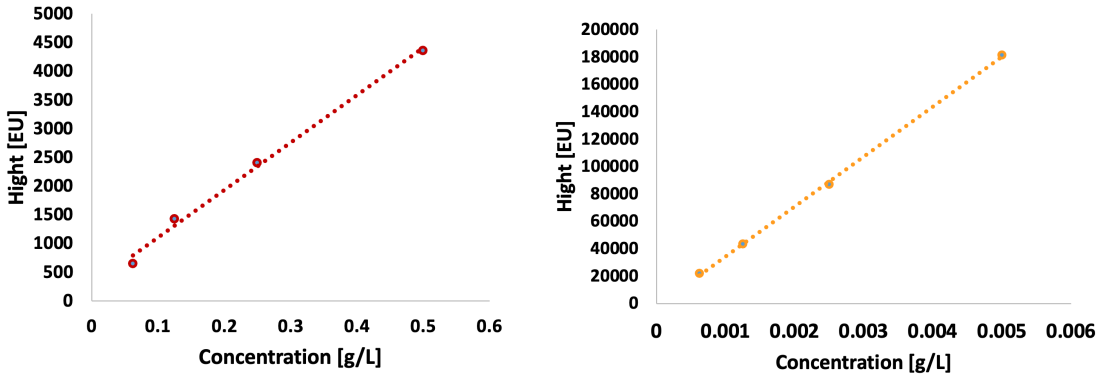

Figure D.1: The titers of the standards (x-values) were plotted against the heights of the peaks of the chromatogram of the standards (y-values). The standards were used for the samples collected in Growth experiment 1. The roseoflavin graph is displayed to the left with function y = 8261x + 274. To the right is the riboflavin graph displayed with function y = $4e^{+7}$x − 2210.

Table D.2: The heights of the peaks and titers of the roseoflavin and riboflavin standards used for samples collected in Growth experiment 2.

$C_{Roseoflavin}$ [g/L]	$H_{Roseoflavin}$ [EU]	$C_{Riboflavin}$ [g/L]	$H_{Riboflavin}$ [EU]
0.500	2312	0.0500	1029833
0.250	1292	0.0250	530705
0.125	630	0.0125	264307
0.063	494	0.0063	139953
0.000	-	0.0000	-

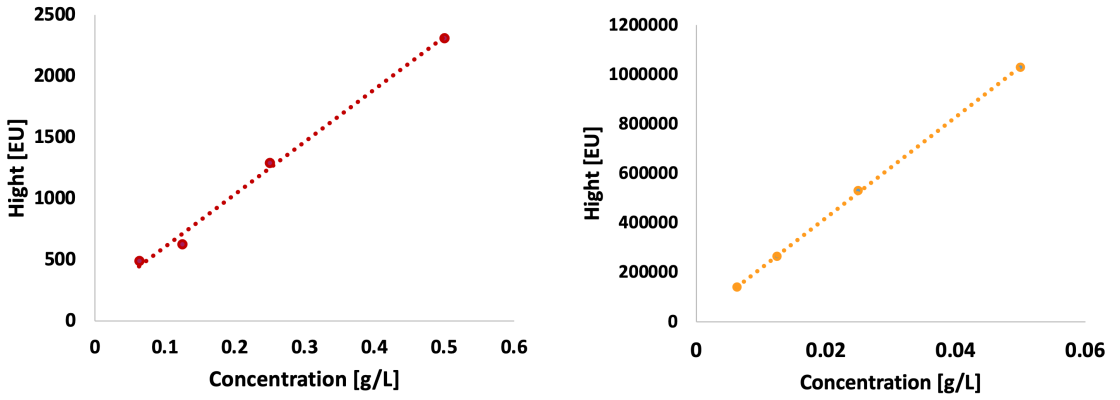

Figure D.2: The titers of the standards (x-values) were plotted against the heights of the peaks of the chromatogram of the standards (y-values). The standards were used for the samples collected in Growth experiment 2. The roseoflavin graph is displayed to the left with function y = 4282x + 178. To the right is the riboflavin graph displayed with function y = $2e^{+7}$x − 12920.

For the samples collected during Growth experiment 1 and Growth experiment 2, all raw data from the HPLC analysis and calculations are found in Appendix E.

For each sample i, collected during the two growth experiments, the titer, C_i, was calculated by the equation,

$$C_i = \frac{\text{Height}_i}{\text{Slope}_r}. \tag{D.1}$$

For each chromatogram of sample i, Height_i was the height of the peaks. Slope_r was the slope found in Figure D.1 or Figure D.2 for either the roseoflavin- or riboflavin standards, r. For roseoflavin in Growth experiment 1, slope_r was 8261, and the slope_r was $4e^{+7}$ for riboflavin. For roseoflavin and riboflavin, the slope_r was 4282 and $2e^{+7}$ in Growth experiment 2, respectively. All C_i and Height_i values for the samples for Growth experiment 1 are found in Figure E.3 in Appendix E in the columns "Concentration [g/L]" and "Height [EU]", respectively. For Growth experiment 2, the C_i and Height_i values are found in Figure E.9 in Appendix E. The average titers and standard deviations were calculated for the triplicates of the strains collected at the 6^{th}, 24^{th}, and 72^{th} hour. The average titer is shown in the column "titer Average [g/L]" in Figure E.3 and Figure E.9. Roseo0 contained the empty vector pVWEx1 and was used as the reference strain. Hence, the average titers of Roseo0 from the samples collected at the 6^{th}, 24^{th} and 72^{th} were subtracted from the values of the other strains collected at the same time, resulting in the titers in Figure E.4 and Figure E.10.

E HPLC raw data

E.1 Growth experiment 1

RoF standards				
Retention Time	Area	% Area	Height [EU]	Concentration [g/L]
3.552	63173	80.95	4360	0.5
3.473	33163	75.25	2404	0.25
3.440	17864	60.02	1428	0.125
3.438	8421	43.13	650	0.063

RoF samples				
Retention Time	Area	% Area	Height [EU]	Abbreviated name
3.576	11349	0.09	549	6ci
3.578	8255	0.07	450	6cii
3.52	5630	0.04	399	6ciii
3.553	10764	0.06	577	6abci
3.596	7500	0.04	451	6abcii
3.613	9847	0.06	510	6abciii
3.556	13259	0.08	595	6mi
3.573	7147	0.04	416	6mii
3.587	6875	0.04	458	6miii
3.558	31965	0.07	1459	24ci
3.568	34183	0.08	1505	24cii
3.587	33255	0.07	1602	24ciii
3.553	39780	0.07	1699	24abci
3.547	36740	0.06	1688	24abcii
3.581	39372	0.06	1816	24abciii
3.551	39857	0.07	1915	24mi
3.554	37436	0.06	1888	24mii
3.581	40229	0.07	1847	24miii
3.586	32874	0.07	1620	72ci
3.573	33260	0.07	1684	72cii
3.605	32285	0.07	1619	72cii
3.571	36918	0.06	1795	72abci
3.564	39857	0.06	1950	72abcii
3.58	39316	0.05	1983	72abciii
3.54	42485	0.06	2039	72mi
3.557	40922	0.07	2007	72mii
3.572	41455	0.06	1999	72miii

Figure E.1: Roseoflavin raw data for Growth experiment 1.

RF standards				
Retention Time	Area	% Area	Height [EU]	Concentration [g/L]
5.543	5313	41.29	315	0
5.577	3272704	95.19	181274	0.005
5.58	1563060	95.62	86779	0.0025
5.583	794615	95.07	43490	0.00125
5.584	397659	95.69	21843	0.00063

RF samples				
Retention Time	Area	% Area	Height [EU]	Abbreviated name
5.588	12115181	97.76	663224	6ci
5.583	11397541	97.66	614715	6cii
5.588	13788175	97.78	719744	6cii
5.595	16536567	98.28	871542	6abci
5.604	17180982	98.26	918104	6abcii
5.605	16870509	98.3	900759	6abciii
5.605	17129993	98.26	920958	6mi
5.608	16284666	98.27	860707	6mii
5.607	16624841	98.25	888655	6miii
5.611	42604816	98.63	2252043	24ci
5.61	40652301	98.6	2163808	24cii
5.604	43754671	98.65	2356378	24ciii
5.615	58278174	99.06	3061029	24abci
5.611	63049846	99.15	3270656	24abcii
5.609	65567850	99.06	3508349	24abciii
5.606	59638012	98.75	3145822	24mi
5.615	60681388	98.78	3233110	24mii
5.618	57361468	98.73	3044646	24miii
5.618	45387708	98.9	2396993	72ci
5.612	45841101	98.95	2419167	72cii
5.616	47873033	98.85	2516255	72cii
5.614	64374007	99.35	3377699	72abci
5.62	70700790	99.3	3692017	72abcii
5.622	71997002	99.34	3787564	72abciii
5.626	66560024	98.96	3358448	72mi
5.622	61141448	98.93	3234651	72mii
5.62	63459753	98.92	3292992	72miii

Figure E.2: Riboflavin raw data for Growth experiment 1.

Roseoflavin	Hight [EU]	Concentration [g/L]	6 h	Hight Average [	STD	Concentration Average [g/L	STD	STD [%]
Control 6h	549.00	0.066	Roseo0	466.00	76.27	0.056	0.009	0.0
	450.00	0.054	Roseo1	512.67	63.04	0.062	0.008	12.3
	399.00	0.048	Roseo2	489.67	93.61	0.059	0.011	19.1
RosABC 6h	577.00	0.070						
	451.00	0.055						
	510.00	0.062						
RosABCM 6h	595.00	0.072						
	416.00	0.050						
	458.00	0.055	24 h	Hight Average [	STD	Concentration Average [g/L	STD	STD [%]
Control 24h	1459.00	0.177	Roseo0	1522.00	73.00	0.184	0.009	0.0
	1505.00	0.182	Roseo1	1734.33	70.94	0.210	0.009	4.1
	1602.00	0.194	Roseo2	1883.33	34.24	0.228	0.004	1.8
RosABC 24h	1699.00	0.206						
	1688.00	0.204						
	1816.00	0.220						
RosABCM 24h	1915.00	0.232						
	1888.00	0.229						
	1847.00	0.224	72 h	Hight Average [	STD	Concentration Average [g/L	STD	STD [%]
Control 72h	1620.00	0.196	Roseo0	1641.00	37.24	0.199	0.005	0.0
	1684.00	0.204	Roseo1	1909.33	100.38	0.231	0.012	5.3
	1619.00	0.196	Roseo2	2015.00	21.17	0.244	0.003	1.1
RosABC 72h	1795.00	0.217						
	1950.00	0.236						
	1983.00	0.240						
RosABCM 72h	2039.00	0.247						
	2007.00	0.243						
	1999.00	0.242						

	Riboflavin						
	Hight [EU]	Concentration [g/L]	6 h	Hight Average [EU]	Hight STD	Concentration Average [g/L]	STD
Control 6h	663224	0.018	Roseo0	665894	52565	0.0182	0.0014
	614715	0.017	Roseo1	896802	23532	0.0246	0.0006
	719744	0.020	Roseo2	890107	30152	0.0244	0.0008
RosABC 6h	871542	0.024					
	918104	0.025					
	900759	0.025					
RosABCM 6h	920958	0.025					
	860707	0.024					
	888655	0.024	24 h	Hight Average [EU]	Hight STD	Concentration Average [g/L]	STD
Control 24h	2252043	0.062	Roseo0	2257410	96397	0.0618	0.0026
	2163808	0.059	Roseo1	3280011	223807	0.0899	0.0061
	2356378	0.065	Roseo2	3141193	94317	0.0861	0.0026
RosABC 24h	3061029	0.084					
	3270656	0.090					
	3508349	0.096					
RosABCM 24h	3145822	0.086					
	3233110	0.089					
	3044646	0.083	72 h	Hight Average [EU]	Hight STD	Concentration Average [g/L]	STD
Control 72h	2396993	0.066	Roseo0	2444138	63431	0.0670	0.0017
	2419167	0.066	Roseo1	3619093	214443	0.0991	0.0059
	2516255	0.069	Roseo2	3295364	61933	0.0903	0.0017
RosABC 72h	3377699	0.093					
	3692017	0.101					
	3787564	0.104					
RosABCM 72h	3358448	0.092					
	3234651	0.089					
	3292992	0.090					

Figure E.3: Calculations and concentrations of roseoflavin and riboflavin samples for Growth experiment 1.

	6 h	24 h	72 h
Roseo0	0.000	0.000	0.000
Roseo1	0.006	0.026	0.032
Roseo2	0.003	0.044	0.045

Strains	STD from % ratio
Roseo0 6h	0.0000
Roseo1 6h	0.0007
Roseo2 6h	0.0005
Roseo0 24h	0.0000
Roseo1 24h	0.0011
Roseo2 24h	0.0008
Roseo0 72 h	0.0000
Roseo1 72 h	0.0017
Roseo2 72 h	0.0005

Figure E.4: Final roseoflavin concentrations for Roseo0, Roseo1 and Roseo2 for Growth experiment 1. The concentration values were used for the histograms in the Results.

E.2 Growth experiment 2

RoF standards				
Retention Time	Area	% Area	Height [EU]	Concentration [g/L]
3.217	37348	62.94	2312	0.5
3.603	22773	44.26	1292	0.25
3.617	3027	18.22	630	0.125
3.568	9461	60.33	494	0.063

RoF samples				
Retention Time	Area	% Area	Height [EU]	Abbreviated name
3.651	4961	0.1	160	6h Control i
3.675	3346	0.08	122	6h Control ii
3.631	6514	0.16	182	6h Control iii
3.654	9831	0.16	239	6h AB i
3.625	6039	0.09	182	6h AB ii
3.711	6996	0.1	223	6h AB iii
3.762	5910	0.13	175	6h ABM i
3.545	9456	0.19	235	6h ABM ii
3.595	7663	0.15	199	6h ABM iii
3.45	2168	86.73	98	6h ABC i
3.595	1882	0.06	65	6h ABC ii
3.862	2766	0.09	85	6h ABC iii
3.587	2635	100	75	6h ABCM i
3.578	1532	0.05	81	6h ABCM ii
3.467	1182	0.04	76	6h ABCM iii
3.783	6263	0.04	256	6h FABCM i
3.76	5824	0.03	284	6h FABCM ii
3.824	13141	100	455	6h FABCM iii

Figure E.5: Roseoflavin raw data for Growth experiment 2.

3.791	33643	0.08	921	24h Control i
3.781	10816	0.02	496	24h Control ii
3.814	24878	0.05	830	24h Control iii
3.779	35555	0.06	1073	24h AB i
3.821	34636	0.06	1075	24h AB ii
3.821	24927	0.04	988	24h AB iii
3.8	54444	0.11	1438	24h ABM i
3.768	64550	0.13	1489	24h ABM ii
3.817	32958	0.06	1142	24h ABM iii
3.748	26393	0.04	766	24h ABC i
3.737	27285	0.04	765	24h ABC ii
3.743	31972	0.05	895	24h ABC iii
3.75	13507	0.02	579	24h ABCM i
3.674	47041	0.09	1108	24h ABCM ii
3.734	42757	0.08	1170	24h ABCM iii
3.75	97553	0.2	2792	24h FABCM i
3.756	149856	0.22	4081	24h FABCM ii
3.758	150468	0.22	4066	24h FABCM iii
3.777	25328	0.05	939	72h Control i
3.759	19862	0.04	781	72h Control ii
3.783	14158	0.03	671	72h Control iii
3.76	138392	0.11	4015	72h AB i
3.752	161553	0.13	4641	**72h** AB ii
3.764	89602	0.07	2976	72h AB iii
3.746	265710	0.22	7199	72h ABM i
3.743	282909	0.24	7735	72h ABM ii
3.698	180051	0.17	4789	72h ABM iii
3.745	20409	0.03	822	72h ABC i
3.722	17681	0.02	734	72h ABC ii
3.761	19525	0.02	796	72h ABC iii
3.734	32406	0.05	1095	72h ABCM i
3.72	27311	0.04	1034	72h ABCM ii
3.725	45496	0.06	1317	72h ABCM iii
3.729	537927	0.49	14629	72h FABCM i
3.734	829728	0.54	22575	72h FABCM ii
3.735	651923	0.48	17403	72h FABCM iii

Figure E.6: Roseoflavin raw data for Growth experiment 2.

RF standards				
Retention Time	Area	% Area	Height [EU]	Concentration [g/L]
5.849	28888115	99.75	1029833	0.05
5.845	15015954	99.74	530705	0.025
5.838	7277601	99.68	264307	0.0125
5.845	3894634	99.72	139953	0.0063

RF samples				
Retention Time	Area	% Area	Height [EU]	Abbreviated name
5.843	1993952	99.53	71537	6h Control i
5.852	4283822	98.15	151728	6h Control ii
5.853	4105851	98.09	144839	6h Control iii
5.85	6243257	98.65	218448	6h AB i
5.849	6568655	98.67	228171	6h AB ii
5.854	6874916	98.58	238116	6h AB iii
5.847	4384352	98.5	150691	6h ABM i
5.845	4836137	98.43	165176	6h ABM ii
5.849	4877970	98.49	165653	6h ABM iii
5.841	3039513	98.73	104152	6h ABC i
5.832	3017451	98.86	102934	6h ABC ii
5.838	3076534	98.88	104083	6h ABC iii
5.835	2906769	98.7	98642	6h ABCM i
5.842	1980540	69.18	95037	6h ABCM ii
5.845	2807254	98.61	94048	6h ABCM iii
5.841	13941256	99.06	464879	6h FABCM i
5.848	14355499	67.39	697684	6h FABCM ii
5.839	14810016	68.84	698081	6h FABCM iii

Figure E.7: Riboflavin raw data for Growth experiment 2.

5.846	29031936	66.53	1405511	24h Control i
5.834	29952449	67.74	1441104	24h Control ii
5.844	30069176	66.19	1463121	24h Control iii
5.853	40386798	66.69	1902804	24h AB i
5.839	38993951	63.88	1902456	24h AB ii
5.847	43650714	65.19	2087284	24h AB iii
5.849	31479174	64.6	1490369	24h ABM i
5.843	32576281	63.89	1545762	24h ABM ii
5.839	33442907	63.35	1619645	24h ABM iii
5.836	46365164	64.84	2256209	24h ABC i
5.835	44820063	64.51	2177727	24h ABC ii
5.832	47210063	67.27	2233863	24h ABC iii
5.838	36163172	64.39	1723330	24h ABCM i
5.83	33492063	63.05	1649336	24h ABCM ii
5.837	36119565	64.24	1755891	24h ABCM iii
5.827	32256379	65.52	1512575	24h FABCM i
5.817	43759206	62.91	2112591	24h FABCM ii
5.823	40896271	61	2033393	24h FABCM iii
5.827	30695720	61.76	1509972	72h Control i
5.82	31601828	65.63	1525393	72h Control ii
5.818	32814511	65.14	1585897	72h Control iii
5.813	75786116	62.94	3708091	72h AB i
5.819	73300887	60.65	3643462	72h AB ii
5.807	77574184	64.75	3692826	72h AB iii
5.803	77176913	64.43	3693958	72h ABM i
5.792	73746061	62.77	3601290	72h ABM ii
5.795	64742080	62.77	3151221	72h ABM iii
5.812	50623271	64.18	2475582	72h ABC i
5.813	53638546	63.99	2591927	72h ABC ii
5.817	49833943	62.15	2482206	72h ABC iii
5.819	41884736	62.2	2058390	72h ABCM i
5.817	42366996	61.43	2094328	72h ABCM ii
5.797	42984028	61.15	2149122	72h ABCM iii
5.813	65720283	60.37	3289771	72h FABCM i
5.804	89140463	58.37	4552556	72h FABCM ii
5.806	79214868	58.61	3988347	72h FABCM iii

Figure E.8: Riboflavin raw data for Growth experiment 2.

Roseoflavin	Hight [EU]	STD	Concentration Average [g/L]	STD	STD [%]
Roseo0 6h	154.67	30.35	0.036	0.007	0.0
Roseo4 6h	214.67	29.40	0.050	0.007	13.7
Roseo5 6h	203.00	30.20	0.047	0.007	14.9
Roseo1 6h	82.67	16.62	0.019	0.004	20.1
Roseo2 6h	77.33	3.21	0.018	0.001	4.2
Roseo3 6h	331.67	107.72	0.077	0.025	32.5
Roseo0 24h	749.00	223.78	0.175	0.052	0.0
Roseo4 24h	1045.33	49.66	0.244	0.012	4.8
Roseo5 24h	1356.33	187.36	0.317	0.044	13.8
Roseo1 24h	808.67	74.77	0.189	0.017	9.2
Roseo2 24h	952.33	324.80	0.222	0.076	34.1
Roseo3 24h	3646.33	739.91	0.852	0.173	20.3
Roseo0 72h	797.00	134.71	0.186	0.031	0.0
Roseo4 72h	3877.33	840.99	0.905	0.196	21.7
Roseo5 72h	6574.33	1569.20	1.535	0.366	23.9
Roseo1 72h	784.00	45.21	0.183	0.011	5.8
Roseo2 72h	1148.67	148.94	0.268	0.035	13.0
Roseo3 72h	18202.33	4032.86	4.251	0.942	22.2

Riboflavin	Hight [EU]	STD	Concentration Average [g/L]	STD
Roseo0 6h	122701	44443	0.0060	0.0022
Roseo4 6h	228245	9834	0.0112	0.0005
Roseo5 6h	160507	8504	0.0079	0.0004
Roseo1 6h	103723	684	0.0051	0.0000
Roseo2 6h	95909	2418	0.0047	0.0001
Roseo3 6h	620215	134525	0.0304	0.0066
Roseo0 24h	1436579	29070	0.0704	0.0014
Roseo4 24h	1964181	106610	0.0963	0.0052
Roseo5 24h	1551925	64858	0.0761	0.0032
Roseo1 24h	2222600	40435	0.1090	0.0020
Roseo2 24h	1709519	54604	0.0838	0.0027
Roseo3 24h	1886186	325971	0.0925	0.0160
Roseo0 72h	1540421	40131	0.0755	0.0020
Roseo4 72h	3681460	33780	0.1805	0.0017
Roseo5 72h	3482156	290320	0.1707	0.0142
Roseo1 72h	2516572	65344	0.1234	0.0032
Roseo2 72h	2100613	45691	0.1030	0.0022
Roseo3 72h	3943558	632583	0.1934	0.0310

Figure E.9: Calculations and concentrations of roseoflavin and riboflavin samples for Growth experiment 2.

	6 h	24 h	72 h
Roseo0	0.0	0.0	0.0
Roseo4	0.0	0.1	0.7
Roseo5	0.0	0.1	1.3
Roseo1	0.0	0.0	0.0
Roseo2	0.0	0.0	0.1
Roseo3	0.0	0.7	4.1

Strains	STD from % ratio
Roseo0 6h	0.0000
Roseo4 6h	0.0019
Roseo5 6h	0.0017
Roseo1 6h	0.0034
Roseo2 6h	0.0008
Roseo3 6h	0.0134
Roseo0 24h	0.0000
Roseo4 24h	0.0033
Roseo5 24h	0.0196
Roseo1 24h	0.0013
Roseo2 24h	0.0162
Roseo3 24h	0.1373
Roseo0 72h	0.0000
Roseo4 72h	0.1560
Roseo5 72h	0.3220
Roseo1 72h	0.0002
Roseo2 72h	0.0106
Roseo3 72h	0.9006

Figure E.10: Final roseofavin concentrations for Roseo0, Roseo1, Roseo2, Roseo3, Roseo4 and Roseo5 for Growth experiment 2. The concentration values were used for the histograms in the Results.

F Raw data and calculations for the antimicrobial tests

The raw data for Antimicrobial test 1, Antimicrobial test 2, and Antimicrobial test 3 is displayed in Figure F.1, Figure F.2, and Figure F.3, respectively. To calculate the final biomass in the figures, the raw data of the blank row G was subtracted from all the reminding rows, yielding the values in Figure F.4 for Antimicrobial test 1, Figure F.5 for Antimicrobial test 2, and Figure F.6 for Antimicrobial test 3. After, the average and standard deviations were calculated from each triplicate in Figure F.4-Figure F.6, to determine the final biomass for a strain at a specific roseoflavin dilution. One triplicate is defined as the values of one of the columns and either row A-C or D-F. The final biomass and standard deviations of Antimicrobial test 1, Antimicrobial test 2, and Antimicrobial test 3 are displayed in Figure F.7, Figure F.8, and Figure F.9, respectively. The equations for average and standard deviations are shown in Appendix B in Equation B.1 and Equation B.2, respectively.

<>	1	2	3	4	5	6	7	8	9	10	11	12
A	0.1327	0.2117	0.2353	0.2574	0.2057	0.3071	0.2691	0.2646	0.2590	0.3554	0.3558	0.3000
B	0.1177	0.2425	0.2466	0.2565	0.2975	0.2859	0.3160	0.2941	0.3731	0.3663	0.3282	0.3632
C	0.1339	0.2302	0.2449	0.2555	0.2646	0.2632	0.2655	0.3018	0.3427	0.3459	0.3073	0.3540
D	0.1248	0.2746	0.3006	0.3306	0.3747	0.4033	0.4503	0.4683	0.4429	0.4591	0.3988	0.4820
E	0.1422	0.2742	0.2584	0.3170	0.3722	0.3959	0.4153	0.4103	0.4306	0.4422	0.4159	0.4489
F	0.1382	0.2700	0.3068	0.2878	0.3670	0.4071	0.4029	0.4022	0.4346	0.4287	0.4389	0.4735
G	0.0494	0.0473	0.0460	0.0459	0.0457	0.0454	0.0453	0.0455	0.0451	0.0442	0.0450	0.0453

Figure F.1: Raw data for Antimicrobial test 1.

<>	1	2	3	4	5	6	7	8	9	10	11	12
A	0.1544	0.1340	0.1447	0.1318	0.1247	0.1277	0.1332	0.1697	0.3083	0.6863	0.6893	0.9541
B	0.1556	0.1438	0.1340	0.1494	0.1257	0.1433	0.1530	0.1830	0.3468	0.6099	0.6516	1.0555
C	0.1463	0.2021	0.1663	0.1443	0.2101	0.1630	0.1758	0.2175	0.2473	0.6504	0.6078	0.9802
D	0.1407	0.1616	0.1552	0.1365	0.1736	0.1434	0.1536	0.2348	0.3286	0.6780	0.9089	1.0286
E	0.1365	0.2058	0.1410	0.1476	0.2122	0.1782	0.1971	0.2419	0.4428	0.6839	0.8566	0.9932
F	0.1453	0.1835	0.1355	0.1324	0.1629	0.1797	0.1911	0.1784	0.3202	0.6880	0.9007	1.0691
G	0.0407	0.0405	0.0400	0.0398	0.0393	0.0383	0.0387	0.0401	0.0395	0.0407	0.0376	0.0367

<>	1	2	3	4	5	6	7	8	9	10	11	12
A	0.1560	0.1499	0.1610	0.1548	0.1350	0.1424	0.1416	0.1583	0.2582	0.5371	0.9868	1.0378
B	0.1544	0.1421	0.1522	0.1708	0.1387	0.1569	0.1528	0.1838	0.2272	0.5220	0.8613	0.9669
C	0.1466	0.1515	0.1452	0.1489	0.1276	0.1231	0.1246	0.1269	0.1795	0.3851	0.6430	1.0940

Figure F.2: Raw data for Antimicrobial test 2.

<>	1	2	3	4	5	6	7	8	9	10	11	12
A	0.1403	0.3096	0.5012	0.5340	0.6514	0.6825	0.7279	0.7594	0.7431	0.7093	0.7379	0.6026
B	0.1337	0.2535	0.4111	0.5406	0.6412	0.7031	0.7124	0.7503	0.7415	0.7417	0.7133	0.6963
C	0.1336	0.2597	0.4475	0.5511	0.6460	0.6919	0.7333	0.7681	0.7644	0.7575	0.7439	0.6655
D	0.2271	0.4309	0.6112	0.7118	0.7767	0.8732	0.8613	0.8789	0.8911	0.8738	0.8436	0.8887
E	0.2220	0.4939	0.6182	0.7018	0.8055	0.8630	0.8898	0.8621	0.9120	0.8795	0.8589	0.8210
F	0.3393	0.5031	0.6252	0.7282	0.8217	0.8823	0.9068	0.8247	0.9049	0.8945	0.9041	0.8557
G	0.0425	0.0399	0.0390	0.0386	0.0392	0.0388	0.0386	0.0381	0.0391	0.0385	0.0390	0.0378

<>	1	2	3	4	5	6	7	8	9	10	11	12
A	0.0991	0.1177	0.1597	0.1758	0.2153	0.1925	0.2041	0.2594	0.2385	0.2260	0.3171	0.2267
B	0.0895	0.1250	0.1819	0.2777	0.2805	0.3143	0.3268	0.3359	0.3208	0.3335	0.3349	0.2106
C	0.0906	0.1141	0.1696	0.1863	0.2127	0.2181	0.2344	0.2541	0.3101	0.3105	0.2855	0.2124

Figure F.3: Raw data for Antimicrobial test 3.

<>	1	2	3	4	5	6	7	8	9	10	11	12
A	0.083	0.164	0.189	0.212	0.160	0.262	0.224	0.219	0.214	0.311	0.311	0.255
B	0.068	0.195	0.201	0.211	0.252	0.240	0.271	0.249	0.328	0.322	0.283	0.318
C	0.084	0.183	0.199	0.210	0.219	0.218	0.220	0.256	0.298	0.302	0.262	0.309
D	0.075	0.227	0.255	0.285	0.329	0.358	0.405	0.423	0.398	0.415	0.354	0.437
E	0.093	0.227	0.212	0.271	0.327	0.351	0.370	0.365	0.385	0.398	0.371	0.404
F	0.089	0.223	0.261	0.242	0.321	0.362	0.358	0.357	0.389	0.385	0.394	0.428
G	0.000	0.000	0.000	0.000	0.000	0.000	0.000	0.000	0.000	0.000	0.000	0.000

Figure F.4: Values after subtraction of row G in Antimicrobial test 1.

<>	1	2	3	4	5	6	7	8	9	10	11	12
A	0.114	0.094	0.105	0.092	0.085	0.089	0.095	0.130	0.269	0.646	0.652	0.917
B	0.115	0.103	0.094	0.110	0.086	0.105	0.114	0.143	0.307	0.569	0.614	1.019
C	0.106	0.162	0.126	0.104	0.171	0.125	0.137	0.177	0.208	0.610	0.570	0.943
D	0.100	0.121	0.115	0.097	0.134	0.105	0.115	0.195	0.289	0.637	0.871	0.992
E	0.096	0.165	0.101	0.108	0.173	0.140	0.158	0.202	0.403	0.643	0.819	0.957
F	0.105	0.143	0.095	0.093	0.124	0.141	0.152	0.138	0.281	0.647	0.863	1.032
G	0.000	0.000	0.000	0.000	0.000	0.000	0.000	0.000	0.000	0.000	0.000	0.000

<>	1	2	3	4	5	6	7	8	9	10	11	12
A	0.115	0.109	0.121	0.115	0.096	0.104	0.103	0.118	0.219	0.496	0.949	1.001
B	0.114	0.102	0.112	0.131	0.099	0.119	0.114	0.144	0.188	0.481	0.824	0.930
C	0.106	0.111	0.105	0.109	0.088	0.085	0.086	0.087	0.140	0.344	0.605	1.057

Figure F.5: Values after subtraction of row G in Antimicrobial test 2.

<>	1	2	3	4	5	6	7	8	9	10	11	12
A	0.098	0.270	0.462	0.495	0.612	0.644	0.689	0.721	0.704	0.671	0.699	0.565
B	0.091	0.214	0.372	0.502	0.602	0.664	0.674	0.712	0.702	0.703	0.674	0.659
C	0.091	0.220	0.408	0.513	0.607	0.653	0.695	0.730	0.725	0.719	0.705	0.628
D	0.185	0.391	0.572	0.673	0.738	0.834	0.823	0.841	0.852	0.835	0.805	0.851
E	0.180	0.454	0.579	0.663	0.766	0.824	0.851	0.824	0.873	0.841	0.820	0.783
F	0.297	0.463	0.586	0.690	0.782	0.844	0.868	0.787	0.866	0.856	0.865	0.818
G	0.000	0.000	0.000	0.000	0.000	0.000	0.000	0.000	0.000	0.000	0.000	0.000

<>	1	2	3	4	5	6	7	8	9	10	11	12
A	0.057	0.078	0.121	0.137	0.176	0.154	0.165	0.221	0.199	0.187	0.278	0.189
B	0.047	0.085	0.143	0.239	0.241	0.275	0.288	0.298	0.282	0.295	0.296	0.173
C	0.048	0.074	0.131	0.148	0.173	0.179	0.196	0.216	0.271	0.272	0.246	0.175

Figure F.6: Values after subtraction of row G in Antimicrobial test 3.

		1	2	3	4	5	6	7	8	9	10	11	12
Average	Transport0	0.079	0.181	0.196	0.211	0.210	0.240	0.238	0.241	0.280	0.312	0.285	0.294
SD		0.006	0.012	0.005	0.001	0.038	0.018	0.024	0.017	0.051	0.009	0.021	0.030
Average	Transport1	0.086	0.226	0.243	0.266	0.326	0.357	0.378	0.381	0.391	0.399	0.373	0.423
SD		0.006	0.002	0.022	0.019	0.003	0.005	0.022	0.032	0.006	0.014	0.018	0.016

Figure F.7: Biomass [g/L] and standard deviation of Antimicrobial test 1.

		1	2	3	4	5	6	7	8	9	10	11	12
Average	Transport0	0.111	0.119	0.108	0.102	0.114	0.106	0.115	0.150	0.261	0.608	0.612	0.960
SD		0.005	0.037	0.016	0.009	0.049	0.018	0.021	0.025	0.050	0.038	0.041	0.053
Average	Transport1	0.100	0.143	0.104	0.099	0.144	0.129	0.142	0.178	0.324	0.643	0.851	0.994
SD		0.004	0.022	0.010	0.008	0.026	0.021	0.024	0.035	0.068	0.005	0.028	0.038
Average	Transport2	0.112	0.107	0.113	0.118	0.094	0.102	0.101	0.116	0.182	0.441	0.793	0.996
SD		0.005	0.005	0.008	0.011	0.006	0.017	0.014	0.029	0.040	0.084	0.174	0.064

Figure F.8: Biomass [g/L] and standard deviation of Antimicrobial test 2.

		1	2	3	4	5	6	7	8	9	10	11	12
Transport3	Av	0.093	0.234	0.414	0.503	0.607	0.654	0.686	0.721	0.711	0.698	0.693	0.617
	SD	0.004	0.031	0.045	0.009	0.005	0.010	0.011	0.009	0.013	0.025	0.016	0.048
Transport4	Av	0.220	0.436	0.579	0.675	0.762	0.834	0.847	0.817	0.864	0.844	0.830	0.817
	SD	0.066	0.039	0.007	0.013	0.023	0.010	0.023	0.028	0.011	0.011	0.031	0.034
Transport5	Av	0.051	0.079	0.131	0.175	0.197	0.203	0.216	0.245	0.251	0.251	0.273	0.179
	SD	0.005	0.006	0.011	0.056	0.038	0.064	0.064	0.046	0.045	0.057	0.025	0.009

Figure F.9: Biomass [g/L] and standard deviation of Antimicrobial test 3.

NTNU

Norwegian University of
Science and Technology